NASA-CR-200508

MARS PATHFINDER LANDING SITE WORKSHOP II: CHARACTERISTICS OF THE ARES VALLIS REGION AND FIELD TRIPS IN THE CHANNELED SCABLAND, WASHINGTON

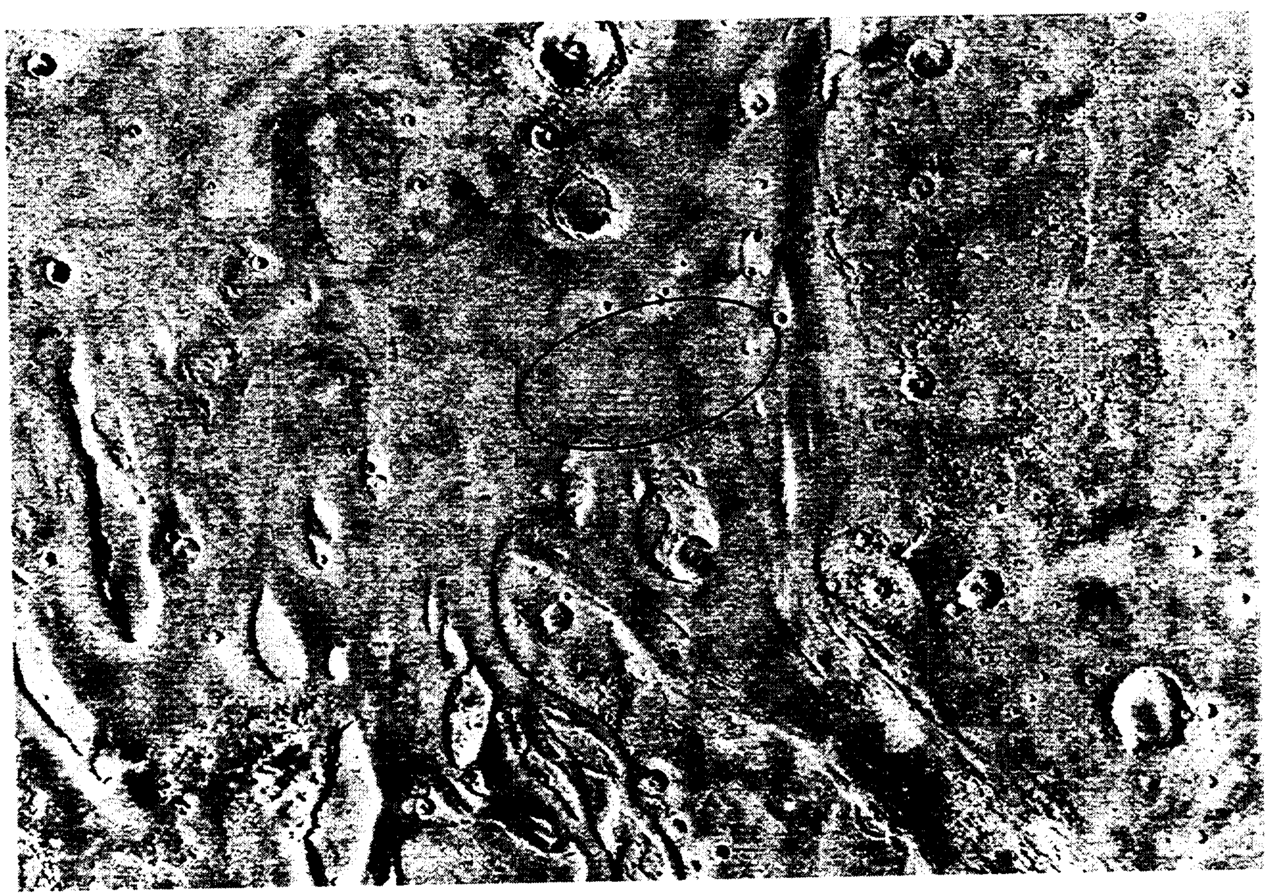

LPI Technical Report Number 95-01, Part 1

Lunar and Planetary Institute 3600 Bay Area Boulevard Houston TX 77058-1113
LPI/TR--95-01, Part 1

MARS PATHFINDER LANDING SITE WORKSHOP II: CHARACTERISTICS OF THE ARES VALLIS REGION AND FIELD TRIPS IN THE CHANNELED SCABLAND, WASHINGTON

Edited by

M. P. Golombek, K. S. Edgett, and J. W. Rice Jr.

Held at
Spokane, Washington

September 24–30, 1995

Sponsored by
Arizona State University
Jet Propulsion Laboratory
Lunar and Planetary Institute
National Aeronautics and Space Administration

Lunar and Planetary Institute 3600 Bay Area Boulevard Houston TX 77058-1113

LPI Technical Report Number 95-01, Part 1
LPI/TR--95-01, Part 1

Compiled in 1995 by
LUNAR AND PLANETARY INSTITUTE

The Institute is operated by the University Space Research Association under Contract No. NASW-4574 with the National Aeronautics and Space Administration.

This report may be cited as

Golombek M. P., Edgett K. S., and Rice J. W. Jr., eds. (1992) *Mars Pathfinder Landing Site Workshop II: Characteristics of the Ares Vallis Region and Field Trips to the Channeled Scabland, Washington.* LPI Tech. Rpt. 95-01, Part 1, Lunar and Planetary Institute, Houston. 63 pp.

This report is distributed by

ORDER DEPARTMENT
Lunar and Planetary Institute
3600 Bay Area Boulevard
Houston TX 77058-1113

Mail order requestors will be invoiced for the cost of shipping and handling.

Cover: Regional mosaic showing the Mars Pathfinder landing site (100 km × 200 km landing ellipse shown). The mosaic shows large catastrophic outflow channels debouching into Chryse Planitia. Ares Vallis flowed to the northwest (from the southeast) across the landing site. Tiu Valles is just to the west of Ares Vallis and may also have flowed across the landing area. The landing site itself is a very smooth depositional surface, where the flood waters deposited the sediments carved from the channels. Landing at this location should allow analysis of a wide variety of rock types deposited by the flood. These catastrophic outflow channels on Mars are much larger analogs to the Channeled Scabland in Washington state.

Preface

This volume contains papers that have been accepted for presentation at the Mars Pathfinder Landing Site Workshop II: Characteristics of the Ares Vallis Region, September 24–30, 1995, in Spokane, Washington. Also included in this volume is the field trip guide to the Channeled Scabland and Missoula Lake Breakout. The organizer for this workshop was Matthew Golombek from Jet Propulsion Laboratory. The field trip organizers were Kenneth Edgett and James Rice Jr. from Arizona State University.

Logistics and administrative and publications support were provided by the Publications and Program Services Department staff at the Lunar and Planetary Institute.

Contents

Field Guide

Mission Description

INTRODUCTION

The Mars Pathfinder Project received a new start in October 1993 as one of the next missions in NASA's long-term Mars exploration program. The mission involves landing a single vehicle on the surface of Mars in 1997. The project is one of the first Discovery-class missions and is required to be a quick, low-cost mission ($150M development cost cap, excluding launch vehicle and mission operations, in less than a three-year development period) and achieve a set of significant but focused engineering, science, and technology objectives. The primary objective is to demonstrate a low-cost cruise, entry, descent, and landing system required to place a payload on the martian surface in a safe, operational configuration. Additional objectives include the deployment and operation of various science instruments and a microrover (an additional $22M development). Pathfinder paves the way for a cost-effective implementation of future Mars lander missions.

This section gives an overview of the Mars Pathfinder mission, with special reference to scientific aspects of the project. First, the flight system and mission are briefly described. A general description of the scientific objectives and investigations afforded by Pathfinder is followed by a description of each science instrument. Finally, the process for selecting a landing site on Mars is described along with the proposed Mars Pathfinder landing site.

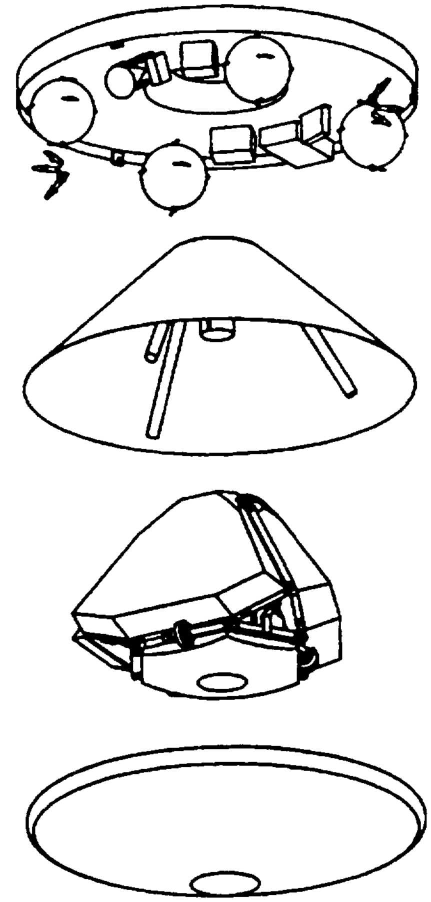

Fig. 1. Exploded view of Mars Pathfinder flight system, showing from top to bottom: back-pack-style cruise stage, backcover with three solid rockets, tetrahedron-shaped lander, and aeroshell.

MISSION AND SPACECRAFT OVERVIEW

The Pathfinder flight system is an aerocraft consisting of three major elements (Fig. 1): a simple back-pack style cruise stage; the deceleration subsystems, including an aeroshell, backcover, parachute, small solid rockets, and airbags; and a tetrahedron-shaped lander (containing the rover and science instruments) packaged within the aeroshell and backcover. The current spacecraft launch mass is approximately 850 kg, including 25 kg of payload (science instruments, rover, and rover support equipment).

Mars Pathfinder will be launched in December 1996 on a Type 1 Earth-Mars transfer trajectory on a McDonnell Douglas Delta II launch vehicle, with a Star upper stage. The primary activities during the 6–7-month cruise phase include periodic attitude control maneuvers required to remain Earth pointed and four trajectory correction maneuvers needed to ensure accurate arrival targeting at Mars. The back-pack-style cruise stage consists of a solar array and additional related power equipment, a medium-gain antenna, propulsion thrusters, propulsion valves and tanks, and attitude determination sensors. It will be jettisoned prior to entry into the martian atmosphere.

At Mars arrival on July 4, 1997, the spacecraft will enter the atmosphere directly from the hyperbolic approach trajectory and will be slowed by a Viking heritage aeroshell and disk-gap-band parachute. During descent the lander will be lowered beneath the backcover on a 20-m-long tether. A radar altimeter will trigger the firing of three small solid tractor rockets mounted on the backcover, and airbags will be inflated to cushion any remaining vertical and horizontal velocity at surface impact. After landing, the airbags will be deflated and the triangular petals of a tetrahedron-shaped lander will be opened, righting the lander regardless of which side the lander comes to rest upon.

The tetrahedron-shaped lander consists of four similarly shaped triangular panels. All lander equipment except the solar arrays, rover, and meteorology mast are attached to a

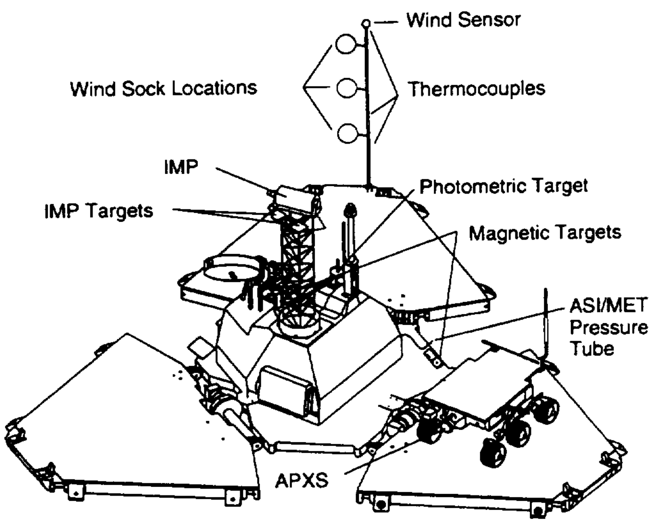

Fig. 2. Perspective view of lander opened on the surface showing the location of the instruments and rover. IMP is the Imager for Mars Pathfinder. IMP targets are the flat field and magnetic targets near the IMP head, as well as the photometric target on top of the electronics box. Magnetic targets are mounted on the base plate as well as the top of the electronics box; magnetic targets on the rover ramps are not shown. APXS is the α proton X-ray spectrometer mounted on the back of the rover. Temperature and wind sensors are mounted on the 1-m-high mast. Entry and descent pressure and temperature measurements are made in the indicated triangular space between the lander panels, where the ASI/MET pressure tube is shown.

single center panel (Fig. 2). All thermally sensitive electronics are contained in an insulated enclosure on the center panel. Specific hardware components inside this enclosure include a high-performance central computer, a Cassini heritage transponder, a solid-state power amplifier for telecommunications, and a high-capacity rechargeable battery. Hardware outside the thermal enclosure includes a steerable high-gain antenna capable of approximately 5.5 kbps into a 70-m Deep Space Network antenna and solar arrays capable of providing enough power to transmit for at least 2 hr per sol and maintain 128 MB of dynamic memory through the night. All engineering and science data obtained during the entry, descent, and landing phase are recorded for playback at the initiation of lander surface operations. The lander is capable of surviving for a minimum of 30 sols, with a possible lifetime of up to a year.

The rover on Mars Pathfinder is a small (10 kg), six-wheel-drive rocker-bogie design vehicle, which is 65 cm long × 48 cm wide × 32 cm high. The rocker-bogie chassis has demonstrated remarkable mobility, including the ability to climb obstacles that are as high as a full wheel diameter and the capability of turning in place. The vehicle communicates through the lander via a UHF antenna link and operates almost entirely within view of the lander cameras, or within a few tens of meters of the lander. It is a solar-powered vehicle, with a primary battery backup, which moves at 0.4 m/min, and carries 1.5 kg of payload. The payload consists of monochrome stereo forward cameras for hazard detection and terrain imaging and a single rear color camera. On the rear of the vehicle is the α proton X-ray spectrometer (APXS) mounted on a deployment device that enables placing the APXS sensor head up against both rocks and the soil. The rear-facing camera will image the APXS measurement site with 1 mm resolution (a few hundred meters per pixel). The rover also carries instruments for two technology experiments described later and a variety of hazard detection systems for safing the vehicle. General scientific guidance for the rover is provided by an appointed Rover Scientist, Henry Moore of the U.S. Geological Survey, Menlo Park.

The rover will also perform a number of technology experiments designed to provide information that will improve the design of future planetary rovers. These experiments include terrain geometry reconstruction from lander/rover imagery, basic soil mechanics by imaging wheel tracks and wheel sinkage, dead reckoning sensor performance and path reconstruction/recovery, logging/trending of vehicle data, rover thermal characterization, rover vision sensor performance, UHF link effectiveness, material abrasion by sensing loss of coverings of different thickness on a rover wheel, and material adherence by measuring dust accumulation on a reference solar cell with a removable cover and by directly measuring the mass of the accumulated dust on a quartz crystal microbalance.

MARS PATHFINDER SCIENCE OBJECTIVES AND INVESTIGATIONS

The science payload chosen for Mars Pathfinder includes an imaging system, an elemental composition instrument, and an atmospheric structure instrument/meteorology package. These instruments, used in conjunction with selected engineering subsystems on board both the lander and rover vehicles, provide the opportunity for a number of scientific investigations. The scientific objectives and investigations afforded by Pathfinder include surface morphology and geology at meter scale, elemental composition and mineralogy of surface materials, and a variety of atmospheric science investigations (*Golombek*, 1995).

The surface imaging system will reveal martian geologic processes and surface-atmosphere interactions at a scale currently known only at the two Viking landing sites. It will observe the rock distribution, surface slopes, and general physiography in order to understand the geological processes that created the surface. This will be accomplished by panoramic stereo imaging at various times of the day as well as before and after the imager deploys on its pop-up mast. Images will be calibrated by observing a flat-field target near the imager head and shadowed and illuminated portions of reference or calibration targets. In addition, observations over the life of the mission will allow assessment of any changes in the scene over time that might be attributable to frost, dust, or sand deposition or erosion or other surface-atmosphere interactions. The rover will also take close-up images of the terrain during its traverses. A basic understanding of near-surface stratigraphy and soil mechanics will be obtained by imaging (from both rover and lander) rover tracks, holes dug by rover wheels, and any surface depressions left by the spacecraft landing.

The APXS and the visible to near-infrared (0.4–1 μm) spectral filters on the imaging system will determine the elemental composition and constrain the mineralogy (particularly sensitive to pyroxene and Fe oxides) of rocks and other surface materials, which can be used to address questions concerning the composition of the crust, its differentiation, and the development of weathering products. These investigations will represent a calibration point ("ground truth") for orbital remote sensing observations. The imaging system will obtain full multispectral panoramas of the surface and any subsurface layers exposed by the rover and lander. Because the APXS is mounted on the rover it will characterize the composition of rocks and soil in the vicinity of the lander (tens of meters), which will represent a significant improvement in our knowledge over that obtained by Viking or that likely to be obtained by the Russian Mars '96 small stations, which deploy the APXS on single-degree-of-freedom arms. The rover-mounted APXS sensor head on Pathfinder will also be placed in holes dug by the rover wheels and against rocks that have been abraded by a rover wheel. Multispectral images are also planned for two sets of magnetic targets distributed at two locations (and heights) on the spacecraft that will discriminate the magnetic phase of accumulated airborne dust. In addition, a single magnetic target mounted near the imager head will be viewed by a magnifying lens to determine the size and shape of individual magnetic particles. The APXS will also measure the composition and, in particular, the Ti content of dust adhering to magnetic targets at the end of the rover ramps, which is critical for discriminating the various magnetic phases. A rear-facing imager will enable close-up images with millimeter resolution of every APXS measurement site. Between these images and auxiliary information from lander imaging spectra, it is likely that mineralogy can be constrained from the elemental abundances measured by the APXS.

The atmospheric structure instrument will determine a pressure, temperature, and density profile of the atmosphere (with respect to altitude) during entry and descent at a new location, time, and season. Measurements of pressure and temperature will be made in a triangular space between the petals at the base of the lander during descent. Redundant three-axis accelerometers will allow extraction of atmospheric density profiles and hence pressure and temperature profiles during entry. Diurnal variations in the atmospheric boundary layer will be characterized by regular surface meteorology measurements (pressure, temperature, atmospheric opacity, and wind). Three thermocouples mounted on a 1-m-high mast located on a petal away from the thermally contaminating lander electronics will determine the ambient temperature profile with altitude. A wind sensor on the top of this mast, along with three wind socks below it, will allow determination of wind speed and direction vs. altitude in the boundary layer as well as calculation of the aerodynamic roughness of the surface. Regular sky and solar spectral observations by the lander imager will also monitor dust particle size and shape, refractive index, vertical aerosol distribution, and water vapor abundance.

MARS PATHFINDER SCIENTIFIC INSTRUMENTS

Imager for Mars Pathfinder (IMP)

The Imager for Mars Pathfinder (IMP), proposed by P. Smith of the University of Arizona, was selected through a NASA Announcement of Opportunity as a principal investigator experiment. In addition to the camera hardware, the investigation includes a variety of spacecraft targets, including radiometric calibration targets, magnetic properties targets, and wind socks (*Smith,* 1994; *Smith et al.*, 1995).

The stereoscopic imager is deployed on a jack-in-the-box pop-up mast that is roughly 1.5 m above the surface (Fig. 2). It includes two imaging triplets, two fold mirrors separated by 15 cm for stereo viewing, two filter wheels in each path, and a fold prism to place the images side by side on the CCD focal plane. Each of the stereo frames has 256 × 256 active elements. The pixel instantaneous field of view is 1 mrad. Each filter wheel has 12 positions, with most filters for geologic studies (0.4–1.1 μm, which are particularly sensitive to Fe oxides and pyroxene) and stereo viewing, others for atmospheric water vapor and dust, and a magnifying close-up lens for viewing the magnetic target near the imager head (*Singer et al.*, 1994). Azimuth and elevation drives provide a nearly complete field of view. IMP co-investigators include D. Britt, L. Doose, R. Singer, and M. Tomasko (University of Arizona); L. Soderblom (U. S. Geological Survey, Flagstaff); H. U. Keller (Max Planck Institüt für Aeronomie), who is providing the CCD and associated electronics; J. M. Knudsen (Niels Bohr Institute, University of Copenhagen), who is providing the magnetic targets; F. Gliem (Technical University of Braunschweig), who is providing the image compression software; and R. Greeley (Arizona State University), who is providing the three wind socks. The JPL Investigation Scientist is K. Herkenhoff.

Alpha Proton X-ray Spectrometer (APXS)

This instrument is a foreign-provided copy of an instrument design flown on the Russian Vega and Phobos missions and is planned for flight on the Russian Mars '96 mission.

Accordingly the instrument has extensive, applicable flight heritage. The α and proton spectrometer portions are provided by the Max Planck Institüt für Chemie, Mainz, Germany, under the direction of the principal investigator, R. Rieder, and co-investigator H. Wänke. The X-ray spectrometer portion is provided by the co-investigator, T. Economou (University of Chicago). J. Crisp is the JPL Investigation Scientist.

This elemental composition instrument consists of α particle sources and detectors for back-scattered α particles, protons, and X-rays (*Rieder et al.*, 1994). The APXS will determine elemental chemistry of surface materials for most major elements except H and He. The analytical process is based on three interactions of α particles with matter: elastic scattering of α particles by nuclei of light elements, α proton nuclear reactions with certain elements with atomic numbers from 9 to 14, which are very characteristic of the individual elements, and excitation of the atomic structure of atoms by α particles, leading to the emission of characteristic X-rays for heavier elements. The approach used is to expose material to a Cu radioactive source that produces α particles with a known energy, and to acquire energy spectra of the α particles, protons, and X-rays returned from the sample. Accordingly, the instrument can identify and determine the amounts of most chemical elements.

The APXS sensor head is mounted on the rear of the rover chassis (Fig. 2) on a deployment mechanism that allows the instrument to be placed in contact with both rock and soil surfaces at a wide variety of elevations and angles. The APXS electronics are mounted within the rover, in a temperature-controlled environment.

Atmospheric Structure Instrument/Meteorology Package (ASI/MET)

The ASI/MET is implemented as a facility experiment, developed by JPL, to provide engineering support to the measurement of the entry descent and landing conditions and to acquire science data both before and after landing (*Seiff*, 1994). An appointed Science Advisory Team, under the leadership of A. Seiff (NASA Ames Research Center/San Jose State University), with team members J. Barnes (Oregon State University), D. Crisp (JPL), R. Haberle (NASA Ames Research Center), and J. Tillman (University of Washington) provides scientific guidance to the JPL instrument team. T. Schofield is the JPL Investigation Scientist.

Data acquired during the entry and descent of the lander permit the reconstruction of profiles of atmospheric density, temperature, and pressure from altitudes in excess of 100 km to the surface. The accelerometer portion of the experiment consists of redundant x-, y-, and z-axis sensors. Three gain states are provided to cover the wide dynamic range from the microgravity accelerations experienced upon entering the atmosphere to the peak deceleration experienced during entry into the atmosphere.

The ASI/MET instrument hardware consists of four thermocouples and a wind sensor mounted on a 1-m-long mast that deploys upright from the end of a lander petal after landing (Fig. 2). A pressure sensor is mounted within the thermal enclosure of the lander with a tube leading to a triangular opening between the petals for measurement of the pressure during descent and after landing. Pressure and temperature sensors are sampled twice per second while entering and descending through the atmosphere. Temperature, pressure, wind speed, and direction are sampled hourly throughout the landed mission at multiple heights above the local surface.

MARS PATHFINDER LANDING SITE SELECTION

Engineering Constraints

A variety of engineering considerations constrain the location of potential landing sites for Pathfinder. The site must be between 0°N and 30°N latitude so that the lander and rover solar arrays can generate the maximum possible power (the subsolar latitude on July 4, 1997, is 15°N) and to facilitate communication with Earth (the sub-Earth latitude at this time is 25°N). Note that detailed calculations of power available from the solar arrays later forced narrowing of the latitudinal band to be within 5° of 15°N. The reference altitude of the site must be below 0 km so that the descent parachute has sufficient time to open and slow the lander to the correct terminal velocity. Landing will occur within a 100 km × 200 km ellipse (a 90% probability landing ellipse) along a N74°E axis around the targeted site due to navigational uncertainties during cruise and atmospheric entry. Inspection of the 1:15M geologic and topographic maps of Mars reveals about a dozen different geologic units are available within these altitude and latitude constraints.

Landing Site Workshop

The short time frame required for the development and launch of Pathfinder requires quick decisions where possible to keep costs at a minimum. In keeping with this philosophy, and the unfortunate circumstance that no new spacecraft will be visiting and returning data from Mars before Pathfinder lands, the decision was made to choose the landing site early in the development of the spacecraft/project to provide a specific location for the lander engineering design criteria. The process involved making an initial landing site selection and then validating the selection based on subsequent lander test results (such as altimeter and airbag drop tests) and information relevant to site safety (such as recently acquired Earth-based radar data). Because Mars Pathfinder is the first mission to land on Mars since Viking, about 20 years ago, we decided to hold an open workshop on potential landing sites that solicited participation by the entire Mars scientific community. The Mars Pathfinder Landing Site Workshop was held April 18–19, 1994, at the Lunar and Planetary Institute in Houston, Texas (*Golombek*, 1994). Over 60 interested scientists and engineers from around the U.S. and Europe gathered to discuss potential landing sites on Mars. Presentations included a description of the mission, spacecraft and instruments, general landing site perspectives from a variety of disciplines, data pertaining to landing site safety, and over 20 proposed individual landing sites.

A variety of general observations from the workshop and discussions were very successful in helping to choose a landing site and are discussed below. First, there was no unanimous first-choice landing site among all participants. In other words, there was no "dinosaur bone site" on Mars that all felt was so compelling that it had to be the landing site. Second, virtually all types of landing sites proposed are available within the preferred constraints of being within 5° of the 15° north latitude (for maximum solar power) and below 0 km elevation.

Three general types of landing sites were proposed by participants of the workshop:

1. *"Grab-Bag" Site*—a place such as the mouth of a large catastrophic outflow channel in which a wide variety of rocks are potentially available and within reach of the rover. Even though the exact provenance of the samples would not be known, the potential for sampling a large diversity of martian rocks in a small area could reveal a lot about Mars overall. Data from subsequent orbital remote sensing missions would then be used to infer the provenance for the "ground truth" samples studied by Pathfinder.

2. *Large Uniform Site of Unknown Rock Type*. The site appears uniform at Viking resolution, but the interprètation of rock type or composition of the unit is uncertain. Landing at the site would allow determination of the rock type that makes up the unit. Several of these sites were presented and received strong support at the workshop.

3. *Large Uniform Site of Suspected or Known Composition*, such as a lava flow. Landing at such a site would confirm the rock type and measure something about it that was important (e.g., Fe and Mg content of a basalt).

In general, it seemed that many of the attendees and the various science disciplines represented supported a "grab-bag" site that holds the prospect of sampling a diversity of crustal units. These sites are all located where catastrophic flood channels debouch into Chryse Planitia and have cut through a variety of ancient Noachian crustal units as well as the Hesperian ridged plains and a variety of other units. The potential of analyzing a variety of rocks that likely make up two-thirds of the crust of the planet, even without knowing exactly their provenance, is an exciting prospect for the next landed mission to Mars. What makes this type of site potentially more interesting than simply landing in the highlands themselves is the possibility of sampling more different highland materials than might be accessible at a single highland site. These sites are likely similar to the Viking 1 landing site: both rocky and dusty.

The other area of interest to a variety of scientists was the Cerberus Region. This area holds the potential of sampling a widespread low-albedo surface eolian unit, interpreted in this area to be mafic sand. In this region, a variety of different crustal units are available, including what may be unweathered highland material. This area will likely look different from the Viking landing sites, being relatively rock poor and dust free. Going to sample this dark eolian unit is equivalent to going to a large uniform site of unknown origin.

A smaller group of scientists wanted to go to sediments; unfortunately, uniquely identifying sediments from Viking images is difficult and it would be difficult to be sure that the desired sediments would be within reach of the rover after landing. In addition, Pathfinder's instruments are much better suited to determining the mineralogy of rock rather than soil.

In general, few scientists present were very excited about landing at a large uniform site of suspected known composition, given that this effectively involves going to a basalt flow (one of the few rock types on Mars identifiable from Viking orbiter images). This was underscored by the widely accepted hypothesis that we already have samples of young basalts from Mars in the form of the SNC meteorites. Going to Mars to confirm that the SNC meteorites are, in fact, from Mars did not get much support at the workshop. Taken one step farther, this led many to conclude that sampling ancient crust is potentially more compelling than trying to sample other materials, given that the highlands represent most of what Mars is made of and likely record first-order processes such as planetary differentiation. In addition, we have virtually no knowledge about what a highland surface looks like, or what processes were dominant during its formation (topics that could be addressed by a Pathfinder landing).

Landing Site Selection Process

Given these general guidelines, the following decisions were made to narrow down the selection. First, all the sites proposed at the first landing site workshop were plotted on the 1:15M geologic maps. All sites above 0 km elevation or outside 10°–20°N latitude (i.e., 5° around the subsolar latitude of 15°N, required for maximum solar power generation) were omitted. If a proposed site fell outside this latitude band, it was moved within the band if the same general geologic unit was available. In addition, a few other sites that are within the engineering constraints and have preferred science attributes expressed at the workshop were added. (Examples are ridged plains and highland sites with low-albedo eolian cover.) All sites within radar stealth regions or with very low thermal inertia (interpreted to be very-low-density dust of considerable thickness with little or no bearing strength) were omitted on obvious safety grounds (e.g., most of Amazonis Planitia). This left about 10 sites that fit all the constraints. These sites were then prioritized into two categories based on science rationale and safety considerations from a preliminary assessment of the Mars Digital Image Mosaic database and surface hazard data (e.g., radar, thermal inertia). The first group includes two grab-bag sites in outflow channels that debouch into Chryse and two highland sites (one with low-albedo eolian cover, one densely covered with valley networks). The second group consists of sites of large uniform material of essentially unknown composition. These sites include other highlands, ridged plains, and young channel/lava sites. Unfortunately, no site provides both a grab bag of ancient Noachian material and dark eolian material.

The top four sites in the first group were carefully evaluated using virtually all available data and models, including Viking images, thermal inertia, rock abundance, albedo, radar, color, occultation data, and weather data from Viking measurements and atmospheric models. [We gratefully acknowledge data and analyses by nonscience team members P. Christensen of Arizona State University (*Christensen and Edgett*, 1994), M. Slade of JPL, and D. Smith and M. Zuber of NASA Goddard Space Flight Center.] All data were presented and discussed at the June 9–10, 1994, meeting of the Mars Pathfinder Project Science Group (*Second PSG Notes and Handouts*, 1994). Final selection was made by a democratic vote of all attending science team members.

Selected Pathfinder Landing Site

Ares Vallis (19.5°N, 32.8°W, –2 km elevation). This site is a grab-bag site with the potential for sampling a variety of Noachian plateau material (a.k.a. ancient crust) as well as Hesperian ridged plains and a variety of reworked materials deposited at the mouth of this large catastrophic outflow channel. It is about as rocky as the Viking sites, but perhaps a bit less dusty (*Golombek et al.*, 1995). This site has clear streamlined islands nearby (Fig. 3) and a very smooth depositional surface at Viking resolution (order 30 m/pixel), except for large (hundreds of meters) hills (Fig. 4). Selection was made contingent on collection and analysis of Earth-

Fig. 3. Regional mosaic showing the Mars Pathfinder landing site (100 km × 200 km landing ellipse shown). The mosaic shows large catastrophic outflow channels debouching into Chryse Planitia. Ares Vallis flowed to the northwest (from the southeast) across the landing site. Tiu Valles is just to the west of Ares Vallis and may also have flowed across the landing area. The landing site itself is a very smooth depositional surface, where the flood waters deposited the sediments carved from the channels. Landing at this location should allow analysis of a wide variety of rock types deposited by the flood. These catastrophic outflow channels on Mars are much larger analogs to the Channeled Scabland in Washington state.

Fig. 4 High-resolution mosaic of the Pathfinder landing site. Ellipse is 100 km × 200 km 90% probability ellipse centered at 19.5°N, 32.8°W. Images are at a scale of about 38 m/pixel. Most of the ellipse is covered by stereo (48° separation angles) at this resolution.

based radar data during the December 1994–April 1995 opposition.

Alternative Sites Identified and Studied

Trouvelot Dark Highlands (12°N, 14°W, 0 km elevation). This is a site extracted from the desire expressed at the workshop to sample ancient highland crust and the desire to sample dark surficial/eolian deposits. The location of the landing ellipse was selected to be entirely within the dark eolian material in Oxia Palus, with reasonably high-resolution Viking images (150 m/pixel) available for much of the site.

Maja Valles Fan (18.8°N, 52°W, –0.5 km elevation). This site is also a grab-bag site with similar sampling opportunities as site 1. A delta/fan is fairly clearly exposed at the location, although the landing ellipse cannot be fit entirely on it. An ancient highland massif just above the fan could improve the likelihood of sampling ancient crustal material.

Maja Highlands (13.5°N, 53°W, 0 km elevation). This site was added because it would sample an ancient highland region cut by a plethora of valley networks. Landing at this site would not only sample the highlands of Mars, but general observations of the local area could help determine whether the valley networks resulted from rain or sapping, which has paleoclimatic implications. Overall the site appears fairly smooth at Viking resolution, except for a number of eroded craters. It is just to the south of the Maja fan/delta site.

Other potential Pathfinder landing sites that were eliminated during the selection process are listed below (in no particular order). All are large uniform sites of unknown composition (except for the Elysium lavas site, which is a large uniform site of known composition).

Dark Hesperian Ridged Plains (14°N, 243°W). This site was added after the workshop to sample the important martian geologic unit known as ridged plains and dark eolian surface material. The site appears smooth in available Viking images, with few wrinkle ridges, giving it a very uncharacteristic appearance for ridged plains.

Marte Vallis (17°N, 176°W). This area was suggested by a number of participants at the conference. At this location Pathfinder would sample either a young channel or young basalts. If it sampled channel material the sediments in the channel would be Hesperian and Amazonian in age.

Hypanis Valley Network (11.5°N, 45.5°W). This site is sort of a hybrid, which includes a grab bag of the local highlands at the mouth of a highland valley network channel system. Rocks are likely to be more locally derived than for a large outflow channel. The site is a fairly smooth depositional surface with some knobby terrain in the eastern part of the ellipse. Unfortunately, high-resolution Viking imagery is not available for this site.

Isidis Planitia (15°N, 275°W). This site was proposed at the workshop to sample late Hesperian plains sediments.

Tartarus Colles (11.5°N, 198°W). This site samples both Hesperian/Noachian material and the dark eolian material. At the available Viking imagery coverage (moderate resolution only) the site appears very rough—a mass of knobs.

Elysium Lavas (13°N, 203°W). This site was proposed to sample known Elysium lava flows. It is also in the dark eolian cover.

Landing Site Validation

Following initial landing site selection in June 1994, work has been going on to validate the landing site. First, the initial Ares Vallis site has been studied in greater detail to provide information on the safety of the site (e.g., *Golombek et al.*, 1995). These data include crater and hill size frequency, albedo, color, thermal inertia, rock abundance, and elevation referenced to an atmospheric surface pressure. In addition, the Ares Vallis site is just to the east of the site initially selected for Viking lander 1. This site was rejected on safety grounds due to Earth-based radar data returns (*Tyler et al.*, 1976) and on imaging data, which showed an unexpectedly complex region at the mouth of this large catastrophic outflow channel (*Masursky and Crabill*, 1976). Only one Viking-era radar track actually has its subradar point within the Ares site (*Downs et al.*, 1978), and these data have low signal to noise, so that the selection of this site was made contingent on acquisition of higher-quality radar data during the recent opposition. Four altimetry mode radar tracks and a single continuous-wave radar track have been collected over the Ares Vallis site and results will be discussed at this meeting (see radar abstracts in this volume). Finally, a series of tests are being performed on critical subsystems involved in landing safely, which will better define the capabilities of these landing systems. Two particularly critical systems include airbag drop tests designed to determine the capability of the airbags to land on large, sharp rocks without catastrophic failure or unacceptable accelerations and altimeter tests designed for determining the ability of the altimeter to deal with steep slopes and rough terrain. After the test results have been obtained and analyzed and the radar data have been reduced and interpreted, a final decision on the landing site will be made by scientists and engineers at a Project Science Group meeting before the end of 1995.

REFERENCES

Christensen P. R. and Edgett K. S. (1994) Physical properties (particle size, rock abundance) from thermal infrared remote observations: Implications for Mars landing sites (abstract). In *Mars Pathfinder Landing Site Workshop*, pp. 19–20. LPI Tech. Rpt. 94-04, LPI, Houston.

Downs G. S., Green R. R., and Reichley P. E. (1978) Radar studies of the martian surface at centimeter wavelengths: The 1975 opposition. *Icarus, 33*, 441–453.

Golombek M., ed. (1994) *Mars Pathfinder Landing Site Workshop*. LPI Tech. Rpt. 94-04, LPI, Houston. 49 pp.

Golombek M. P. (1995) Mars Pathfinder mission and science investigations (abstract). In *Lunar and Planetary Science XXVI*, pp. 475–476. LPI, Houston.

Golombek M. P., Parker T. J., and Moore H. J. (1995) Mars Pathfinder landing site characteristics (abstract). In *Lunar and Planetary Science XXVI*, pp. 481–482. LPI, Houston.

Masursky H. and Crabill N. L. (1976) The Viking landing sites: Selection and certification. *Science, 193*, 809–812.

Rieder R., Wänke H., and Economou T. (1994) Alpha proton X-ray spectrometer (abstract). In *Mars Pathfinder Landing Site Workshop*, pp. 36–37. LPI Tech. Rpt. 94-04, LPI, Houston.

Second PSG Notes and Handouts (1994) *Notes and Handouts from the Second Mars Pathfinder Project Science Group Meeting*, Mars Pathfinder Project, Mail Stop 230-235, Jet Propulsion Laboratory, Pasadena, California.

Seiff A. (1994) Atmospheric structure and meteorology instrument for Mars Pathfinder (abstract). In *Mars Pathfinder Landing Site Workshop*, p. 37. LPI Tech. Rpt. 94-04, LPI, Houston.

Singer R. B. and the IMP Team (1994) Surface science capabilities from IMP spectral imaging (abstract). In *Mars Pathfinder Landing Site Workshop*, pp. 39–40. LPI Tech. Rpt. 94-04, LPI, Houston.

Slade M. A. and Jurgens R. F. (1995) Mars Pathfinder landing site: Implications of Goldstone radar CW and ranging observations (abstract). In *Lunar and Planetary Science XXVI*, p. 1313. LPI, Houston.

Smith P. H. (1994) Imager for Mars Pathfinder (abstract). In *Mars Pathfinder Landing Site Workshop*, pp. 40–41. LPI Tech. Rpt. 94-04, LPI, Houston.

Smith P. H., Britt D. T., Doose L. R., Tomasko M. G., Gliem F., Greeley R., Sullivan R., Keller H. U., Knudsen J. M., and Soderblom L. A. (1995) Update on the Imager for mars Pathfinder (IMP) (abstract). In *Lunar and Planetary Science XXVI*, pp. 1321–1322.

Tyler G. L., Campbell D. B., Downs G. S., Green R. R., and Moore H. J. (1976) Radar characteristics of Viking landing sites. *Science, 193*, 812–815.

Abstracts

ESTIMATES OF THE MAXIMUM AND MINIMUM FLOW VELOCITIES OF THE CIRCUM-CHRYSE OUTFLOW CHANNELS. R. A. Craddock[1] and K. L. Tanaka[2], [1]Center for Earth and Planetary Studies, National Air and Space Museum, Smithsonian Institution, Washington DC 20560, USA, [2]U.S. Geological Survey, Branch of Astrogeology, 2255 N. Gemini Drive, Flagstaff AZ 86001, USA.

The Mars Pathfinder landing site was chosen in part because of its potential to offer investigators the opportunity to analyze a variety of material from different locations [1]. To know what we're getting out of the "grab bag" it is imperative that the detailed geology and hydraulic history of southern Chryse Planitia and the circum-Chryse outflow channel complex be understood ahead of time. Crude estimates of the maximum channel flow velocities can be made simply by knowing the depth and slopes of the outflow channels themselves. Although these characteristics have been derived in part by stereophotogrammetry [2], they are subject to a considerable amount of error, or ~± 1 km in the southern Chryse area [3]. Fortunately some Earth-based radar data exist that are both reasonably accurate and provide the spatial coverage necessary for determining the slopes of some of the channels [4,5]. Using these data, the bed shear stress of a flow, or the retarding stress at the base of a flow, τ_b, can be estimated from the depth-slope formula

$$\tau_b = \rho g h S \qquad (1)$$

where ρ is the density of the fluid, g is gravitational acceleration, h is the flow (or channel) depth, and S is the slope of the channel. This is equal to the bottom stress created by a flow, τ, where

$$\tau = \rho C_f \bar{u}^2 \qquad (2)$$

C_f is a dimensionless drag coefficient and $\bar{u}$ is the mean flow velocity. Thus, the mean flow velocity for a channel can be calculated from

$$\bar{u} = \left(\frac{ghS}{C_f}\right)^{1/2} \qquad (3)$$

The dimensionless drag coefficient can be adjusted for gravity by the expression

$$C_f = g\left(\frac{n^2}{h^{1/3}}\right) \qquad (4)$$

where n is the Manning roughness coefficient (units of $s/m^{1/2}$), which has been derived empirically from terrestrial observations. Application of an appropriate Manning roughness coefficient, n, to martian outflow channels is uncertain, so Robinson and Tanaka [6] used a range of values (0.015–0.035) in estimating the flow velocities of Kasei Valles. Because these values describe most environments free of vegetation, they appear to be reasonable values to apply to the circum-Chryse channels. Estimates of the mean flow velocities were calculated from this method (Table 1); however, at best these represent maximum values. Large-scale geologic mapping indicates that most channels were subjected to multiple episodes of flooding [7–9], which suggests that the channels may not have been completely full of water at any one time (i.e., bankful discharge). This method is also not directly applicable to Simud and Tiu Valles because the Earth-based radar data indicate a positive downslope gradient [4,5], which may be due to modification (e.g., slack-water deposition) postdating channel formation.

TABLE 1. Estimates of channel flow velocities determined from Earth-based-radar-derived measurements of channel depths and slopes.

Valles	Depth (km)	Slope	Roughness coefficient (n)	Flow Velocity $\bar{u}$ (m/s)
Ares	1.0*	−0.0005†	0.015	32.1
			0.025	19.3
			0.035	13.8
Maja	0.6*	−0.0026†	0.015	52.1
			0.025	31.2
			0.035	22.3
Shalbatana	1.7*	−0.0001*	0.015	20.5
			0.025	12.3
			0.035	8.77
Simud	3.01*	+0.0011†	0.015	N/A
			0.025	N/A
			0.035	N/A
Tiu	2.2*	+0.0005†	0.015	N/A
			0.025	N/A
			0.035	N/A

* Data from Downs et al. [4].
† Data from Lucchitta and Ferguson [5].

An alternative method for calculating lower channel flow velocities may be in the thermal inertia data made available by the Viking Infrared Thermal Mapper (IRTM) [10] and the Phobos Thermoskan [11] instruments. These data can be used to estimate the critical shear stress, τ_{cr}, by assuming (1) the effective particle size measured by the IRTM represents the median-sized bed material, D_{50}; (2) the channel bed is planar; (3) the sorting coefficient (standard deviation) is 2.0ϕ, implying that the material is poorly sorted, typi-cal of most gravel-bed streams; (4) the calculated D_{84} particle size was the minimum-sized particle in motion at one time; (5) the density of the material is that of basalt (3.3 g/cm^3); and (6) the fluid that formed Shalbatana Vallis was water at 10°C. The tacit assumption made is that the thermal inertia values measured in the channel represent unmodified channel materials. The validity of this assumption is discussed in general by Betts and Murray [11].

Shields [12] derived empirical relations for the dimensionless grain parameter, ζ_*, and the dimensionless boundary shear stress, τ_*. The dimensionless grain parameter is defined as

$$\zeta_* \frac{D^3(\rho_s - \rho)g}{v^2\rho} \qquad (5)$$

where D is the particle diameter (in this case the D_{84} particle size derived from the thermal inertia data expressed in centimeters), ρ_s is the particle density (3.3 g/cm^3), ρ is the fluid density (water at 10°C or ~1.0 g/cm^3), g is the acceleration of gravity, and v is the kinematic viscosity of the fluid (1.304 × 10^{-2} cm^2/s for water at 10°C). From the assumptions given, ζ_* simplifies to

$$\zeta_* = D^3 \times 5.07 \times 10^6 \text{ cm}^{-3} \qquad (6)$$

From Shields' [12] curve, values for the dimensionless boundary shear stress, τ_*, can be determined. For values of ζ_* less than ~400, Shields extrapolated his curve. Although equation (7) shows that it is unlikely derived values of ζ_* will be <400, White's [13] experimental data can be used to determine values for τ_* in this range. The dimensionless boundary shear stress, τ_*, is

$$\tau_* = \frac{\tau_{cr}}{(\rho_s - \rho) gD} \qquad (7)$$

where τ_{cr} is the critical boundary shear stress needed to initiate sediment motion. This is assumed to be the bottom shear stress, τ_b, during the waning stages of channel formation and can be used to estimate lower values of the channel velocities. The shear velocity, u_* (expressed in centimeters per second), is

$$u_* = \sqrt{\frac{\tau_{cr}}{\rho}} = \sqrt{\frac{\tau_b}{\rho}} \qquad (8)$$

By substituting equation (1) for τ_b, equation (9) becomes

$$u_* = \sqrt{ghS} \qquad (9)$$

which also allows the depth (h) of the water in the channel during the low flood stages to be determined. This depth should be much less than the full depth of the channel.

As Komar [14,15] notes, it is better to analyze the flow in terms of u_* than $\bar{u}$ due to the uncertainties in estimating reasonable values for C_f. However, values of $\bar{u}$ are more intuitive. These can be calculated from the following relationship.

$$\bar{u} = \sqrt{C_f u_*} = g^{1/2} n h^{-1/6} u_* \qquad (10)$$

TABLE 2. Estimates of channel flow velocities determined from thermal-inertia-derived measurements of channel-effective grain sizes.

Valles	Thermal Inertia	D_{85} (cm)	n	ζ_* (× 10^6)	τ_*	Flow Velocity $\bar{u}$ (m/s)	Flow Depth¶ (m)
Ares	9.0*	0.28	0.015	1.4	0.052	0.51	0.67
			0.025			0.85	
			0.035			1.19	
Maja	N/A						
Shalbatana	9.0†,‡	0.28	0.015	1.4	0.052	0.39	3.34
			0.025			0.65	
			0.035			0.91	
Simud	8.4†,‡	0.24	0.015	1.2	0.052	0.55	0.25
			0.025			0.91	
			0.035			1.27	
Tiu	10.8†,‡	0.40	0.015	2.0	0.054	0.58	0.99
			0.025			0.97	
			0.035			1.36	

* Data from Henry and Zimbelman [16].
† Data from Craddock [10].
‡ Data from Betts and Murray [11].
¶ Derived from equations (8–10).

Of course, in order to estimate values of $\bar{u}$ from the thermal-inertia-derived values of u_*, reasonable values of the Manning coefficient, n, must be used. Obviously these should be the same range of values used to determine the channel flow velocities at bankful discharge (0.015–0.035). Table 2 lists the possible channel flow velocities and depths determined from the available thermal inertia data. They represent minimum estimates because the material contained on the surface of the channel floors, if unmodified, was probably emplaced during the waning stages of flooding. Actual channel flow velocities probably fall between the two values presented in Tables 1 and 2.

Acknowledgments: This research is supported in part by NASA grant NAGW-3365 (Smithsonian Institution).

References: [1] Golombek M. P. (1995) *LPS XXVI*, 475–476. [2] U.S. Geological Survey (1991) Map I-2160 1:15M-scale. [3] Wu S. S. C. and Howington-Kraus A. (1988) *NASA TM 4041*, 551. [4] Downs G. S. et al. (1982) *JGR, 87*, 9747–9754. [5] Lucchitta B. K. and Ferguson H. M. (1983) *Proc. LPSC 13th*, in *JGR, 88*, A553–A568. [6] Robinson M. S. and Tanaka K. L. (1990) *Geology, 18*, 902–905. [7] Chapman M. G. and Scott D. H. (1989) *Proc. LPSC 19th*, 367–375. [8] DeHon R. A. and Pani E. A. (1992) *Proc. LPS, Vol. 22*, 63–71. [9] Craddock R. A. et al. (1993) *LPS XXIV*, 335–336. [10] Craddock R. A. (1988) M.S. thesis, Arizona State Univ., 110 pp. [11] Betts B. H. and Murray B. C. (1994) *JGR, 99*, 1983–1996. [12] Shields A. (1936) U.S. Dept. Agriculture, Soil Conservation Service Coop. Lab., Calif. Inst. Tech, 26. [13] White S. J. (1970) *Nature, 228*, 152–152. [14] Komar P. D. (1979) *Icarus, 37*, 156–181. [15] Komar P. D. (1980) *Icarus, 42*, 317–329. [16] Henry L. Y. and Zimbelman J. R. (1987) Papers Presented at the Third Annual Summer Intern Conf., LPI, 13–14.

GEOLOGIC MAPPING TRAVERSE OF THE HIGHLAND-TO-LOWLAND TRANSITION IN AN AREA ADJACENT TO THE MARS PATHFINDER REGION.

L. S. Crumpler, Department of Geological Sciences, Brown University, Providence RI 02912, USA.

Introduction: Mapping in the region between Central Chryse Planitia and Xanthe Terra is of relevance to understanding the Ares Vallis region because (1) it is the closest area to the proposed Pathfinder landing site for which regional 1:500,000-scale mapping and local ground-surface geologic characteristics have been determined (Fig. 1); (2) it traverses a region of the highland-lowland transition at a similar latitude and in an area of similar overall geologic units as the Pathfinder site; and (3) in contrast to the proposed landing site in Ares Vallis, it represents a portion of the Chryse Basin margin that is relatively little modified by outflow channels, and thus offers the opportunity to establish the nature of the regional surface in the transition as it might have appeared prior to Ares Vallis outwash. Thus, detailed mapping in this region is important to both the characterization of the highland-to-lowland transition in a region of extensive fluvial deposition and erosion, and to making educated inferences about the regional substrate geology of the Mars Pathfinder site.

Objectives: *Geotraverse mapping.* This work builds on mapping recently completed in central Chryse Planitia in the vicinity of Mutch Memorial Station (MMS or VL-1) from central Chryse Planitia southward onto the Noachian highlands (MTM 15047, 10047, and 05047 1:500,000-scale photomosaic sheets) in an effort

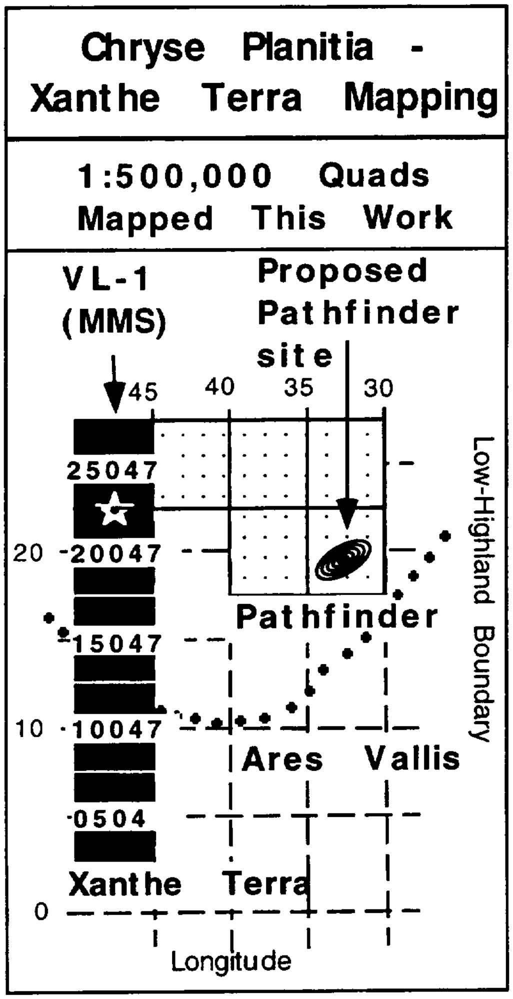

Fig. 1. Area previously mapped in central Chryse Planitia (solid boxes). The proposed Mars Pathfinder site is located several hundred kilometers to the east in a similar regional setting, but the Xanthe-Chryse transect may preserve substrate geologic characteristics that were originally present in the Ares Vallis area prior to outwash effects. Approximate location of highland-lowland boundary as mapped by Scott and Tanaka [4] is shown as a sinuous dashed line.

to extend our detailed surface geologic knowledge outward from the Viking Lander 1 site, where we have actual ground truth, to surrounding geologic units. The approach taken by stacking three 1:500,000-scale quadrangles [1,2] is that of a geologic traverse along a relatively narrow corridor (transect or geotraverse) at a large map scale from a relatively young but typical surface in a lowland region to the complex and older surface of an adjacent highland. The goal is a geologic cross section across the lowland-to-highland boundary in an area where the transition is both topographically and geologically relatively gradual in comparison with many other localities around the margins of Chryse Planitia.

Regional setting. The oldest map units are Noachian to Hesperian surface materials near the southern edge of Chryse Planitia. These continue northward where they are overlain in central Chryse Planitia, in the vicinity of MMS, by younger ridged plains that are interpreted to be outwash deposits from Maja Vallis to the west [1,2]. Hesperian ridged plains are among the oldest post-Noachian materials exposed in the highland-lowland boundary regions, and the large exposure here in southern Chryse Planitia affords an opportunity to assess some characteristics of this surface prior to outwash deposition and surface scouring. The highland-lowland boundary strikes approximately northwest-southeast across the center of the map area. At 1:500,000 scale the actual contact between the Hesperian ridged plains and the highland material appears transitional in character, as numerous low hills or knobs, possibly residuals of cratered highland material, protrude through the ridged plains unit. Similar low knobs occur in the central basin east of MMS within the 1:500,000-scale quads connecting this area with the Pathfinder region.

Numerous mare-type ridges, generally interpreted to be the result of small amounts of shortening and compression [5,6], occur on the Hesperian plains. Some arcuate arrangements of maretype ridges, near the highland-lowland boundary within the Hesperian plains, are clearly superimposed on the buried rims of large highland craters. This observation implies that the highland surface may be preserved to some extent beneath the adjacent plains materials.

Several sinuoustype channels (Hypanis and Nanedi Valles) trend southwest to northeast within the highland part of the proposed map area. High-resolution images across one of these affords the opportunity to map this channel in detail and an assessment may be made of the local evidence for the origin and modification of this type of channel. Bends in Mars sinuous channels are frequently characterized by circular or constant radius curvature in contrast to the more asymptotic curvature of river meanders on Earth. This might suggest that factors in addition to normal stream dynamics, such as variation in material properties resulting from the probable brecciated or cratered nature of the highlands, among other environmental influences (re-used lava channels), may have exerted a control on the sinuosity [7].

Summary: Several questions of regional, local, and topical significance to the Pathfinder site can be addressed through mapping the Xanthe Terra to Chryse Planitia traverse: What is the geologic history and stratigraphy of the transitional boundary between the highlands and lowlands throughout this region [8]? What is the origin of the numerous knobs within the transitional region; are they residual highland materials? What evidence is there for the origin and the nature of the emplacement of the Hesperian ridged plains? What are the gradients in thickness of the Hesperian ridged plains material at the boundary, and what might these tell us about the underlying gradients of the highland surface? Are the surfaces of the intercrater highland plains the same material that forms the lowland plains? If not, why are the crater ages similar? What is the regional geologic section and how does it relate to the regional topographic characteristics? And finally, what is the evidence for the origin of the highland-lowland boundary in this region and can it test theories [3] of the origin of the global dichotomy?

References: [1] Crumpler et al. (1995) 1:500,000 scale Misc. Inv. Geol. Map, USGS, in preparation. [2] Craddock R. A. et al. (1992) *LPS XXIII*, 257–258. [3] McGill G. E. and Squyres S. W. (1991) *Icarus, 93*, 386–393. [4] Scott D. H. and Tanaka K. L. (1986) USGS, 1:15,000,000 Series, Atlas of Mars, Western Region, 1-1 802A. [5] Plescia J. B. and Golombek M. P. (1989) *LPI Tech Rpt. 89-04*, 64–65. [6] Watters T. R. (1988) *JGR, 93*, 10236–10254. [7] Mars Channel Working Group (1983) *GSA Bull., 94*, 1035–1054; Rotto S. and Tanaka K. (1993) USGS Misc. Inv. Map 1-2441.

AFTER THE FLOOD: A PREVIEW OF EOLIAN FEATURES AT THE MARS PATHFINDER LANDING SITE IN ARES VALLIS.
K. S. Edgett, Department of Geology, Arizona State University, Box 871404, Tempe AZ 85287-1404, USA.

After the last floods poured through Ares Vallis, wind was the main sedimentary agent at work in the Mars Pathfinder landing site region. Based upon field observations of the Ephrata Fan, a major flood deposit in the Channeled Scabland of Washington, it appears likely that wind should have reworked the fine sediment that was left after the Ares floods, while other sediments, especially airborne dust, were deposited in the area. On the Ephrata Fan, flood-deposited sand was reworked by wind to form dunes [1], and where sand was not present, windborne silt and volcanic ash accumulated between rocks [2].

Relative to the Viking landers, Mars Pathfinder is very well suited to study eolian features. The origin and physical nature of some eolian landforms at the Viking lander sites remain unresolved. For example, the particle size of sediments in the drifts at the Viking 1 site is undetermined [3,4]. Because of its stereo/multispectral imaging [5] and microrover capabilities, Mars Pathfinder might resolve similar puzzles in Ares Vallis. If Viking 1 had had the microrover, it could have driven out to the nearby drifts and determined (1) if the drifts have cross beds, (2) if the drifts are cohesive and/or cemented sand or dust, (3) if features identified as sand ripples [4] were such, and (4) if all the drifts are dark with bright red coatings, as suggested by the presence of one low-albedo drift [4]. If Viking 2 had had a microrover, its tiny cameras could have been used to determine whether ripples in nearby troughs [6] consisted of granules (2–4-mm sizes) [4]. Finally, if the Vikings had had Mars Pathfinder's multispectral imaging ability [5], some information about the mineralogy of eolian deposits could have been obtained.

Albedo, thermal inertia, and rock abundance offer clues to the nature and distribution of eolian debris [7]. In a global context, the Ares landing site has an intermediate albedo and thermal inertia [8–10]; it is not dust covered like Arabia, nor is it sandy like the north polar sand sea. Rock abundance at the Ares site is similar to the Viking 1 site, but the albedo is slightly lower and the thermal inertia is slightly higher [9,10]. Thermal and albedo properties of the landing ellipse change from east to west, with darker surface materials (probably sand) occurring in the northeast near the margin of Acidalia [10]. The low-albedo Acidalia Planitia is thought to be rocky with sand in the form of sand sheets or drifts [7,8]. The dark sands of Acidalia are probably mobile and moving slowly into the northeast end of the Ares Vallis landing ellipse.

Mars Pathfinder's wind sock experiment and meteorological station should provide information about eolian events that occur during the mission. The July 1997 landing corresponds to L_s 141°, or mid-northern summer. Northern summer should be the least windy season, according to GCM work [11]. Little eolian activity is to be expected during the 30-day primary mission; the strongest winds (needed to move sediment) typically occur during the seasons that have the strongest annual winds (late northern autumn through winter) [12].

No eolian dunes will be found at the Ares landing site; none are observed in Viking orbiter images. It is possible, however, that dark sand might be accumulated in eolian drifts and/or granule ripples, particularly in the eastern half of the landing ellipse. The two fields of small "crater clusters" [13] within the landing ellipse have dark material surrounding them. This dark material must be sandy to have maintained a low albedo over time, and might be (1) sand-sized impact glass [14] or (2) an indicator that the craters penetrated to a lens of flood-deposited sand.

Like on the Ephrata Fan of Washington, the Ares site is probably located in a rocky or gravelly facies [15]. The site has probably accumulated some airborne dust, forming a discontinuous mantle between rocks like at the Viking 1 site. The light-toned "etched terrain" [16] just outside the southwest end of the landing ellipse might be eolian scoured, similar to features Sharp [17] described elsewhere on Mars. If so, then the southwestern part of the landing ellipse might have small eolian deflation pits and/or remnant knobs and mesas. Other features, like ventifacts or pitted rocks, might be found, but their presence is difficult to predict.

The Mars Pathfinder landing site in Ares Vallis is not likely to be a vigorously active eolian environment, but may be more active than the Viking lander sites. The Mars Pathfinder site is probably most similar to the Viking 1 site, although with somewhat more windblown sand. The new capabilities of Mars Pathfinder will allow more detailed investigation of eolian features, giving new clues about the particle sizes and compositions of eolian sand and dust. In turn, Mars Pathfinder offers a chance to re-interpret the geology of the Viking lander sites, provided that there are features similar to those seen by Viking 1 or 2.

References: [1] Petrone A. (1970) M.S. thesis, Washington State Univ., Pullman, Washington. [2] Edgett K. S. field notes, 1990–1995. [3] Mutch T. A. et al. (1976) *Science, 193,* 791–801. [4] Sharp R. P. and Malin M. C. (1984) *GSA Bull., 95,* 1398–1412. [5] Reid R. J. and Singer R. B. (1995) *LPS XXVI,* 1155–1156. [6] Mutch T. A. et al. (1977) *JGR, 82,* 4452–4467, Fig. 6a. [7] Christensen P. R. and Moore H. J. (1992) in *Mars* (H. H. Kieffer et al., eds.), 686–729, Univ. of Arizona, Tucson. [8] Arvidson R. E. et al. (1989) *JGR, 94,* 1573–1587. [9] Golombek M. P. et al. (1995) *LPS XXVI,* 481–482. [10] Edgett K. S., this volume. [11] Greeley et al. (1993) *JGR, 98,* 3183–3196. [12] Edgett K. S. and Blumberg D. G. (1994) *Icarus, 112,* 448–464. [13] Greeley R. et al. (1977) *JGR, 82,* 4093–4109. [14] Schultz P. (1994) *Eos Suppl., 45,* 406. [15] Rice J. W. and Edgett K. S., this volume. [16] Parker T. J., this volume. [17] Sharp R. P. (1973) *JGR, 78,* 4222–4230.

VIKING IRTM OBSERVATIONS OF THE ANTICIPATED MARS PATHFINDER LANDING SITE AT ARES VALLIS.
K. S. Edgett, Department of Geology, Arizona State University, Box 871404, Tempe AZ 85287-1404, USA.

Albedo, rock abundance, and thermal inertia derived from Viking Infrared Thermal Mapper (IRTM) observations provide some insight as to the nature of the surface materials that occur at the Ares Vallis landing site [1,2]. Observations of the Ares Vallis site are compared here with the Viking 1 and 2 lander sites, which offer some measure of "ground truth."

Moderate-resolution (30–60-km-sized areas) observations are the best available for the Ares Vallis site, and include an IRTM-derived albedo map (1° latitude/ longitude bins) compiled by Pleskot [3], thermal inertia (0.5° bins) from Christensen and Malin [4,5], and rock abundance and fine-component thermal inertia maps (1° bins) derived from IRTM data by Christensen [6].

In the landing ellipse, albedo ranges from about 0.19 to 0.23 and is generally lower at the eastern end of the landing ellipse, higher toward the west. The comparable albedo at the Viking lander sites is about 0.25 at both.

Thermal inertia, computed using the Kieffer thermal model [7] with the "2% assumption" (wherein the atmospheric contribution to downgoing radiation is 2% of the maximum solar insolation) varies between 410 (9.8) and 540 (12.9) J m^{-2} $s^{-0.5}$ K^{-1} (10^{-3} cal cm^{-2} $s^{-0.5}$ K^{-1}). (Note that both S.I. units and commonly used "Kieffer" units for thermal inertia are given here; the latter is in parentheses). In general, thermal inertia is higher at the eastern end of the landing ellipse and lower toward the west. For comparison, the Kieffer model thermal inertia of the Viking 1 site is about 360 (8.5) and for Viking 2 is about 330 (7.9).

Rock abundance, a parameter derived from thermal inertia and differences in temperature at 7, 9, 11, and 20 µm, ranges from about 25% at the east end of the ellipse down to about 18% at the west end. The uncertainty here is on the order of 5% to 10% rocks [6]. Modeled rock abundance at the Viking 1 site is about 15 ± 5%; at Viking 2 it is 20 ± 10% [8]. The rock abundances estimated for the Ares Vallis landing ellipse are similar to the rock abundances of the two Viking lander sites. The corresponding fine-component (Kieffer model) thermal inertia, a by-product of the rock abundance modeling, is about 350 (8.4) to 460 (10.9) from west to east in the Ares landing ellipse, as opposed to 300 (7.1) and 260 (6.2) for the Viking 1 and 2 sites, respectively.

A search was conducted for high-resolution (2–5-km-sized areas) IRTM observations of areas within the Ares Vallis landing ellipse. One Viking orbiter track meeting appropriate search criteria (spacecraft range ≤2500 km, emission angle ≤60°, L_s = 350°–115°, hour 0–6) was found to pass about 200 km to the north of the landing ellipse; the thermal inertias there were consistent with the moderate-resolution results, but allowed a more detailed map along the orbiter's flight path. Unfortunately, no such IRTM data were found to pass through the Ares landing ellipse. One daytime (10–14 h) high-resolution IRTM track from Viking 2 was found, but accurate computation of thermal inertia is problematic for daytime data. In general, this track indicates thermal inertias similar to those in moderate resolution.

Lately there has been considerable discussion about the uncertainty in thermal inertia derived under the relatively dusty atmosphere of the Viking era [9–13]. Hayashi et al. [10], using the Haberle-Jakosky coupled surface-atmosphere model approach [9], note that the Kieffer model thermal inertias for the Viking 1 and Viking 2 sites are about 60–80 (1.4–1.9) thermal inertia units too high. The corresponding range of thermal inertias for the Ares Vallis site would also drop by about 100 (2.4) units, thus ranging from about 310 (7.4) in the west to 440 (10.5) in the east. The general trend from higher thermal inertia in the east to lower in the west remains unchanged. From the conclusions of Hayashi et al. [10], it seems that the fine-component thermal inertias (by-product of rock abundance) for the Ares landing ellipse would drop by about 90 (2.2) units, to range from 260 (6.2) in the west to 370 (8.8) in the east.

The Ares Vallis landing site has the potential for being somewhat different from the two Viking lander sites. However, the differences might turn out to be as subtle as the differences observed when one compares the two Viking sites. The Ares site in general is not radically different from the previous sites; this may turn out to be helpful for reinterpretation of the geology of the Viking sites. In general, the Ares site is about as rocky as the two Viking sites, but the somewhat lower albedo and higher fine-component thermal inertias suggests there might be more sand (or at least, less dust) at the Ares site. The fine-component thermal inertias suggest effective particle sizes in the medium to medium-coarse sand range (300–600 µm) throughout the region; this assessment is consistent with new thermal conductivity results from Presley [14]. The east-to-west variation in thermophysical properties might indicate that there are coarser deposits of sediment at the eastern end of the landing ellipse. It seems likely that the landing site will look less like the Viking 1 and 2 sites if Mars Pathfinder touches down at the eastern end of its landing ellipse. The implications for eolian features that might occur at the landing site are discussed elsewhere [15].

References: [1] Golombek M. P. et al. (1995) *LPS XXVI*, 481–482. [2] Edgett K. S. (1995) *LPS XXVI*, 353–354. [3] Christensen P. R. (1988) *JGR, 93*, 7611–7624. [4] Christensen P. R. and Malin M. C. (1988) *LPS XIX*, 180–181. [5] Christensen P. R. and Malin M. C. (1993) *LPS XXIV*, 285–286. [6] Christensen P. R. (1986) *Icarus, 68*, 217–238. [7] Kieffer H. H. et al. (1977) *JGR, 82*, 4249–4291. [8] Christensen P. R. (1982) *JGR, 87*, 9985–9998. [9] Haberle R. M. and Jakosky B. M. (1991) *Icarus, 90*, 187–204. [10] Hayashi J. N. et al. (1995) *JGR, 100*, 5277–5284. [11] Paige D. A. et al. (1994) *JGR, 99*, 25959–25991. [12] Edgett K. S. and Christensen P. R. (1994) *JGR, 99*, 1997–2018. [13] Bridges N. T. (1994) *GRL, 21*, 785–788. [14] Presley M. A. (1995) Ph.D. dissertation, Arizona State Univ., Tempe, 237 pp. [15] Edgett K. S., this volume.

SIZE-FREQUENCY DISTRIBUTIONS OF ROCKS ON MARS.

M. Golombek and D. Rapp, Jet Propulsion Laboratory, California Institute of Technology, Pasadena CA 91109, USA.

Predicting the size-frequency distribution of rocks at different locations on Mars is difficult owing to the limited dataset (ground truth from only two sites at the surface), but is critical for determining potential landing hazards for future Mars landers. In this abstract we (1) review rock frequency data at the two Viking landing sites and a variety of sites on Earth, with special reference to larger rocks that could be hazardous to a lander, (2) describe the data in terms of simple mathematical expressions, and (3) provide a means of extrapolating the data to any location on Mars from relationships between the rock frequency curves and remote sensing data.

We used rock lengths, widths, and heights carefully measured from the stereo Viking landing images by Moore and co-workers [1] consisting of a total of 421 and 486 rocks in areas of 83.7 m^2 and 83.76 m^2 at the Viking 1 and 2 sites (VL 1, VL 2) respectively. The rock data plotted in either cumulative number per square meter or cumulative fractional area vs. diameter have similar shapes at both Viking sites, displaying a convex up-curved shape on log-log plots that can be fit well with simple exponential functions. The rock data do not appear linear on log-log plots, so that power-law functions (commonly used to fit crater size-frequency data) overestimate the frequency and fractional area covered by both large-diameter and small-diameter rocks (Fig. 1).

Similar shaped size-frequency distributions of rocks are found at a wide variety of rocky surfaces on the Earth (Fig. 1). Data collected by Malin [2] for (1) Icelandic catastrophic outflow deposits, (2) Antarctic dry valley wall talus, and (3) Hawaiian volcanic ejecta, as well

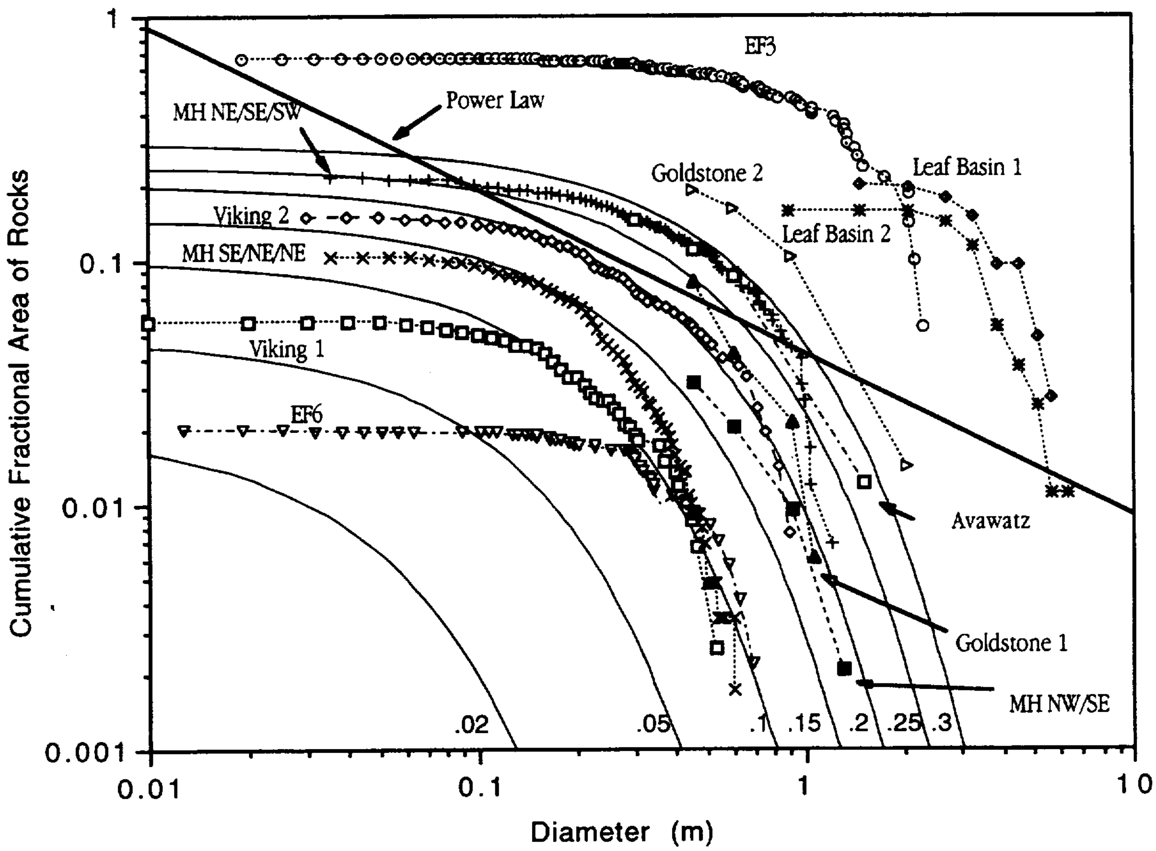

Fig. 1. Cumulative fractional area covered by rocks vs. diameter for each rock at VL 1 and 2, Mars Hill sites (MH), Ephrata Fan sites (EF), and highly binned data (only 4–5 data points) from a variety of surfaces on the Earth. Power-law distribution suggested for VL 2 [1] also shown. Solid curves are the rock distributions predicted for various rock abundances (2–30%) on Mars derived from a combined exponential fit to VL 1 and 2. Sites on the Ephrata Fan, a depositional fan in the Quincy Basin of the Channeled Scabland, and potentially analogous to the Pathfinder landing site in Ares Vallis, Mars, include one with extreme rock coverage (70%), near the field trip stop in Rocky Ford Creek and another with 2% rock coverage.

as data we have collected from (4) Mars Hill, (5) an abandoned and washed alluvial fan in Death Valley, (6) a presently active alluvial fan on the eastern side of the Avawatz Mountains in the Mojave Desert, (7) two eroded and mass-wasted volcanic surfaces (basalt and tuff breccia) in the Eastern Mojave Desert (Goldstone), (8) catastrophic outflow deposits of the Ephrata Fan in Washington state, and (9) a giant boulder field in the Leaf Basin of northern Quebec, in which boulders are transported downslope and washed in an intertidal zone [3], all show convex up-curved size-frequency rock distributions on a log-log plot. Data from these sites have all been fit reasonably well with simple exponential functions, which describe both the precipitous drop-off in rocks with large diameters as well as the shallowing in cumulative number or area of rocks at small diameters.

The VL 2 site is believed to be ejecta from the nearby crater Mie [4], whereas VL 1 is believed to be a partially covered and eroded lava flow surface, possibly with some local crater ejecta and flood deposits [5]. As a result, they appear to have formed by very different geologic processes, yet the shape of the rock size-frequency distributions at both sites are the same. The sites on Earth include alluvial fan water-rich debris flows (active and abandoned), catastrophic flood deposits, eroded volcanic surfaces, volcanic ejecta, and talus slopes, yet the rock size-frequency distributions are all similarly shaped. All sites show a precipitous fall-off in number or fractional area of rocks at large diameters, which may have something to do with the dearth of large coherent blocks of material and the inability of geologic processes to transport such large blocks without breaking them into smaller pieces.

The consistency of the size-frequency rock distributions found on Earth and the two Viking landing sites suggests that similar shaped rock size-frequency distributions are applicable to other areas on Mars. A combined fit to both VL cumulative fractional area of rocks vs. diameter data was made with a general exponential function of the form $F_k(D) = k \exp\{-q(k)\ D\}$, in which $F_k(D)$ is the cumulative fractional area covered by rocks of a given diameter or larger, k is the total area covered by rocks at the site, and $q(k) = (0.571 + 0.492/k)$. Simple linear height vs. diameter relationships, related to k, $H = (0.25 + 1.4\ k)\ D$, were also derived from H/D ratios of ~3/8 and ~1/2 at VL 1 and 2 respectively, which suggest that less rocky areas on Mars have rocks with lower H/D ratios than more rocky areas. Height was then substituted into the general exponential function derived for diameter, which yielded $F_k(H) = k \exp\{-p(k)\ H\}$ and $p(k) = (0.571 + 0.492/k)/\{0.25 + 1.4\ k\}$, which describes the cumulative fractional area of rocks vs. height for any given total rock coverage.

Viking thermal inertia measurements and models developed by

Christensen [6] have been used to estimate the fractional surface area covered by high thermal inertia rocks greater than about 10 cm diameter vs. smaller particles, such as sand and dust, with low thermal inertia for 1° latitude by 1° longitude remotely sensed areas on Mars. Because the cumulative fractional area covered by rocks of 10 cm diameter and larger is fairly close to the total rock coverage, it can be used as the pre-exponential constant k in the general exponential function fit to the VL rock data to describe the cumulative fractional area vs. diameter or height at any location on Mars. This calculation is conceptually equivalent to Christensen and Malin's [7] suggestion that rock abundances on Mars reflect the thickness of mantling fine material. In this simple model, the maximum rock abundances (~30%) occur in areas with no mantling sand or dust, and less rocky areas (down to 2%) are mantled by progressively greater thicknesses of dust (up to 1 m thick). The exponential curves in Fig. 1 show these distributions in terms of cumulative area vs. diameter for any value of rock abundance, and the equations derived above show the decrease in H/D for less rocky areas.

Results indicate that most of Mars is rather benign with regard to hazards from landing on large rocks. Roughly 50% of Mars has rocks covering only 8% or less of its exposed surface [6]. For total rock coverage of 8% analogous to VL 1, about 0.2% of the surface is covered by 20 cm or higher rocks. A surface covered with 12% rocks has only 1% of its surface area covered by rocks higher than 20 cm. The Mars Pathfinder lander airbag system is being designed to accommodate landing on 0.5-m-high boulders. Such a landing system could land on a surface covered by about 20% rocks, similar to VL 2, with 1% of the surface covered by rocks of 0.5 m or higher. Surfaces with 20% or fewer rocks account for over 90% of the surface of Mars, so that such a landing system could be sent to all but the rockiest 10% of Mars with a low probability of landing on a ≥0.5-m-high rock. The Ares Vallis landing site being considered for Mars Pathfinder has total rock abundances of ~20% [8], indicating a low probability of failure due to landing on large rocks.

References: [1] Moore and Keller (1990) *NASA TM-4210*, 160; 1991, *NASA TM-4300*, 533. [2] Malin (1989) *NASA TM-4130*, 363. [3] Lauriol and Gray (1980) *G. Soc. Can., Pap. 80-10*, 281. [4] Mutch et al. (1977) *JGR, 82*, 4452. [5] Binder et al. (1977) *JGR, 82*, 4439. [6] Christensen (1986) *Icarus, 68*, 217. [7] Christensen and Malin (1993) *LPSC XXIV*, 285. [8] Golombek et al., this volume.

CHARACTERISTICS OF THE MARS PATHFINDER LANDING SITE.

M. P. Golombek[1], T. J. Parker[1], H. J. Moore[2], M. A. Slade[1], R. F. Jurgens[1], and D. L. Mitchell[1], [1]Jet Propulsion Laboratory, California Institute of Technology, Pasadena CA 91109, USA, [2]U.S. Geological Survey, Menlo Park CA 94025, USA.

The preliminary landing site selected for Mars Pathfinder and a candidate for final validation is at the mouth of Ares Vallis in southeastern Chryse Planitia (19.5°N, 32.8°W) [1]. Ares Vallis is a large outflow channel that drained the highlands to the southeast. The region contains large streamlined islands of older plateau materials and smooth outflow deposits in the channels. Many of the streamlined islands have terraces that may represent layering, downcutting stages during flooding, or both. Linear features extending downstream from many of these islands may be longitudinal grooves [2] or other primary flow features, indicating a surface composed of materials deposited by the floods. Potential source materials for the outflow deposits include ancient Noachian crustal units (Npl_1, Npl_2), Hesperian Ridged Plains (Hr), and a variety of reworked channel materials (Hcht, Hch, Hchp). The 100 × 200 km landing ellipse is located on a broadly undulating, level surface between (1) streamlined islands and knobby terrain to the east, (2) large streamlined islands to the south, (3) large fresh impact craters to the north, and (4) scabby or etched terrain to the west (Fig. 1). Scabby or etched terrain appears rough in high-resolution images (~40 m/pixel), with 10–30-m-high scarps that may have resulted from fluvial plucking or eolian deflation [3]. Portions of the landing site are peppered with secondary craters with dark rims of either excavated or partly buried low-albedo material; morphologies of the secondaries indicate a primary or source crater to the south.

Crater counts in the landing ellipse indicate a Late Hesperian age [4] with a –2 power-law size-frequency distribution and 2419 craters ≥1 km diameter, 445 craters ≥2 km diameter, 64 craters ≥5 km diameter, all normalized per million square kilometers. The following numbers of craters lie within the 15,700 km^2 landing ellipse: 49 <0.5 km in diameter, 38 between 2 and 3 km in diameter, and part of one 10-km-diameter crater. There is about a 3% chance of landing within a crater at this site.

Within the landing ellipse there are approximately 275 small hills that range from 60 m (which is close to the resolution limit) to 7 km in diameter, although most are <1 km in diameter. Some streamlined islands have concentrations of hills on their downstream sides, which suggests that they were carried as bedload during flooding and deposited where flow velocities decreased; flow reconstruction calculations, however, suggest a maximum boulder of only 10 m diameter could have been carried [2]. Cumulative frequencies of hills within the landing ellipse roughly fit a –1.6 power-law size-frequency distribution between diameters of 0.2 and 1 km. There are 828 hills ≥1 km diameter, 382 hills ≥2 km diameter, and 64 hills ≥5 km diameter (all normalized per million square kilometers). The actual number of hills in the landing ellipse ≥0.25 km diameter is 168, with 62 hills ≥0.5 km diameter, 13 hills ≥1 km diameter, 6 hills ≥2 km diameter, and 1 hill ≥5 km diameter. Photoclinometry (symmetric method) was used to estimate the heights and slopes of 12 hills. Results indicate most hills have overall slopes of about 10°, with maximum local slopes up to 25°. A general relationship exists between hill diameter and height $h = -33.2 + 0.15d$, where h is height and d is diameter ($r = 0.86$). There is about a 1% chance of landing on a hill at this site.

Albedo, color, thermal inertia, and rock abundance suggest that the Ares Vallis landing site shares many of the same characteristics as the Viking landing sites. A combined albedo, thermal inertia (reported in 10^{-3} cgs units), and rock abundance dataset kindly provided by Christensen [5] was used in our evaluation of the landing site. Albedo varies from 0.19 to 0.23 (1° bin data [6]), thermal inertia varies from 9.8 to 12.9 (0.5° bin data [7]), fine-component thermal inertia varies from 8.4 to 10.9 (1° bin data [8]), and rock abundance varies from 18% to 25% (1° bin data [9]) over the Pathfinder landing ellipse. For comparison, the Viking 1 and 2 landing sites have values of rock abundances of 16% and 23%, albedos of 0.25, thermal inertias of 8.4 and 7.8, and fine-component thermal inertias of 7.1 and 6.2 respectively. Red (0.155–0.187) and violet (0.058–0.079) radiances of the Ares landing site using Viking orbiter frames in the 344S series yield an average red-to-violet ratio of 2.3 (range: 2.05–2.95); Viking lander 1 red (0.165–0.184) and violet (0.062–0.071) radiances yield an average red-to-violet ratio of 2.6 (range: 2.4–2.8), derived from the same orbiter images. The lower albedo, lower red-to-violet ratios, greater rock abundances, and higher thermal inertias for the Ares Vallis site suggest a slightly rockier and less dusty surface than the Viking landing sites.

Surface materials at the Ares Vallis site should be similar to those at the Viking landing sites [10]. Color radiances and their ratios suggest a variety of materials that include cohesive soil-like materials, dust, and coated and uncoated rocks [11]. Rather high fine-component thermal inertias also suggest that cohesive soil-like materials, compatible with successful landing and roving, dominate the surface, with less low-cohesion, low-strength drift material prevalent at the Viking lander 1 site. Rock abundance estimates suggest ample rocks are present and available for analysis with the imaging system and the rover-mounted alpha proton X-ray spectrometer.

In contrast with the weak radar echoes received during 3.5-cm wavelength observations for the Viking mission in 1976 [12], strong radar echoes were received from the site during 3.5-cm wavelength Goldstone observations in early 1995. Preliminary analysis of selected delay-Doppler echoes with subradar points between 19.7°and 20.2°N and 31.1° and 34.6°W yields rms slopes of 4.6° ± 0.7° and normal reflectivities of 0.057 ± 0.008. Continuous-wave (CW) echoes with subradar points along 18.7°N between 31.9° and 34.6°W yield an rms slope of 6.4° ± 0.7° and the following cross sections: total polarized –0.101, quasispecular –0.048, polarized diffuse –0.053, and depolarized –0.020. A conservative estimate for the experimental uncertainty in these CW cross sections is ~25%.

Preliminary comparisons with CW observations at the same wavelength in the southern hemisphere imply that the surface of the Ares site may be rougher at a scale of 0.4–10 m (rms slope 6.4° ± 0.7°) and has reflectivities (about 0.058 when integrated from 0° to 30° [13]) that are comparable to or smaller than averages in the south. At these southern latitudes [14], average rms slopes are 4.04° ± 1.47° (1988 data) and 4.25° ± 0.71° (1990 data) with average reflectivities of 0.0603 ± 0.0296 (1988 data) and 0.1062 ± 0.0175 (1990 data). Diffuse echo strengths and their ratio are more or less normal at the Ares site; spectra show little or no unusual structure. Delay-Doppler reflectivities (0.057 ± 0.008) are consistent with dry soil-like materials with poorly constrained bulk densities of 1.3 ± 0.3 g/cm^3 [15]. Bulk densities such as these indicate a surface that is consistent with our interpretations of the remote sensing data described above—namely a surface compatible with successful landing and roving, with less of the drift material present at the Viking lander 1 site. The average radar reflectivities also suggest a surface that will adequately reflect radar altimeter transmissions during descent of the Pathfinder spacecraft used for firing the solid rockets and inflating the airbags.

The elevation of the landing site appears to be well below the 0 km elevation required to provide sufficient atmosphere for the flight system parachute. The USGS topographic map [16] lists the Ares site at about –2.0 km elevation (relative to the reference surface), which is also the elevation listed for the Viking 1 site. Earth-based radar tracks at 22.71°N obtained on January 20, 1980, and 22.89°N latitude obtained on January 15, 1980, cross the longitudes of both the Ares landing site and the Viking lander 1 site (22°N, 46.5°W), yielding elevations of –1.7 km and –1.8 km vs. –1.6 and –1.8 km respectively. Other radar tracks at latitudes of 21.59°N obtained on February 16, 1980, and 21.3°N obtained on February 22, 1980, suggest an elevation of –2.0 km for the Ares landing site. Because of uncertainties in relating an elevation, with respect to some reference martian figure, to atmospheric pressure (which is what is important for operation of the parachute), we have simply assumed that the elevation of the Ares site is the same as Viking lander 1 and determined the atmospheric surface pressure from the extremely repeatable surface pressure measurements for the appropriate landing season and day (6.85 mbar).

References: [1] Golombek, this volume. [2] Komatsu et al. (1995) *LSC XXVI*, 779; *LSC XXVI*, 781. [3] Greeley et al. (1977) *JGR, 82*, 4093. [4] Tanaka (1986) *Proc. LPSC*, in *JGR, 81*, E139. [5] Christensen and Edgett (1994) *LPI Tech Rpt. 94-04*, 19. [6] Pleskot and Minor (1981) *Icarus, 45*, 447. [7] Christensen and Malin (1993) *LPS XXIV*, 285. [8] Christensen and Moore (1992) in *Mars*, 687–729, Univ. of Arizona, Tucson. [9] Christensen (1986) *Icarus, 68*, 217. [10] Moore et al. (1987) *USGS Prof. Paper, 1389*, 222. [11] Arvidson et al. (1989) *JGR, 94*, 1573; Dale-Bannister (1988) *LPS XIX*, 239. [12] Tyler et al. (1976) *Science, 193*, 812; Downs G. S. et al. (1978) *Icarus, 33*, 441–453. [13] Moore and Thompson (1991) *Proc. LPS, Vol. 21*, 457. [14] Thompson et al. (1992) *LPS XXIII*, 1431–1432. [15] Moore and Jakosky (1989) *Icarus, 81*, 164–184. [16] USGS, 1989, Misc. Inv. Map I-2030.

ASSESSMENT OF PATHFINDER LANDING SITE WITH GOLDSTONE RADAR RANGING AND GOLDSTONE-VLA DUAL-POLARIZATION IMAGING. A. F. C. Haldemann[1], D. O. Muhleman[1], R. F. Jurgens[2], and M. A. Slade[2], [1]Division of Geological and Planetary Sciences, California Institute of Technology, Pasadena CA 91125, USA, [2]Jet Propulsion Laboratory, California Institute of Technology, 4800 Oak Grove Drive, Pasadena CA 91109, USA.

The preliminary landing site for the Mars Pathfinder lander/rover has been chosen in southeastern Chryse Planitia (19.5°N, 32.8°W) [1]. The region is believed to be relatively smooth. Its location at the mouth of the Ares Vallis outflow will hopefully provide a variety of sampling opportunities for the rover experiments. A more detailed review of the landing site characteristics can be found elsewhere in this volume [2]. The Ares Vallis site had been rejected as a Viking lander site, however, due to Goldstone CW radar echoes with low signal-to-noise (SNR). We will present an updated assessment based on two types of recent radar observations: radar ranging with the Goldstone DSN antenna and radar imaging with the Goldstone-VLA combination. Both experiments were at X band (3.5 cm).

TABLE 1. Dates and locations of radar tracks on Mars to be used in the radar ranging part of the study.

Date	Latitude	Longitude Begin	Longitude End	Locations
18 Dec. 1994	21.8	56.5	94.2	Kasei, northeastern Tharsis
25 Dec.	21.7	330.8	25.1	Arabia, eastern Chryse
27 Jan. 1995	19.9	336.2	76.2	Arabia, Chryse, Kasei
29 Jan.	19.8	322.9	48.7	Arabia, Ares, Tiu
30 Jan.	19.7	321.2	39.9	ibid.

Goldstone radar ranging measurements were performed during Mars' most recent opposition in the winter of 1994–1995, when the planet was at a distance of about 0.6 AU. Five radar tracks of interest for the primary landing site were recorded and are listed in Table 1. Three of the tracks pass over the site itself or its immediate vicinity. The Goldstone radar system is now 12 dB more sensitive than it was at the time of the Viking landing site assessment, so we expect that a correspondingly more detailed assessment can be carried out.

The data are in the form of delay-Doppler views, which fall along a subradar track on the planet. Views are collected during 10-min receive cycles separated by 10-min radar transmit cycles. Each view has about a 4 s integration time, and are summed in groups of 4 to improve SNR. The Doppler frequency resolution provides a longitudinal resolution of about 4 km, while the delay resolution makes for a latitudinal resolution of about 100 km. The data are of good quality, and should certainly provide consistent topographic profiles, which will be compared to the Mars digital elevation model [2]. The topographic profiles will be used to assess the kilometer-scale roughness in the landing site region.

The delay-Doppler data can be fit with radar models, in particular the Hagfors scattering law, to extract reflectivity and the Hagfors C parameter, a proxy for rms slope. The reflectivity relates to the dielectric properties of the upper meter, and contain information about the bulk density of the material and some information about chemistry, e.g., mafic vs. silicic material. It will be interesting to find out how well these material property assessments are borne out when the lander and rover return results. The C parameter can be used in a comparative manner to assess surface texture or roughness, both on the scale of the wavelength and on scales large compared to the wavelength. The texture may be expressed on the surface, and thus is evident in visual images, or may be covered by up to a meter of soil and appear smooth in visual images. Our investigation will make comparisons of the radar results with Viking imagery, and these analyses may drive some choices of model parameters to aid the fitting routines. Indeed, the study will require careful analysis of the applicability of the Hagfors scattering model, and the limits of its interpretation (see for example [3]).

The second dataset at our disposal was produced by interferometric imaging at the VLA of radar echoes from Mars. This is a huge dataset, which first observed the Stealth region on Mars, an essentially radar-absorbing region to the southwest of Tharsis [4]. These data were also used to observe the radar properties of the martian poles [5]. The resolution of these images is only on the order of the landing site ellipse, but the image data cover a much larger range of incidence angles than the delay-Doppler data, and will thus be extremely useful to constrain the models used to fit the delay-Doppler data.

Further, the Goldstone-VLA image data are in both circular polarizations. Polarization characteristics are a vital but complex part of the radar experiments. The details of the surface morphology are encoded into the polarization properties through multiple scattering, critical angle internal reflections, locally coherent scattering processes, and effects we have yet to imagine. Particular polarization signatures have been exploited for Mars [4], and will further provide constraints on the interpretation of the regional variation in wavelength-scale roughness. The results will be presented at the workshop.

References: [1] Golombek, this volume. [2] USGS (1993) Mars Global Topography CD-ROM, v.7. [3] McCollum and Jakosky (1993) *JGR, 98,* 1173–1184. [4] Muhleman D. O. et al. (1991) *Science, 253,* 1508–1513. [5] Butler B. J. et al. (1994) *LPSC XXV.*

RADAR SCATTERING CHARACTERISTICS OF ARES VALLIS AND ENVIRONS FROM ARECIBO OBSERVATIONS. J. K. Harmon[1] and B. A. Campbell[2], [1]Arecibo Observatory, Arecibo PR 00613, USA, [2]National Air and Space Museum, Washington DC 20560, USA.

Quasispecular radar echoes can provide estimates of surface roughness (rms slope θ_r) and the dielectric constant along the sub-Earth track on Mars. Such measurements were used for landing hazard assessment by the Viking 1 lander site selection team [1,2]. The radar θ_r measurements were partly responsible for the decision to reject the original A1 site in favor of the smoother A1WNW site. Since the Mars Pathfinder lander site lies very close to the rejected VL1-A1 site, it makes sense to take a fresh look at the radar characteristics of this area. The sub-Earth track crossed the Pathfinder site during the most recent Mars opposition in early 1995, and preliminary results from Goldstone 3.5-cm ranging observations indicate high radar roughness ($\theta_r > 10°$) over the landing site [3]. Although telescope upgrading work prevented us from making similar observations at Arecibo in 1995, we do have some Arecibo 12.6-cm radar data from earlier oppositions covering portions of the Ares Vallis region. Here we present some results from those observations.

In Fig. 1 we show θ_r values estimated from Arecibo ranging observations at 20.6°N in 1980 (filled boxes) and at 23.2°N in 1982 (open boxes); each of these points is obtained by fitting a single delay template to the region within 4° of the sub-Earth point for a given 30-s data block. Also shown are θ_r estimates from CW observations taken at 23.1°N in 1976 (solid line) and at 22.5°N in 1967 (dashed line); both these lines are adapted from Fig. 1 of Tyler et. al. [2]. These data all agree in showing that the Chryse plains are rough compared to the ridged plains and cratered plains to the east and west. Superimposed on this general trend are more localized roughness variations that can only be properly analyzed by making template fits to narrow Doppler slices. For example, the delay-Doppler array in Fig. 2 shows a "hole" at the central leading edge that corresponds to relatively weak echoes from the main channel of Ares Vallis at 23.2°N, 31°W. Template fits to this channel feature

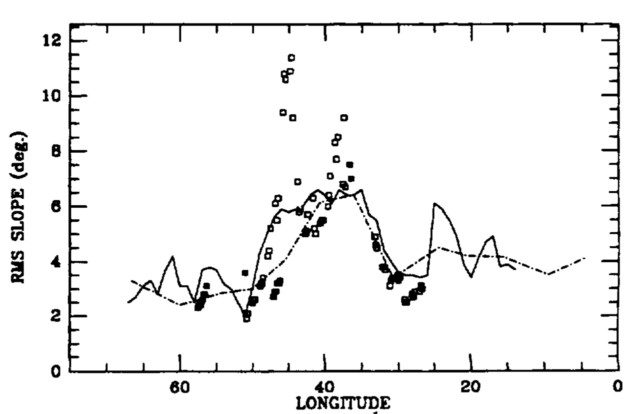

Fig. 1.

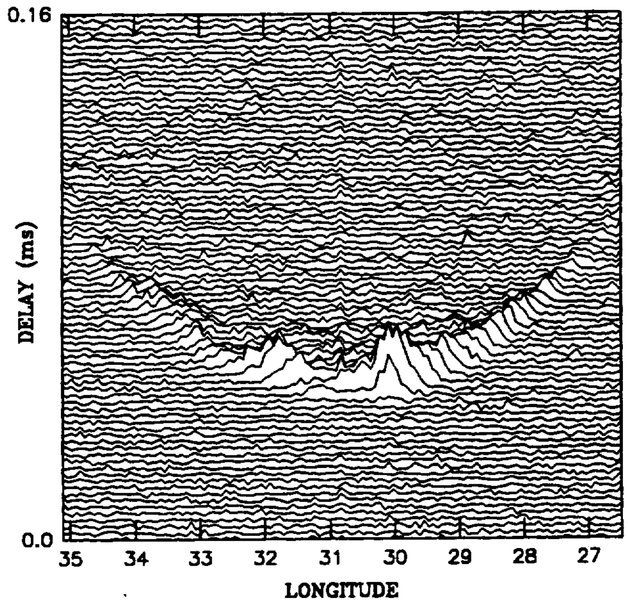

Fig. 2.

give $\theta_r \approx 5°$ for an assumed reflectivity of $\rho_0 = 0.07$, indicating that at this latitude Ares Vallis is rougher than the terrain to the east, but not particularly rough in an absolute sense. In Fig. 3 we show a delay-Doppler plot taken at a sub-Earth point of 20.6°N, 36.5°W, closer to the Pathfinder landing site. The single delay template fit to this entire array gives $\theta_r = 7.2°$ and $\rho_0 = 0.068$, values typical of Chryse in general. The righthand edge of this plot corresponds to the point where the sub-Earth track grazes the north edge of the Pathfinder landing site ellipse, and the weakness of the echoes at this point in the plot are consistent with some increase in roughness as one approaches the lander site from the west at this latitude. A template fit to a Doppler slice centered at 32.8° gives $\theta_r = 8.5°$ for an assumed $\rho_0 = 0.068$. This is significantly rougher than the northern branch of the Ares Vallis channel at 23.2°N. It is smoother than the $\theta_r > 10°$ reported by the JPL group from their track across the lander site, but we do not consider this difference as very significant given that (1) the Arecibo scan is 1°N of the lander site, (2) the observations were made at a longer wavelength, and (3) we have had to assume a ρ_0 value because we do not have sufficient longitude coverage at this latitude to do the same "Downs-style" scattering analysis as was done on the 1995 Goldstone data by the JPL group.

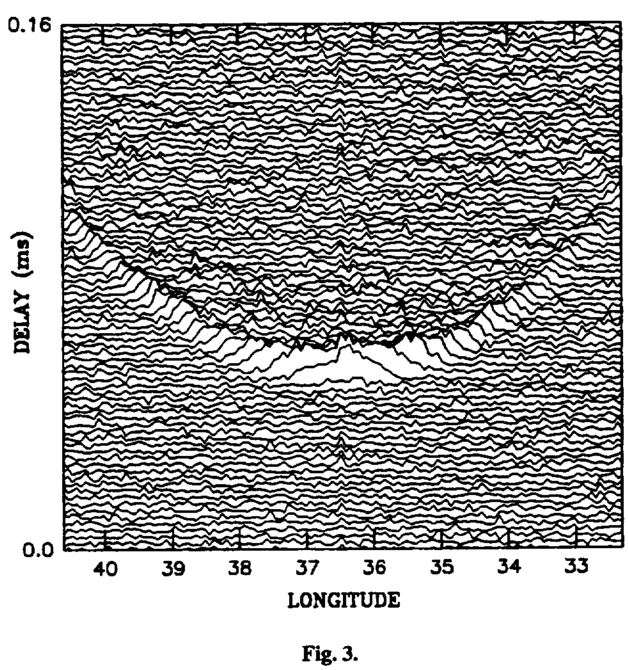

Fig. 3.

In addition to these quasispecular results, we have coverage of the Chryse area in depolarized reflectivity maps from 1990 random-code observations. Depolarized enhancements are indicative of surface roughness at wavelength (decimeter) scales, i.e., scales smaller than those influencing θ_r. The strongest such enhancements are found on the Tharsis volcanos and flows and in the Elysium Basin and outflow channel. In the Chryse channel region the strongest enhancements are found in Maja Vallis and the plateau bordering Simud Vallis. We find no strong feature at the Pathfinder lander site, although we do see a modest enhancement within the Ares Vallis channel south and east of the lander site. This indicates that the Ares Vallis channel is rockier than the cratered and ridged plains through which it flows, but does not have the sort of chaotic texture typical of the major volcanic provinces. We will discuss results from the depolarized maps in more detail at the workshop.

References: [1] Masursky H. and Crabil N. L. (1976) *Science, 193,* 809–812. [2] Tyler G. L. et al. (1976) *Science, 193,* 812–815. [3] M. Slade, private communication.

POSSIBILITY OF HIGHLY CONTRASTING ROCK TYPES AT MARTIAN HIGHLAND/LOWLAND CONTACT. G. G. Kochemasov, IGEM of the Russian Academy of Sciences, 35, Staromonetny, Moscow 109017, Russia.

"Stream sediment sampling" was proposed in 1979 as a rational tool for collecting and studying various rock fragments on the martian surface (9th Gagarin reading on aeronautics and aviation) and was again discussed in 1988 (18th Gagarin reading) [1]. This idea was based on the author's experience in stream sediment, heavy fraction, and rock fragment sampling as a geological prospecting tool in various African and Asian environments. A particular parallel was drawn between the martian environment and that of mountain deserts of northern Africa (Anti-Atlas) where eolian contamination is rather pronounced and which has to be borne in mind during the martian rock-sampling mission. Experiments in the Anti-Atlas have shown that significant eolian contamination exists in fine (<0.5 mm) dry mountain alluvial fractions. Hence, relatively large rock and mineral fragments are more safe for "on-the-spot" study of a catchment area and preparing a return collection.

The majority of planetologists believe, based on remote spectral studies, that the difference between lowland and highland rock types is not very great (as the difference between the fresh and weathered basalts-palagonites [2]). We think that this conclusion is controversial, considering, for example, an enormous albedo difference between Arabia Terra and Syrtis Major Planitia—probably likely the highest difference in the inner solar system. It was recently

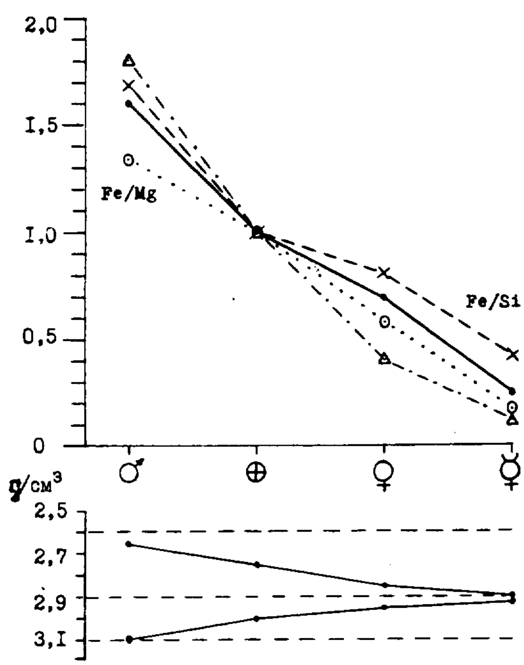

Fig. 1.

shown that there is regular change of crucial planetary crust characteristics with increasing solar distance ([3] and references therein). This resonance behavior is related to wave tectonics, which considers the interference of lithospheric (geospheric) stationary waves warping planetary spheres in four directions (orthogonal and diagonal) and having lengths proportional to the planetary orbital periods (Mercury $\pi R/16$, Venus $\pi R/6$, Earth $\pi R/6$, Earth $\pi R/4$, Mars $\pi R/2$, where R is a planet's radius). This "intricate weaving" produces "rounded" tectonic blocks and surface relief, both increasing with solar distance. Subsided (oceanic) and uplifted (continental) segments of the planetary crusts, composed of relatively dense and light materials (the principles of block angular momentum conservation govern this behavior) tend to have density contrasts growing in the same direction (Fig. 1).

Tracing the chemistry change of basaltic plains is most reliable as their soils were studied directly on Earth, Venus, and Mars. Iron content, and hence the density of mare basalts, correlates with the planetary relief amplitude or the amplitude of producing its lithospheric wave (e.g., the deeper primary Pacific Ocean has more Fe-rich tholeiites than the shallower secondary Indian and Atlantic Oceans, which helps us to understand the governing principle). Basalt contents of the Earth's primary Pacific depression are (in weight %) Fe/Si 0.38 and Fe/Mg 1.89 [4]; martian basalts, respectively, 0.64 and 2.53 [4]; venusian ones 0.31 and 1.10 [5]; and mercurian ones 0.16 and 0.32. For Mercury we took into account a mean estimate of Fe content in the surface rocks (5%), the high Mg content of its mantle, and the closeness of its crust composition to anorthosites with small albedo contrast between "mare" and "highlands" [4]. Figure 1 shows ratios of the above Fe parameters compared to the terrestrial ones taken as 1 (solid line—relief, dashed line—Fe/Si, dots—Fe/Mg).

Highland compositions: andesitic terrestrial [6] changes to alkali basaltic venusian [5]. The composition of the highland regions of Mercury (bright cratered plains) is taken to be somewhat more anorthitic or less dense (enstatite anorthosite) than that of the "smooth dark plains." Decreasing highland densities with increasing solar distance predicts the "lightest" continents on Mars, which is supported by the very sharp albedo contrast between "cratered old terrains" (bright areas) and plains (dark areas), indications of viscous magmas, and low-density rocks (gravity data [7]). "White rock" [8] with its very high (resembling ice) albedo could be albitite—a light acid variety of plagioclasite. High SiO_2 in this rock and in the bulk highland rock, equal to the SiO_2 content of albite (70%), follows from 60% SiO_2 in the bulk crust (= martian dust enriched in feldspar [4]) and 45% SiO_2 in the lowland basalts covering one-third to two-fifths of Mars' surface. Albitite could be magmatic or metasomatic in origin. The formation of this acid Na-rich plagioclasite is consistent with high pressure caused by warping Mars lithospheric waves (high and anisotropic pressure squeezing the planet).

As the lowland rocks recede from the Sun they become more Fe rich and dense (anorthite enstatitite 2.93 g/cm³; Mg basalt 2.95; tholeiite 3.0; Fe basalt 3.1); the highland rocks, inversely, become less dense (enstatite anorthosite 2.90 g/cm³; alkali basalt 2.85; andesite 2.75; albitite 2.65). The density contrast between the highland and lowland rocks increases: 0.03; 0.1; 0.25; 0.45 g/cm³ (Fig. 1, dot-dashed line, reduced to the terrestrial contrast 0.25 g/cm³), correlating with the relief range. Such regularity is caused by the action of the Le Chatelier rule, according to which equilibrium disturbance brings forces creating obstacles to it: increasing surface warping (relief range) brings increasing density contrast between lowland and highland rocks. This tends to level angular momenta of rising and falling blocks.

We suggest that at the lowland/highland contact in the Ares Vallis outflow area the Pathfinder could encounter rocks of the Fe-tholeiite family mixed with light (not dense) rocks rich in Na such as albitites and syenites (some resemblance with mangerite-anorthosite and anorthosite-granite formations on Earth).

References: [1] Kochemasov G. G. (1989) *Gagarin Reading on Aeronautics and Aviation, 1988*, Moscow, Nauka, 275 (in Russian). [2] Kieffer H. et al (1992) *Mars*, Univ. of Arizona, Tucson. [3] Kochemasov G. G. (1994) 20th Russian-American Microsymposium on Planetology, Abstracts, Moscow, Vernadsky Inst., 46–47. [4] *Basaltic Volcanism on the Terrestrial Planets* (1981) Pergamon, 1286 pp. [5] Basilevsky A. T. et al. (1992) *JGR, 97*, 16315–16335. [6] Taylor S. R. and McLennan S. M. (1985) *The Continental Crust*, Blackwell, Oxford, 312 pp. [7] Phillips R. J. et al. (1973) *JGR, 78*, 4815–4820. [8] Ward A. W. (1979) *JGR, 84*, 8147–8166.

CATASTROPHIC PALEOFLOODING AT THE PATHFINDER LANDING SITE: ARES VALLIS, MARS.

G. Komatsu[1,2] and V. R. Baker[1,3], [1]Lunar and Planetary Laboratory, University of Arizona, Tucson AZ 85721, USA, [2]Geological Institute, University of Tokyo, Tokyo, Japan, [3]Department of Geosciences, University of Arizona, Tucson AZ 85721, USA.

Paleodischarges for the martian outflow channels have been estimated by several researchers [1–3] using a modified Manning equation. This study updates our preliminary work [4]. The flow velocity (v) can be estimated by the Chezy equation, $v = C\ (ds)^{1/2}$

TABLE 1. Flow reconstruction using Manning equation.

	Section 10	Section 1
Manning Coefficient	0.032	0.032
Depth (m)	398.40	985
Slope	0.02	0.0001
Velocity (m/s)	148.91	25.43
Froude Number	5.46	0.49
Discharge (10^9 m^3/s)	0.57	0.57

in which C is the Chezy coefficient, $C = (2g/C_f)^{1/2} = 1/n\,(d)^{1/6}$ (where g is gravity, C_f is the friction coefficient, n is the Manning coefficient, and d is depth) and s is energy slope. The Manning coefficient for Mars (n_M) can be related to the empirical terrestrial Manning coefficient (n_E), by the equation $n_M = n_E(g_E/g_M)^{1/2} = 1.62n_E$ (where g_E is terrestrial gravity and g_M is martian gravity). More realistically, the empirical Manning coefficient on Earth ranges over a factor of about 2 and, for our application, the influence on the final result is minimal. The Manning coefficient chosen for Mars (n_M) paleoflooding is 0.0324 ($n_E = 0.02$). We selected a reach where the channel is well defined and unusually deep. For simplicity, the 10 cross sections of the Ares Vallis are assumed to represent the paleogeometry of the channel at the time of flooding [4]. The slope between cross sections 1–8 is too small to measure, so we have assumed it to be 0.0001. Because high-water marks, such as trim lines and deposits, are not apparent on the available Viking imagery, we assumed that the water surface reached the rims of the channel. We also assumed that the flood did not overflow the rims of the channel. The peak discharge was calculated for each cross section, and we took the lowest peak discharge out of the 10 as the best estimate for the entire reach (Table 1).

The resulting peak discharge is 0.57×10^9 m^3/s. This discharge rate is of the same order as the estimates for the Kasei Vallis [2]. For this discharge, the flow velocity ranges from tens of meters per second to over 100 m/s. Froude numbers suggest that, at the steep section, the flow was supercritical and, at the less steep section, the flow was subcritical. We expect that the water may have incised the channel and, therefore, may not have filled it to the rim. In this case, the discharge could well have been much lower than the estimated peak. Calculations by [5] show that flow velocities of tens of meters per second transport basalt fragments of one to several meters in diameter. A 100 m/s flow would transport basalt boulders larger than 10 m in diameter even by suspension. However, basalts are prominently jointed due to cooling, and fragmentation during the transportation would cause considerable reduction of boulder sizes.

The above calculation was applied to the deep section of the channel to estimate the peak discharge. The next U.S. Mars mission, Mars Pathfinder, has its primary candidate landing site located about 100 km to the north of the mouth of the Ares Vallis, which is one of several huge outflow channels debouching into the Chryse Planitia. At the landing site, the flood levels were estimated to be lower than the constricted section. This is the result of the pronounced expansion of the channel reach. However, the rich evidence of erosional landforms around the landing site suggests that even on the outwash fan deposited in this expansion, the peak flood power was still very high. The maximum flow velocity may still have been several tens of meters per second. As the flow velocity decreases, the sorting of sediments occurs. The sediments transported through constricted reaches will settle on the outwash fan of the expanding reach. Hence, on the outwash fan, it is considered that the largest-sized boulders accumulated near the mouth, and the grain size should have decreased away from the mouth of the channel. As the flood level lowers toward the end of the flood event, the sediment transport decreases. This leads to deposition of smaller grains. As a result, the flood deposit stratigraphy probably displays an upward decrease of grain size. Moreover, the flooding may have occurred in multiple events, which would have caused redistribution of flood deposits. The preservation of the original flood deposits is also subject to modification by other geological processes, including glaciation, impact cratering, and eolian processes. The size distribution of the boulders and smaller grains observed at the landing site depends on these factors as well as on the primary flood depositional processes.

References: [1] Baker V. R. (1982) *The Channels on Mars.* [2] Robinson M. S. and Tanaka K. L. (1990) *Geology, 18,* 902–905. [3] De Hon R. A. and Pani E. A. (1993) *JGR, 98,* 9129–9138. [4] Komatsu G. et al. (1995) *LPSC XXVI,* 781–782. [5] Komar P. D. (1980) *Icarus, 42,* 317–329.

MARS PATHFINDER: GEOLOGY OF THE LANDING SITE ELLIPSE. R. O. Kuzmin[1] and R. Greeley[2], [1]Vernadsky Institute of Geochemistry and Analytical Chemistry, Russian Academy of Sciences, Kosygin Street, 19, Moscow 117975, GSP-I, Russia, [2]Department of Geology, Arizona State University, Tempe AZ 85287-1404, USA.

Nineteen years after the last successful landing on Mars by Viking, the Mars Pathfinder mission will provide new data for the martian surface and atmosphere. An important advance will be the inclusion of a microrover for sampling and imaging surface rocks [1].

The Mars Pathfinder landing site must satisfy engineering constraints such as topographic level, surface roughness, and latitude to provide maximum solar power for the lander and rover. For scientific goals, the landing site should be in a region that has a wide variety of rock types in a small area. From terrestrial experience [2], such a site is typical for channel and canyon deltas that drain highland or mountain areas of various ages and rock types. For example, the Furnace Creek alluvial fan in Death Valley contains basalt, rhyolite, diorite, quartzite, limestone, and gabbro within 1 m radius of a simulated landing site. These rocks were transported from the surrounding mountains by intermittent streams. There is a good probability that a similar depositional regime can be found on Mars in deltas of the large outflow valleys. Ares and Tiu Valles are among the largest outflow channels on Mars. Their watersheds include various ancient Noachian highland materials and Hesperian-age ridged plains. Consequently, the delta-fluvial deposits of these channels, selected as the nominal site for Pathfinder, should include a wide variety of rock types and ages.

Analysis of Viking images (30 m/pixel) for the nominal landing site ellipse on the delta deposits of Ares-Tiu Valles shows that the surface is mostly smooth and slightly undulating, resembling the surface of the Viking 1 landing site. Crater counts of the landing site ellipse suggest a late Hesperian age. The surface of the site is complicated locally by streamlined islands that have terraces. About eight terrace levels are recognized on the flanks of the streamlined islands. The terraces could result from erosion of layered highlands or from fluvial deposition during different stages of flooding. The ellipse area also includes knobs and fluidized ejecta from large impact craters. Scabby or etched terrain occupies the western edge of the landing site ellipse. This terrain may have resulted from fluvial plucking and subsequent eolian deflation. The main trend of the etched terrain is parallel with Tiu Vallis, suggesting an origin related to the formation of the channel. To the north, the etched terrain grades into incipient chaotic terrain, indicating that the etching process may have been enhanced by ground-sapping processes [5].

Large blocks, ranging from the limit of resolution to 1 km, are found in the northwestern part of the ellipse. Some blocks may be remnants of crater rims and highland material; others could be remnants of eroded fluvial deposits. Craters and blocks constitute about 4% of the surface area [4]. Locally, many small impact craters (100–200 m in diameter) have dark halos, suggesting that they excavated dark-albedo subsurface material.

Albedo variations on the plains of the landing site ellipse may be due to variations in thickness of sand and dust. Typical values of the thermal inertia in the area range from 9.8–12.9 [6] to 8.4–10.9 [7] for fine-component material. This suggests possible particle sizes of 500–2300 µm [8], typical sizes for medium and very coarse sand. Thermal remote sensing data of Mars [9] suggest a rock abundance of the landing site to be similar to the Viking 1 landing site, except for the fine-component material. The current modification of the landing site by eolian processes is demonstrated by crater streaks and fine lineations on the surface.

The Ares-Tiu Valles delta is characterized by weak radar echoes [10], high values of fine-component thermal inertia, and moderate rock abundances. We suggest that a reasonable explanation for this discrepancy is that sand-gravel-rocky surface material is interbedded with finer deposits and scattered rock fragments, and that the thickness of the fine component is less than the penetration depth of the radar. On the Earth, such a surface structure is typical for some fluvial plains and desert pavements.

References: [1] Golombek M. P. (1995) *LPSC XXVI*, 475–476. [2] Greeley R. and Kuzmin R. O. (1994) *LPI Tech Rpt. 94-04*, 33–34. [3] Kuzmin R. O. et al. (1994) *LPI Tech Rpt. 94-04*, 35–36. [4] Golombek M. P. (1995) *LPSC XXVI*, 481–482. [5] Carr M. H. et al. (1976) *Science, 193*, 766–776. [6] Christensen P. R. and Moore H. (1992) in *Mars*, 687–729, Univ. of Arizona, Tucson. [7] Christensen P. R. and Malin M. (1993) *LPS XXIV*, 285. [8] Edgett K. S. and Christensen P. R. (1994) *JGR, 99*, 1997–2018. [9] Christensen P. R. (1986) *Icarus, 68*, 217. [10] Tyler G. L. et al. (1976) *Science, 193*, 812.

GROUND ICE AT THE MARS PATHFINDER LANDING SITE.

M. T. Mellon, NASA Ames Research Center, Moffett Field CA 94035, USA.

Water on Mars is of central interest to many areas of martian research, ranging from climate studies to geologic evolution. Ice in the martian subsurface (ground ice) is proving to be an important and dynamic reservoir. Its presence during recent geologic history may have had some influence on the geomorphic character of the Pathfinder landing site. The presence and implications of ground ice will be discussed.

At present epoch, ground ice is not likely to be stable at the low latitude of the intended Pathfinder landing site. In addition to low latitude, the relatively high average thermal inertia and low albedo typical of this region produce surface and subsurface temperatures much in excess of the atmospheric frost point. (The frost point is the temperature at which atmospheric water vapor would condense and, below which subsurface ice is stable with respect to sublimation and loss to the atmosphere). With the exception of higher long-term atmospheric water abundances than have been observed (raising the frost point) and small localized regions of unusually low thermal inertia (lowering mean ground temperatures), ground ice present in the near-surface regolith would rapidly sublime, diffuse to the surface, and be lost to the atmosphere.

In the recent geologic past, however, the situation was probably very different. Large oscillations in the martian orbit would have caused considerable changes to the pattern of insolation and to the martian climate as a whole. Primarily, an increase in the obliquity (tilt of the spin axis relative to the orbital plane) would increase the amount of solar energy being deposited in the polar regions, while simultaneously decreasing that in the equatorial and midlatitude regions. An increase in polar insolation would have increased the rate at which water sublimes from the polar caps during the summer season and generally increased the atmospheric water content and the frost point temperature. Similarly a decrease in equatorial solar heating would have lowered the regolith surface and subsurface temperatures, allowing ground ice to become stable (and rapidly condense from atmospheric vapor) in regions in which it was previously unstable. This would have been the case for the intended Pathfinder landing site. Such episodes of stability have occurred periodically throughout history when the obliquity reaches moderately high values, the last episode occurring mearly 500,000 yr ago.

On Earth ground ice present in regions of permafrost influences the geomorphic character of the surface, producing such periglacial landforms as ice-wedge polygons, thermokarst pits, and solifluction lobes. The episodic presence of ground ice at the Mars Pathfinder landing site may have had a similar impact. It is possible that the formation of thermal-tension fractures in the ice-cemented martian permafrost may have produced polygonal terrain on a scale similar to terrestrial counterparts. Polygonal terrain has been suggested in the Viking lander 2 images and may be observed in Pathfinder images. Although such polygons will not be active at the Pathfinder landing site in the present absence of ground ice, abundant ground ice at high obliquity would facilitate their development, which may in turn leave a geomorphic signature until the present epoch. In addition, periodic inflation and deflation of the ground due to "frost heave," which may be associated with the episodic condensation and sublimation of ground ice, might have produced thermokarst topography (differential collapse related to differences in regolith structure and composition).

The Pathfinder landing site may exhibit a geologic character, in part due to the influences of ground ice. Certainly, other processes, such as eolian and impact, are in force. These processes will compete with periglacial processes, particularly since the last occurrence of ground ice, making periglacial landforms difficult to identify. Despite this difficulty, the impact of ground ice may be evident at the lander site.

WHAT WILL PATHFINDER SEE AND DO ON MARS? H. J. Moore, U.S. Geological Survey, Menlo Park CA 94025, USA.

Experiences of the Viking landers are excellent guides for Pathfinder. Lander 1 operated for nearly four martian years after landing on July 20, 1976. Like the Viking landers, Pathfinder will observe materials, sample them, deform and disturb them, estimate their physical properties, witness their response to martian winds, and measure things. Major differences between the Viking landers and Pathfinder include the cameras and analyses sampling techniques. Cameras on both spacecraft have similar resolutions and stereometric capabilities, but spectral capabilities are better for Pathfinder. Samplers on the landers acquired and delivered samples to analytical instruments aboard the landers, but the Pathfinder microrover will carry an analytical instrument to soil-like materials and rocks. Things that Pathfinder might see and do are illustrated below with Viking lander observations and results.

Bright drifts, deflated by wind, are striking features seen in Lander 1 images. These drifts, with cross laminations that dip northeastward [1], are superposed on a rocky substrate. In the distance, a couple of undeflated duneforms rest on the rocky substrate. The substrate includes a cohesive soil-like material atop and admixed with rocks and rock fragments ejected from nearby impact craters; there may be outcrops of bedrock [2]. Rocks are striking features seen in the Lander 2 images [3]. Among the rocks are crusty to cloddy soil-like materials and thin deposits that appear to be fine grained—like drift material.

Estimates of the mechanical properties of soil-like materials were derived from the responses of the materials to the footpads and sampler [4]. In order of increasing strength, the sampled materials are (1) drift (Lander 1), (2) crusty to cloddy (Lander 2), and (3) blocky (Lander 1). Drift material is fine grained with grain sizes near 0.1–10 µm [5,6]. Friction angles estimated from deformations in front of the sampler during trenching are near 18° and imply that drift material is porous with a low bulk density; its bulk density in the X-ray fluorescence spectrometer (XRFS) analysis chamber is 1100 ± 150 kg/m^3 [7]. Cohesions range from 0 to 3.7 kPa. Disruption of crusty to cloddy materials produces crusts and fines in places and more or less equidimensional prismatic clods about 0.04 m across and less in other places. Local surfaces are littered with small clodlets (a few millimeters across), but surfaces of crusts are also seen at the surface. Individual mineral grains are in the 0.1–10 µm range [6,8]. The friction angle is about 34° and compatible with moderately dense soil-like materials. Cohesions range from 0 to 3.2 kPa. Disruption of blocky material produces strong prismatic clods. Smooth, tamped, and compressed surfaces in some sample trenches of blocky material argue for the presence of particles generally finer than 50 µm, but large comminutor motor currents suggest that significant amounts of strong millimeter-sized objects (such as rocks) are present. Some small unweathered rocks may be imbedded in blocky material because several centimeter-sized objects deposited on the XRFS funnel are dark gray with color reflectances consistent with mafic igneous rocks [9]. Blocky material is the strongest of the three soil-like materials, chiefly because of its cohesion, which is near 5 kPa. Its friction angle is about 31°. Friction angles and cohesions of blocky material are compatible with moderately dense loess on Earth.

Chemical compositions of the soil-like materials determined by the XRFS are remarkably similar at both sites [10] although the sites are separated by about 6500 km. The mineralogy of the surface materials are unknown, but the surface materials may be weathering or alteration products of mafic igneous rocks or smectite clays. Palagonite was suggested as an analog for the soil-like materials because of its spectral properties [11], but palagonite does not reproduce the results of the Viking Labeled Release experiments [11]. The weight percents of SO_3 and Cl in soil-like materials correlate directly with their visual classification and relative mechanical strengths of the materials. The gas chromatograph mass spectrometer detected water and CO_2 in the soil-like materials [12]. It appears probable that adsorbed water and CO_2 are present in the soil-like materials.

Little is known about the rocks at both sites because they were never sampled by Viking. Textures and appearances of the rocks vary [13]. Most of the rocks have irregular shapes but a few appear to be rectangular prisms. Surfaces of most rocks are pitted, others are smooth and unpitted, and others are knobby. The surface sampler did not chip, scratch, or spall surfaces of the rocks, so they do not have thick, weak, punky rinds [14]. The rocks are probably like terrestrial rocks with bulk densities near 2600 kg/m^3, cohesions near 10^3–10^4 kPa, and friction angles in the range of 40°–60°. Many surfaces of rocks have red colorations, while others are decidedly less red and nearly gray [15]. Red surfaces are consistent with coatings of a palagonite-like material on unaltered rocks produced by eolian deposition, weathering, or both. Gray surfaces suggest that the underlying rock is mafic. Hopefully, Pathfinder will obtain chemical compositions of both red and dark gray rock surfaces.

Modifications of the surface by natural processes were mild. Two small slope failures occurred on steep slopes of drifts at the Lander 1 site. A few to tens of micrometers of bright red dust were deposited from great dust storms in the falls of the first and fourth years and the winter of the first year. Mild winds from local dust storms reworked thin layers of dust during the second and third years [16]. At the Lander 1 site, a local dust storm occurred during the late winter of the first year. Late in the winter of the third year, a local dust storm eroded trenches, conical piles, and other surface materials around Lander 1 [16]. Finally, a great dust storm was in progress in the fall of the fourth and final martian year [17].

Surface phenomena were different at Lander 2 because ices and dusts were deposited during the first two great dust storms [18]. During the second winter, ices and dusts were again deposited on the surface but no great dust storm was in progress. The ices evaporated and a few micrometers of dust remained behind. No strong winds capable of eroding the surface or the conical piles of loose materials placed on and among rocks by the sampler ever occurred while Lander 2 observed Mars.

References: [1] Mutch et al. (1976) *Science, 194*, 87. [2] Binder et al. (1977) *JGR, 82*, 4439. [3] Mutch et al. (1977) *JGR, 82*, 4452. [4] Moore et al. (1982) *JGR, 87*, 10043; (1987) *USGS Prof. Paper 1389*, 222. [5] Ballou et al. (1978) *Nature, 271*, 644. [6] Moore and Jakosky (1989) *Icarus, 81*, 164. [7] Clark et al. (1977) *JGR, 82*, 4577. [8] Oyama and Berdahl (1977) *JGR, 82*, 4669. [9] Dale-Bannister et al. (1988) *LPSC XIX*, 239. [10] Toulmin et al. (1977) *JGR, 82*, 4625; Clark et al. (1982) *JGR, 87*, 10059. [11] Banin et al. (1992) in *Mars*, 594. [12] Arvidson et al. (1989) *Rev. Geophys. Space Phys., 27*, 39. [13] Garvin et al. (1981) *Moon Planets, 24*, 355; Sharp and Malin (1984) *GSA Bull., 95*, 1398. [14] Moore et al. (1978) *USGS Prof. Paper, 1081*, 21. [15] Guinness et al. (1987) *Proc. LPSC 17th*, in *JGR, 92*, E575. [16] Arvidson et al. (1983) *Science, 222,* 463; Moore (1985) *Proc. LPSC 15th,* in *JGR, 90,* D163. [17] Tillman (1988) *JGR, 93,* 9433. [18] Jones et al. (1979) *Science, 204,* 799; Wall (1981) *Icarus, 47,* 173; Svitek and Murray (1990) *JGR, 95,* 1495.

VIKING STEREO OF THE ARES VALLIS SITE: SEDIMENTOLOGICAL IMPLICATIONS.

T. J. Parker, Jet Propulsion Laboratory, California Institute of Technology, Pasadena CA 91109, USA.

The Ares Vallis site has one very important advantage over other potential grab-bag sites on Mars that might be accessible to the spacecraft. Because this site was one of the first choices for Viking Lander 1, excellent, same-orbit stereo images were acquired early in the Viking mission. These stereo pairs are on the order of 40-m/pixel resolution with a separation angle between looks of about 48°, corresponding to about a 40-m vertical precision for topographic measurements based on parallax displacement. Subtle topography on the plains is most easily viewed in stereo, and is indispensable to studying the geology of the landing site and surrounding region. In addition, it will be extremely useful in determining the exact location of the Pathfinder lander on the martian surface after the landing, by potentially providing a correlation between objects viewed on the horizon with a three-dimensional aerial view at least several months earlier than Mars Global Surveyor images could "find" the lander.

The Pathfinder landing ellipse was placed within a plains region beyond the mouth of Ares Vallis to avoid large topographic hazards. But this plains region is not without its interesting, and in some cases very problematic, landforms. The ellipse contains the following features: (1) primary impact craters; (2) small secondary impact craters; (3) streamlined islands and (4) longitudinal grooves [e.g., 1]; (5) "scabland" or "etched" terrain [e.g., 1], mostly outside ellipse to west); (6) pancakelike shields, (7) dikelike structures [e.g., 2,3], and (8) knobs or "buttes" [e.g., 3]; and (9) a previously undetected, subtle undulating or hummocky topography to the plains surface. The nature of these landforms has important bearing on what we can anticipate Pathfinder may see once the first images are transmitted to Earth.

But why is there even the least confusion about the nature of the landing site? After all, it lies just beyond the mouth of one of the largest outflow channels on Mars, orders of magnitude larger than the Channeled Scablands on Earth. Shouldn't we expect a fluvial sedimentary deposit? Probably. But a number of things could have happened to the site to change that in the more than 1.8 Ga since the latest Ares Vallis flood, including (1) eolian reworking or burial; (2) permafrost modification; (3) burial by lacustrine or marine sediment; (4) desiccation; and (5) burial by volcanic plains. Points (2) and (4) would have little effect on the lithology at the lander scale, since they involve the least modification of the postflood surface. Points (1), (3), and (5), on the other hand, could drastically affect the kinds of materials Pathfinder would examine. Thankfully, due to the relatively high thermal inertias (see discussions elsewhere in this volume) any eolian or fine lacustrine blanket is not likely to be thick enough to preclude access to surface rocks.

To further complicate the picture, even without subsequent modifiers, fluvial processes may leave behind (1) fluvial deposits; (2) relatively unmodified, pre-existing terrain (sediment "bypassing" or throughput); or (3) an eroded, pre-existing bedrock surface. The differences between these three are determined by the channel's energy at this location relative to reaches both upstream and downstream. High-energy flows will transport sediment through the site or scour the existing bedrock surface, whereas a drop in transport energies beyond the mouth of the channel will result in sediment deposition. Again, based on these considerations, we should probably expect a fluvial sedimentary deposit. What about the problematic landforms? How does the range of interpretations for these features affect what Pathfinder is likely to find? Taking these one at a time and based on a preliminary examination of the stereo pairs, I offer nine suggestions.

(1) and (2): Large craters are relatively few within the landing ellipse. Small secondaries are much more abundant and occur in a number of large clusters across the ellipse. Small craters probably won't pose a serious landing hazard. Landing near, even within, a crater may increase the grab-bag potential of the specific landing site by providing blocks of ejected material.

(3) and (4): Streamlined islands and longitudinal grooves scattered within and around the landing ellipse suggest a primary fluvial plains surface not buried by thick eolian, lacustrine, or volcanic deposits.

(5): "Scabland" terrain to the west of the ellipse appears to be due to eolian deflation after, rather than fluvial plucking during, the flood. Etching of the plains from around a few of the pancakelike shields and exhumation of several dikes appears to have occurred in this area. In addition, at least one small crater's ejecta blanket appears to have locally armored the plains surface, protecting it from the etching process. Other occurrences in this region of less-pronounced "scabland" terrain are more intriguing. One notable example in Viking images 004a19 and 004a79 (stereo pair) has an almost parabolic shape oriented ~45° with respect to local channel scour, and therefore probably unrelated to it.

(6) and (7): The pancakelike shields and dikes exhibit no evidence of either channel scour or streamlining, further indicating they formed after the flood. Although there is no reason volcanic landforms couldn't be found in a fluvial setting (they often are on Earth), these occur exclusively on the plains surface in this region, never on the flanks or "tails" of streamlined islands. This might suggest that they are related in some way to the plains "deposits," perhaps as pseudovolcanic sedimentary structures, such as sand volcanos, mud laccoliths, and clastic dikes. Although there are no terrestrial analogs to these features at such large scales, the martian floods were certainly capable of rapidly emplacing thick, wet sedimentary deposits that could have experienced dewatering on a grand scale after cessation of the flood.

(8): The knobs may be remnants of resistant material left behind after the flood. However, most show no streamlining, whereas several similar-sized streamlined knobs can be found throughout the southern Chryse Basin. In addition, many clusters of these knobs can be found, particularly in the "shadows" of flow obstructions, similar to occurrences of large boulders in the scablands, but on a scale too large for suspension, or even bedload transport. Alternatively, they could be similar to "rafted" blocks in terrestrial floods. Most notable of these are fragments of concrete from the Saint Francis Dam in southern California, which are on the order of thousands of tons in mass and were rafted more than a kilometer downstream when the 47 × 10^6 m^3 reservoir failed catastrophically in 1928.

(9): The gently undulating surface of the plains within the ellipse (most pronounced near its center) became apparent when I contrast-enhanced the Viking images to bring out subtle details within the plains (typically saturating sunward and shaded slopes of knobs and craters). This surface almost appears rippled, although the ripples are poorly organized and trend with their crests parallel to the flow direction. The wavelengths are on the order of a few kilometers and amplitudes are up to a few tens of meters. They may be hummocks or lobes of sediment deposited by the flood.

References: [1] Baker V. R. (1973) *GSA Spec. Paper 144*, 79. [2] Greeley R. et al. (1977) *JGR, 82*, 4093. [3] Hodges C. A. and Moore H. J. (1994) *USGS Prof. Pap. 1534*, 194.

THE GEOLOGIC MAPPING OF THE ARES VALLIS REGION.

J. W. Rice Jr., Department of Geography, Arizona State University, Tempe AZ 85287-0104, USA.

Geologic mapping is being conducted at a scale of 1:500,000 on the Ares Vallis outflow region in southern Chryse Planitia. Ares Vallis is a 1500-km-long outflow channel that drains the cratered highlands to the south before debouching into the vast, topographically enclosed Chryse Basin. This area contains both erosional and depositional landforms (streamlined islands, flood-flow-modified impact craters and associated ejecta blankets, terraces, and knobby and etched terrains). The identification of deltaic deposits on Mars has been documented [1,2]. However, a more detailed account is being put forth for the depositional and erosional history of Ares Vallis based on the mapping being conducted.

The region mapped contains the landing site (19.5°N, 32.8°W) for Mars Pathfinder. This site was chosen by Mars Pathfinder science personnel in June 1994. The Ares Vallis site was originally proposed by Rice and Kuzmin et al. in April 1994 [3,4]. This mapping effort will aid in the analysis and interpretation of landforms and surface materials found at the landing site. The landing is scheduled for July 4, 1997.

The 1:500,000-scale mapping of Ares Vallis is an order of magnitude better than previous maps of this region [5,6]. Viking orbiter images with resolutions on the order of 40 m/pixel are being used to define the various materials present in this region. Information on physical properties [7–10] are also being incorporated into this map. Finally, a more complete picture of the depositional history of the Chryse Basin is emerging and a facies model has been proposed [11] that should help explain both the Viking 1 and Pathfinder landing sites.

References: [1] Rice J. W. and Scott D. H. (1993) *LPI Tech. Rpt. 93-06*, 45–46. [2] Rice J. W. and De Hon R. A. (1995) *USGS Map I-2432*. [3] Rice J. W. (1994) *LPI Tech. Rpt. 94-04*, 36. [4] Kuzmin R. O. et al. (1994) *LPI Tech. Rpt. 94-04*, 30–31. [5] Wilhelms D. E. (1976) *USGS Map I-895*. [6] Greeley R. et al. (1977) *JGR, 82*, 4093–4109. [7] Golombek M. P. et al. (1995) *LPSC XXVI*, 481–482. [8] Edgett K. S. (1995) *LPSC XXVI*, 353–354. [9] Edgett K. S., this volume. [10] Parker T. J., this volume. [11] Rice J. W. and Edgett K. S., this volume.

FACIES ON MARS: A MODEL FOR THE CHRYSE BASIN OUTFLOW SEDIMENTS BASED ON ANALOG STUDIES OF ICELANDIC SANDAR AND THE EPHRATA FAN OF THE CHANNELED SCABLAND, WASHINGTON.

J. W. Rice Jr.[1] and K. S. Edgett[2], [1]Department of Geography, Arizona State University, Tempe AZ 85287-0104, USA, [2]Department of Geology, Arizona State University, Tempe AZ 85287-1404, USA.

Nicholaus Steno introduced the concept of facies to the study of geology in 1669 [1]. Here, we describe "facies" in terms of laterally adjacent coeval sedimentary units. In this paper we extend the facies concept to the surface of Mars, specifically the basin of Chryse Planitia. This should aid in the interpretation of the Mars Pathfinder landing site. Mars Pathfinder is scheduled to land on the Ares Vallis flood plain on July 4, 1997.

A sedimentary facies model has been developed for Chryse based on the combined analysis of geomorphology, albedo, and thermophysical properties. Seven major outflow channels debouch into the topographically enclosed Chryse Basin. We are developing a facies map to illustrate the areal extent of the sedimentary deposits exposed at the surface (those that result from the most recent outflow events in Chryse). A facies map indicates the distribution of different sedimentary facies over a geographic area for a specified moment or interval of geologic time [2]. Such maps are important for interpreting ancient depositional environments and paleogeography.

The sandar of southern Iceland and the Ephrata Fan of the Channeled Scabland, Washington, are the analog surfaces used in this study. Sandar deposits (Icelandic glacial outwash fans/plains) cover extensive areas (up to 800 km^2) of the Icelandic coasts. Most of these deposits were laid down by jokulhlaups, which occur frequently and are caused by the abrupt drainage of ice-dammed lakes or subglacial volcanic eruptions [3,4]. The high current velocities and discharges associated with these outbursts are very significant factors for sediment transport along these fans. Discharges from these floods can be up to 100,000 m^3/s and can last for several days [4]. Sandar deposits display a succession of facies characterized by differences in fan gradient, clast size, bar morphology, and sedimentary structures [5]. These facies are described as follows: (1) "proximal facies," composed of steep gradients, large clasts, longitudinal bars, and few sinuous streams; (2) "mid-fan facies," typified by moderate gradients, clasts ranging from tens of centimeters to sand size, longitudinal bars, and numerous anabranching and bifurcating streams; and (3) "distal facies," characterized by low gradients, mostly sand-sized material, linguoid bars, and branches that merge and form very wide shallow streams.

Sandar are relevant to martian outflow channel deposits because they are the direct result of rapid sediment deposition from an expanding flow after leaving a constricted area. This is observed at the mouth of Maja Vallis, where the channel emerges from its constriction in the highlands and empties into the vast Chryse Basin [6]. Another important point to note is that discharge rates on sandar vary greatly. Discharges into Chryse were also probably variable due to the sudden and sporadic release of water associated with the production of the chaotic terrain.

The other analog surface is the Ephrata Fan. This fan is an extensive coarse gravel unit deposited subfluvially [7]. The Ephrata Fan was emplaced as flood waters emerged from the Soap Lake constriction, located at the mouth of the Lower Grand Coulee, and expanded outward into the Quincy Basin. Clast sizes on the fan surface range from house-sized boulders in the proximal fan zone to the sand of the Moses Lake dune field located in the fan's distal zone. We postulate that the Ephrata Fan in Quincy Basin is a very small analog/model of the outflow deposits in Chryse Basin.

Rock abundance, thermal inertia, albedo, and geomorphic evidence indicate that the Chryse Basin follows the general sedimentary facies models of Icelandic sandar deposits and the Ephrata Fan. The transition to distal facies in Chryse Basin is most easy to recognize; it is indicated by the change in albedo from Chryse Planitia (0.21–0.26) to Acidalia Planitia (0.14–0.16). The lower albedo of Acidalia results from the presence of windblown sand [8], similar to the presence of eolian-reworked sand in the Moses Lake dune field on the Ephrata Fan. Viking 1 lander investigators in the 1970s commented on the relative paucity of sand at the landing site [e.g., 9]; we argue that this is because very little sand was deposited at that location; instead, the outflow floods washed most sand further out into Acidalia. Today, Acidalia is both sandy and rocky, probably owing to eolian erosion that has exposed buried rocks and possibly stripped away sand (perhaps transported to the north polar dune field).

Both the Viking 1 and Mars Pathfinder landing sites occur in what we map as the mid-fan facies; these areas are rocky with little sand, and the rocks tend to trap windblown silt and dust. That the Viking 1 site might once have been inundated by floods is apparent, considering its proximity to the mouths of Maja and Kasei Valles.

Our facies model for the last flood deposits in Chryse Basin is outlined as follows: (1) The proximal facies zone extends from chaotic terrain (channel sources) to the mouth of channels, a distance of ~1000 km; (2) mid-fan facies zone (transition zone) extends from channel mouths to about 800 km into Chryse Basin; and (3) the distal facies zone begins at the albedo change between Chryse and Acidalia.

References: [1] Walker R. G., ed. (1984) *Facies Models*, Geoscience Canada Reprint Ser. 1, 317. [2] Dott R. H. and Batten R. L. (1981) *Evolution of the Earth*, McGraw-Hill, 113 pp. [3] Krigstrom A. (1962) *Geog. Ann., 44*, 328–346. [4] Thorarinnsson S. (1960) Inter. Geol. Cong. 21st Session, 33–45. [5] Boothroyd J. and Ashley G. (1975) *SEPM Spec. Pub., 23*, 193–222. [6] Rice J. W. Jr. and DeHon R. A. (1995) *USGS Map I-2432*. [7] Baker V. R. and Nummedal D. (1978) *The Channeled Scabland*, NASA, 186 pp. [8] Arvidson R. E. et al. (1989) *JGR, 94*, 1573–1587. [9] Sagan C. et al. (1977) *JGR, 82*, 4430–4438.

A SOJOURNER'S PROSPECTUS: PROVENANCE OF FLOOD-TRANSPORTED CLASTS AT THE MARS PATHFINDER LANDING SITE.

J. W. Rice Jr.[1] and K. S. Edgett[2], [1]Department of Geography, Arizona State University, Tempe AZ 85287-0104, USA, [2]Department of Geology, Arizona State University, Tempe AZ 85287-1404, USA.

Introduction: Mars Pathfinder and its microrover, recently named Sojourner (after the 19th Century civil rights figure Sojourner Truth), will examine rock and soil composition at the Ares Vallis landing site, centered at 19.5°N, 32.8°W. The Ares site was chosen because it may provide a "grab bag" of flood-transported rock types [1]. This paper discusses terrestrial examples of deposits and processes in catastrophic flood and periglacial settings on Earth, and how these lend credence to the conclusion that the Ares site might provide a rich sampling of diverse materials. The purpose is to generate discussion on the nature of the Ares "grab bag."

What Rocks Might Have Been Sampled?: The units cut by Ares Vallis, according to Scott and Tanaka [2], are "Hesperian ridged plains material" and two types of "Noachian plateau cratered material." Tiu Vallis cuts the same units. An older Noachian proto-Ares Vallis cuts similar units and may have stretched from the Nereidum Montes through Uzboi, Ladon, and Margaritifer Valles to Chryse [3]. The Hesperian ridged plains are likely dominated by mafic or ultramafic lavas, perhaps interbedded with sediments and volcanic ash. The Noachian units likely include impact breccias interbedded with lavas, pyroclasts, and eolian and lacustrine sediment. Hydrothermal minerals/rocks might be among the materials at the Ares site [4], as well as "hardpan" or other low-temperature diagenetic debris [5]. The only clue we have to the composition of Noachian rocks is the Allan Hills 84001 orthopyroxenite meteorite, which might be a ~4-Ga sample from the martian highlands [e.g., 6].

Missoula Flood Deposits in Washington and Oregon: The Missoula flood deposits suggest how a diversity of lithologies can be deposited in a location like the Ares site. The late-Wisconsin sediments in the Quincy Basin, Washington, came mainly from floods that poured through the Grand Coulee (see field guide in this volume, and references therein). Most of the larger clasts (cobbles, boulders) were deposited in the Ephrata Fan. Observations made in June 1995 (with M. Golombek [7]) show that about 95% of the rocks on the surface of the fan are basalts, ~5% are granodiorites, and <<1% are others (metamorphic and sedimentary rocks [8]). The two dominant rock types outcrop in the Grand Coulee [9]. The sand dunes south of the Ephrata Fan have a wider variety of flood-deposited clasts: basalt (~55%), metamorphic rock (~6%), quartz (~30%), and other minerals [10] derived from rocks that outcrop as far away as Idaho. At the Ares landing site, we expect that the smaller clasts are most likely to include rock fragments that were carried the greatest distances by water.

There is another way for a flood to carry large clasts great distances. The Missoula flood deposits include ice-rafted debris. The most spectacular ice-rafted features occur in the Willamette Valley, Oregon [11]. The boulders in Willamette Valley include metamorphic, plutonic, and volcanic rocks transported from outcrops occurring from Lake Pend Oreille, Idaho, down to Portland, Oregon [11]. Amazingly, one ice-rafted boulder was the Willamette Meteorite, a 14,000-kg nickel-iron that was originally incorporated into the Cordilleran ice sheet, transported down the Purcell Trench glacial lobe, then brought to Oregon by a flood-borne ice raft [12]. We think that some of the large (~1-km) knobs (which lack streamlining) at the Ares landing site could be ice-rafted blocks.

High-Latitude Fluvial Flood Processes on Earth: Rivers in high northern latitudes provide additional insight as to mechanisms that transport and deposit clasts from a variety of settings. In addition to ice rafting, whole, thick sections of frozen rock and soil may be transported by water following bank collapse. Bank collapse can occur all along the course of a fluvial system, such as the Colville River in Alaska, and is usually initiated by thermo-erosional undercutting of an ice-rich bank by the warmer water in the stream [13,14]. Some high-latitude fluvial systems discharge into ice-covered seas; the ice cover allows sediment to be transported great distances (tens of kilometers on Earth). This process is well documented at the Colville River delta, where springtime flood waters meet the still-frozen Beaufort Sea [15]. Although controversial, this process could have occurred at the Ares site if an ice-covered sea was ever present.

Diversity of Rock Types at Viking 1 Lander Site?: The Ares landing site is thought to be a "grab bag," with rocks and perhaps intact soil units that have been transported by floods. The Ares site may offer new insight into the Viking 1 lander site, the geologic history of which remains controversial. Here we note that the rocks at the Viking 1 lander site appear to have a variety of lithologies [e.g., 16]. Perhaps what will be found at the Ares Vallis site will help us reinterpret what was observed at the Viking 1 site two decades ago.

References: [1] Golombek M. P. et al., this volume. [2] Scott D. H. and K. L. Tanaka (1986) *USGS Map I-1802-A*. [3] Parker T. J. (1989) *LPS XX*, 826–827. [4] Farmer J. D. et al. (1995) *LPS XXVI*, 393–394. [5] Treiman A. H., this volume. [6] McSween H. Y. Jr. (1994) *Meteoritics, 29*, 757–779. [7] Golombek M. and Rapp D., this volume. [8] Grolier M. J. and Bingham J. W. (1971) *USGS Map I-589*. [9] Stoffel K. L. et al. (1991) *Wash. Div. Geol. Earth Res. Map GM-39*. [10] Petrone A. (1970) M.S. thesis, Washington State Univ., Pullman. [11] Allison I. S. (1935) *GSA Bull., 46*, 605–632. [12] Allen J. E. and Burns M. (1986) *Cataclysms on the Columbia*, Timber Press, Portland, Oregon. [13] Williams P. J. and Smith M. W. (1989) *The Frozen Earth*, Cambridge Univ., New York. [14] Walker H. J. (1973) *Arctic Inst. N. Am. Tech. Pap., 25*, 49–92. [15] Reimnitz E. and Bruder K. F. (1972) *GSA Bull., 83*, 861–866. [16] Sharp R. P. and Malin M. C. (1984) *GSA Bull., 95*, 1398–1412.

SPATIAL STATISTICAL ANALYSIS OF THE ARES VALLIS REGION FROM VIKING ORBITER AND WORST-CASE SCENARIO FOR SUBPIXEL-SCALE ROUGHNESS.

M. K. Shepard[1], E. A. Guinness[2], and R. E. Arvidson[2], [1]Department of Geography and Earth Science, Bloomsburg University, Bloomsburg PA 17815, USA, [2]Department of Earth and Planetary Science, Washington University, St. Louis MO 63130, USA.

One of the immediate concerns of the Pathfinder mission team is the surface roughness of the proposed landing site. Is it a reasonably safe area to place a soft lander? This question is a difficult one to answer directly since Viking orbiter images of the proposed site have minimum pixel resolutions of 40 m. Boulders or precipices much smaller than this could cause a mission catastrophe. The objective of our research is to infer some quantitative measure of the subpixel-scale roughness in this region using techniques of spatial statistics.

In an area of homogeneous terrain, i.e., terrain of one geologic provenance, one can expect some statistical behavior of the topography as a whole. When this area is imaged by a satellite sensor, the terrain is essentially broken into equal-sized areas or pixels. A pixel represents the average reflectance behavior of all the area within its purview. The reflectance of each pixel is a function of the surface composition, the topography, and shadows cast by the topography. In the simplest case, the reflectance of a pixel is a linear sum of the reflectance of the surface material and the reflectance of shadows, weighted by their respective fraction of the pixel area.

Assume a surface of single composition, illuminated by the Sun at an incidence angle >45°. If the topography of the surface in question has elements with vertical scales comparable in size to the pixel, those elements will dominate the pixel reflectance because of the shadows present. Furthermore, the larger the topographic elements are with respect to the pixel size, the greater the variance in the number of those elements and shadows present. As a whole, pixels in this area will show a relatively large degree of variance in reflectance because some will have large numbers of shadows and others will not. Furthermore, the greater the contrast between illuminated surface and shadow, the greater the variance.

Conversely, if the topography is dominated by elements with scales much smaller than the pixel size, then any given pixel will have (statistically) the same number of these elements as every other pixel. Therefore, as a whole, the pixels in this area will have less variance in reflectance.

In areas where the surface is not of a single composition, there will be variance from pixel to pixel caused by compositional heterogeneity. The amount of variance caused by compositional heterogeneities can be determined by examining the surface when the Sun is directly overhead. At this point there will be no shadows cast by topography and the entire variance in the scene can be attributed to compositional variation. This variance can then be "subtracted" from the variance in the scene at higher Sun angles, where the variance is a combination of compositional variations and topographic shadows, thereby leaving the variance caused by the topography alone. The scale of subpixel roughness can be quantified by utilizing a combination of analytic methods and forward models of computer synthesized surfaces. This methodology has been developed and tested successfully on an Earth analog site [1].

Unfortunately, all the high-resolution (40 m/pixel) Viking Orbiter scenes of the Ares Vallis region have Sun angles of ~60°. It is therefore impossible to estimate the variance in the images caused by compositional variances. Many (if not all) of the scenes are also plagued by a large atmospheric optical depth that significantly reduces the contrast between shadows and illuminated surface. However, by assuming that the surface is compositionally homogeneous, i.e., no variance due to compositional heterogeneity, a worst-case scenario for subpixel-scale roughness can be developed.

We will present the results of this worst-case scenario, as well as other information gleaned from an analysis of the differences in variance behavior observed in different spectral windows (images acquired through the clear, violet, red, and green filters).

References: [1] Shepard M. K. et al. (1993) *LPSC XXIV*, 1293–1294.

DUAL-POLARIZATION CONTINUOUS-WAVE (CW) OBSERVATIONS FROM THE ARES VALLIS SITE AND ENVIRONS.

M. A. Slade, D. L. Mitchell, and R. F. Jurgens, Jet Propulsion Laboratory, California Institute of Technology, Pasadena CA 91109-8099, USA.

During the 1995 Mars opposition, CW radar observations were performed over the Ares Vallis landing site in order to help assess the type of terrain that the Pathfinder spacecraft and rover would encounter. A total of nine transmit-receive cycles, or runs, were performed on April 17, 1995. For each run, an ~100% circularly

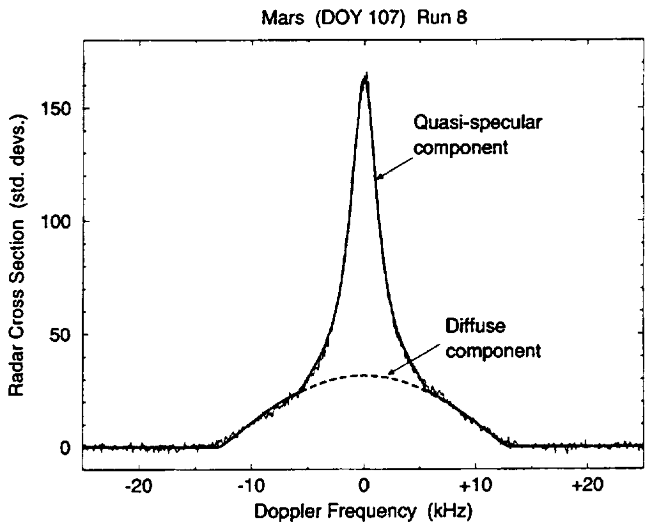

Fig. 1. The OC Doppler spectrum obtained on April 17, 1995, when the mean subradar longitude and latitude were 32.7°W and 18.7°N. The OC echo has been decomposed into two components: (1) a quasispecular echo (heavy solid line) originating from a small region, typically a few degrees in radius, centered on the subradar point, and (2) a diffuse echo (heavy dashed line) reflected from the entire visible disk. The quasispecular component is modeled with a Hagfors law, yielding a C parameter of 80, corresponding to an rms surface slope (on scales much larger than the observing wavelength) of 6.4°. The total OC radar albedo is 0.101, and the quasispecular portion of the OC radar albedo is 0.048.

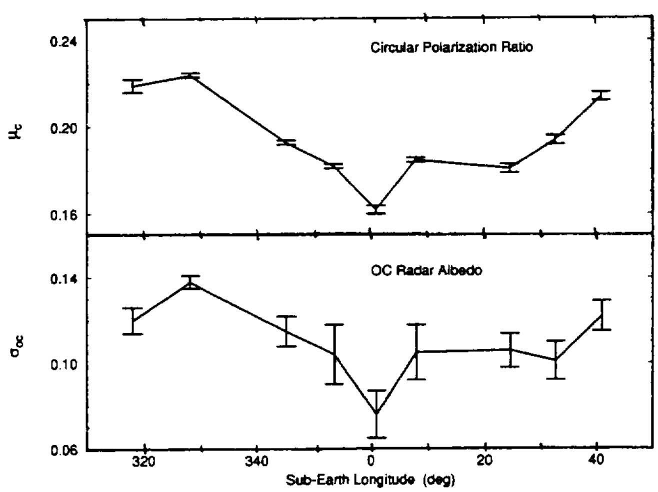

Fig. 2. Results in the context of the day's observations, showing the total OC radar albedo and the circular polarization ratio for this and the other runs of April 17. The implications of this part of the 1995 Mars radar dataset will be discussed at the meeting.

polarized signal was transmitted toward Mars, and echoes were recorded simultaneously in both the same sense of circular polarization as transmitted (the SC sense) and the opposite (OC) sense. The helicity of circular polarization is reversed upon reflection from a surface that is smooth on all scales within about an order of magnitude of the wavelength, but SC echo power can arise from single backscattering from a rough surface, from multiple scattering, or from subsurface refraction. The circular polarization ratio is thus a measure of near-surface complexity, or "roughness," at scales near the 3.5-cm observing wavelength.

A TARGETING STRATEGY FOR ENSURING A HILLSIDE VIEW AT ARES VALLIS. P. H. Smith, Lunar and Planetary Laboratory, University of Arizona, Tucson AZ 85721, USA.

An inspection of the Mars Pathfinder landing site at Ares Vallis with the stereo frames provided by the Viking orbiter cameras shows a number of large-scale features that may be of considerable interest if they are within range of the IMP camera. This paper will characterize the heights of the features resolved by Viking and make estimates of how they might appear to the IMP camera at various distances, with the aim of adjusting the landing ellipse to maximize the probability of seeing one or more hills. Certainly, the most distinctive features within the landing site are the stream-flow islands, which have a tear-drop shape and are sometimes associated with an impact crater. Close inspection of orbiter pictures shows that the slopes of these features are layered, but little can be learned about this layering since it shows up at the limit of resolution. Possible explanations include topography such as sedimentary layers, ancient shorelines, erosion from multiple stream flows, or lava flows. It would be unfortunate to miss seeing such an interesting structure because the actual landing site happens to be 20 km away, below the local horizon.

Naturally, one cannot prevent limiting the horizon if Pathfinder lands in a ditch or local depression. However, barring bad luck of that sort, it is possible to improve the chances of seeing interesting steep terrain by choosing a landing ellipse within the vicinity of the Ares Vallis delta that guarantees large vertical features are within every view circle of the landing ellipse. A view circle can be defined by the distance that IMP (the Pathfinder camera) can resolve a steep slope with better resolution than the Viking orbiter pictures; with a 1-mrad/pixel resolving power, this distance is about 5 km and gives a pixel size of 5 × 5 m. Note that at this distance the surface curvature will only hide the lower 1 m of the feature.

To estimate the density of sites, I divide the landing area by gridlines 10 km apart, twice the radius of the viewing circle. The major tall features within the area are apportioned to a gridbox and are counted. The best landing ellipse is the one that gives the highest probability of putting an observable tall feature within every grid box contained in the landing ellipse. Movements of the ellipse that serve to maximize the chance of viewing tall structures will not take away from the grab-bag nature of the site nor hinder any of the other goals of the mission.

Besides searching for ancient shorelines and layering features, there are other important goals attached to seeing local hills besides studying the hills for themselves. First, the landing site appears to have a high enough density of tall objects that we are likely to be able to see two or more separate hills. This leads to the ability to exactly locate our landing site within the Viking pictures using simple triangulation from our relative coordinate system. It may be difficult for the MOC camera aboard the Mars Global Surveyor to identify our precise location on a rather featureless terrain. And second, the importance of a dramatic view should not be minimized. A 300-m-tall object seen at 3 km distance will subtend about 100 pixels and would be at least 300 pixels wide; a full color image of this hill would be very exciting. Tucsonans know that the beauty of the desert is revealed by the surrounding mountains.

SEDIMENTARY STRATIGRAPHY OF CHRYSE PLANITIA, MARS. K. L. Tanaka, U.S. Geological Survey, Flagstaff AZ 86001, USA.

Geologic/geomorphic mapping of Chryse Planitia and surrounding terrain [1] has revealed assemblages of landforms indicative of the basin's sedimentary stratigraphy. Here I refine the precision of relative ages of basin units and discuss progressive northeastward thickening of these units based on geomorphic indicators.

Using crater densities in units of the geologic map of [1], Late Hesperian and Early Amazonian ages have been cited for deposits resulting from flooding into Chryse Planitia. These crater counts were limited to areas covered by higher-resolution images; area sizes range from 7 to 65 × 10^3 km^2. I have begun a more comprehensive study of crater densities for these same units (see Table 1); thus far I confirm, with much better precision, a Late Hesperian/Early Amazonian age for much larger areas of the units (>2 × 10^5 km^2). Additionally, these ages are based on craters >5 km diameter, which appear fully preserved. Craters <5 km have a somewhat lower density than expected relative to larger craters, which may be explained by obliteration by moderate erosion or deposition. In some areas of the basin, large, partly buried, and heavily modified crater rims outnumber large, relatively unmodified, superposed craters. The density of these large craters in places suggests that the underlying material may be much older than the basin sediments (Early Hesperian or older). In addition, I determine a Late Noachian/Early Hesperian crater density for unmodified ridged plains material (unit Hr) in western Chryse Planitia (Table 1).

A few geomorphic clues indicate that sediments progressively thicken from southern and western Chryse Planitia to northeastern Chryse and southern Acidalia Planitiae (in the direction of fluvial flow, as indicated by teardrop-shaped bars), as follows: (1) channel bars and terraces become progressively thinner and disappear; (2) wrinkle ridges change from pristine to subdued to presumably buried in western Chryse (alternatively, they become lower in height and more subject to other degradational processes); (3) large, presedimentation crater rims form raised channel obstructions in Chryse Planitia (i.e., they are prows for many of the channel bars), then become subtle, mostly buried and modified in southern Acidalia, and finally disappear farther north; and (4) fractures and grooves are sparse and primarily align in the direction of flow in southernmost Acidalia Planitia (including within a large, degraded, infilled crater) and then become more polygonal in pattern farther north; some of the grooves have wide flat floors and have been interpreted to form by compaction of sediments hundreds of meters thick [2,3].

TABLE 1. Crater densities of basin units in Chryse and Acidalia Planitiae, Mars (after mapping of [1]).

Map Unit	Area of Count (km^2)	Cumulative no. of Craters per 10^6 km^2 >2 km	>5 km	Relative Age*
AHcc	514,440	280 ± 23	60 ± 1	LH/EA
AHcs	276,340	326 ± 34	76 ± 17	LH/EA
AHcr	236,100	356 ± 39	93 ± 20	LH/EA
Hchl	410,070	285 ± 26	83 ± 14	LH/EA
Hr	230,240	747 ± 57	230 ± 32	LN/EH

* Based on crater-density stratigraphy of [7]; N = Noachian, H = Hesperian, A = Amazonian, E = Early, L = Late.

How thick are the sediments? Considering that channel terraces, wrinkle ridges, and degraded crater rims may be tens to hundreds of meters high [4], it appears that thicknesses of a few tens of meters may not be readily detected in most Viking images. As thickness approaches 100 m, landforms such as wrinkle ridges, smaller craters, and thinner channel bars may appear subdued. Those features would likely disappear for thicknesses of a few hundred meters, whereas large craters would appear buried and compaction fractures would become evident. As sediment thickness reaches several hundred meters, most large craters would disappear (given that large degraded martian crater rims seldom exceed 500 m in height in the planet's highlands [5], where they generally appear higher than in the northern plains). These geomorphic indicators observed in Chryse indicate progressive, northeastward thickening of basin sediments from on the order of 100 m near the mouths of Kasei and Simud/Tiu/Ares Valles in western and southern Chryse Planitia to a few hundred meters into southern Acidalia Planitia.

The Mars Pathfinder landing site (latitude 19.5°N, longitude 32.8°) lies on unit Hchl below the mouth of Ares Vallis. Here, the unit consists of a broad flood plain marked by bars and a few small knobs. The plain is likely made up of a thin veneer (tens of meters?) of flood deposits (none of the above sediment thickness indicators are observed).

References: [1] Rotto S. and Tanaka K. L. (1995) *USGS Map I-2441*, in press. [2] Lucchitta B. K. et al. (1986) *Proc. LPSC 17th*, in *JGR, 91*, E166–E174. [3] McGill G. E. and Hills L. S. (1992) *JGR, 97*, 2633–2647. [4] Golombek M. P. et al. (1991) *Proc. LPS, Vol. 21*, 670–693. [5] Roth L. E. et al. (1989) *Icarus, 79*, 289–310. [6] Kargel J. S. et al. (1995) *JGR, 100*, 5351–5368. [7] Tanaka K. L. (1986) *Proc. LPSC 17th*, in *JGR, 91*, E139–E158.

HARDPAN AND OTHER DIAGENETIC "ROCK" IN THE CATCHMENT OF ARES VALLIS AND SURROUNDING AREAS. A. H. Treiman, Lunar and Planetary Institute, 3600 Bay Area Boulevard, Houston TX 77058-1113, USA.

The Mars Pathfinder landing site, in the outflow plains of Ares Vallis, will presumably present a "grab bag" of many rock types transported from upstream. Based on the geology of the Valles Marineris (just southwest of Ares Vallis), the Ares Vallis catchment could include hardpan and other diagenetic "rocks" lithified by low-temperature aqueous solutions. The chemical effects of diagenesis may be detectable with the M/P APX instrument; if present, but unrecognized, diagenetic effects could lead to erroneous geochemical inferences.

Extensive Hardpan: The "cliffs" at the wall tops in Valles Marineris represent an extensive hardpan horizon [1] (Fig. 1). The cliffs represent a relatively resistant packet of layers: an upper darker layer (~50 m thick); a central brighter layer (~250 m thick); and a lower dark layer (~100 m thick). The layer packet is exposed on chasma walls from western Noctis Labyrinthus (110°W, VO

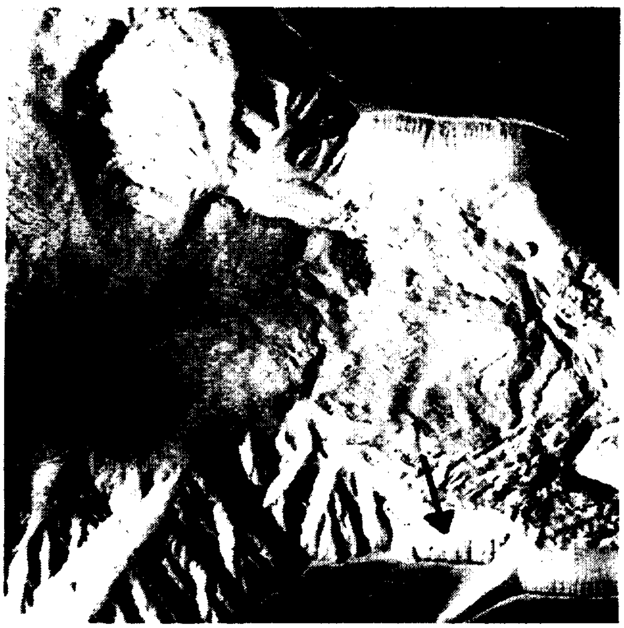

Fig. 1. Wall-top layering, southeast wall of Hebes Chasma (arrow) near top of landslide scarp (~2 km tall, ~30° slope angle). VO915A06 (2.2°S, 73.5°W), scale bar 10 km.

423A75) to eastern Eos Chasma (31°W, VO 964A22), and in continuous reaches of 200–300 km of wall in Hebes, Ius, Eos, and Coprates Chasmae. The packet is visible on all planar chasma walls (fault or landslide) where Viking orbiter or Mariner 9 image resolutions are <150 m, and rarely on spur-and-gully walls or in images of poorer resolution. The packet appears at the same stratigraphic position (<50 m from the wall tops) and thickness (400 ± 200 m) over this huge area, independent of elevation (3–10 km), age of adjoining plateau surface (Noachian through upper Hesperian), and geological structures (e.g., impact craters, Fig. 2).

Fig. 2. South wall of Gangis Chasma, VO014A30 (centered 9.7°S, 44.6°W), oblique view south, scale bar 10 km E–W at wall. Layering (arrows) undeflected from plains to crater floor under crater rim. An extra layer to west thickens and deepens beneath crater.

From its continuity and consistent stratigraphy, the layer packet appears to be a single geologic feature, exposed discontinuously over the whole Valles Marineris (4000 km E–W, 800 km N–S). Age relations between geology of the plateaus and the layering packet suggest that it did not form by deposition. If the layers were deposited in Noachian times, they should dip beneath the resurfacing materials of the Hesperian-aged ridged plains of Lunae and Syria Planae. However, the layers remain at the wall tops. If the layers were deposited in Hesperian times, they should not be present under Noachian-aged plateaus; they are present. Nor can a depositional origin explain the continuity of the packet beneath impact craters (Fig. 2).

However, a diagenetic origin for the layering, alteration of preexisting material *in situ*, can explain its structure transgressions, stratigraphic transgression, and lateral extent. Diagenetic effects controlled by proximity to the ground surface would appear independent of surface elevation, and transgress pre-existing features, including the boundary between Noachian and Hesperian deposits and the structures and lithologic changes beneath and inside impact craters [2]. Given similar compositions and permeabilities to fluids, diagenetic transformations should affect all earlier materials, regardless of their ages. And diagenetic layers can be of regional extent, like hardpans or calcretes on Earth. Diagenesis has been invoked to explain rock shapes at Viking lander sites and clodding of near-surface sediment [3,4], but not for the extent or thickness of the upper-wall layers in Valles Marineris.

Similar upper-wall layering is visible in the Ares Vallis catchment, although neither exposures nor image resolutions are as good as for Valles Marineris. The layering packet appears present at Hydaspis Chaos (1.6°N, 29.6°W; VO083A34) and Iani Chaos (2.6°S, 48.59°W; VO405B09), and in some crater walls (6.5°N, 19.9°W; VO745A31). Hardpan material from these layers could have been transported to the Mars Pathfinder landing site.

Hardened Fault Zones: Some graben-bounding faults on the plateaus adjacent to Valles Marineris appear to continue as ridges on the walls of chasmae. These ridges are most prominent at the boundary between Ophir and western Candor Chasmae (Candor Labes, 4.5°S, 72°W), and are now under study. The ridges are probably relict fault zones, cemented and hardened by precipitates from aqueous solutions [e.g., 5].

Conclusion: Rocks and regolith in the Ares Vallis catchment may have been chemically and structurally affected by aqueous solutions under diagenetic conditions. On Earth, hardpans can be cemented by Ca carbonate, Ca sulfate, salts, iron oxide hydroxides, clays, and silica. The chemical signatures of the first three cements may be directly detectable with the Mars Pathfinder APX instrument (as C, S, and Cl). Chemical signatures of the last three may not be detectable directly, and could lead to geochemical errors. For instance, an ironstone hardpan developed in basalt could masquerade as a ferroan ultramafic lava.

References: [1] Treiman A. H. et al. (1995) *JGR*, in press. [2] Melosh (1989) *Impact Cratering*. [3] Fuller and Hargraves (1978) *Icarus, 34*, 614. [4] Jakosky and Christensen (1986) *JGR, 91*, 3457. [5] Mozely and Goodwin (1995) *Geology, 23*, 539.

Field Trips Accompanying the Mars Pathfinder Landing Site II Workshop: Channeled Scabland and Lake Missoula Break-out Areas in Washington and Idaho

Edited by
Kenneth S. Edgett
Department of Geology
Arizona State University
Box 871404
Tempe AZ 85287-1404

and
James W. Rice Jr.
Department of Geography
Arizona State University
Box 870104
Tempe AZ 85287-0104

with major contributions by
Victor R. Baker
Department of Geosciences
University of Arizona
Tucson AZ 85721

INTRODUCTION

On July 4, 1997, Mars Pathfinder is scheduled to land near 19.5°N, 32.8°W, in a portion of Ares Vallis. The landing ellipse covers a huge (100 x 200 km) area that appears to include both depositional and erosional landforms created by one or more giant, catastrophic floods (Golombek et al., 1995).

One of the best known terrestrial analogs to martian outflow channels (such as Ares Vallis) is the region known as the Channeled Scabland (Figs. 1–4; Baker and Milton, 1974). The Channeled Scabland and other associated landforms in the states of Washington, Idaho, Oregon, and Montana, were carved by multiple catastrophic releases of water from the Ice Age Lake Missoula (Fig. 1; Baker and Bunker, 1985).

This guide describes some of the geomorphological features of the Channeled Scabland and adjacent Lake Missoula break-out area near Lake Pend Oreille, Idaho. The guide is prepared for two field trips that accompany the Mars Pathfinder Landing Site II Workshop in Spokane, Washington, September 28–29, 1995. Field Trip I is based in Moses Lake, Washington, and runs September 24–27, 1995; Field Trip II is based in Spokane, Washington, and occurs on September 30, 1995.

Field Trip I— The Channeled Scabland

Field Trip I, to the Channeled Scabland of Washington, includes aircraft overflights of the Channeled Scabland region in conjunction with a ground trip by chartered bus. The purpose of the field trip is to investigate landforms and geologic features on Earth that are similar to those present at or near the Ares Vallis landing site. The field trip is expected to provide a geomorphic and visual framework for interpreting the Ares Vallis site in 1997. The aircraft overflights are crucial to understanding the full three-dimensional context and history of the immense landforms produced by the Missoula Floods, as well as the much larger flood features in Ares Vallis (Fig. 4). The combination of overflights and ground trips on Field Trip I will help the participants gain an intuitive understanding of the relationship between the flood geomorphology that is obvious when seen from above, and more subtle and difficult to interpret when seen from the ground. Most of the field stops in this guide were chosen to give participants an opportunity to visit, in person, the terrains that are both characteristic of the Channeled Scabland, and might occur at the Ares Vallis landing site. Areas of the Scabland to be investigated include the streamlined loess islands and flood sediments of the Cheney-Palouse area, the Dry Falls, giant current ripples, and the deposits of the Ephrata fan.

Field Trip I Education Outreach

Field Trip I is designed to bring together Mars Pathfinder scientists and engineers, K–12 educators from Washington and Idaho, and other interested members of the Mars scientific community. Eleven K–12 educators (and five alternates) were competitively selected in April 1995 to participate in Field Trip I on the basis of planned

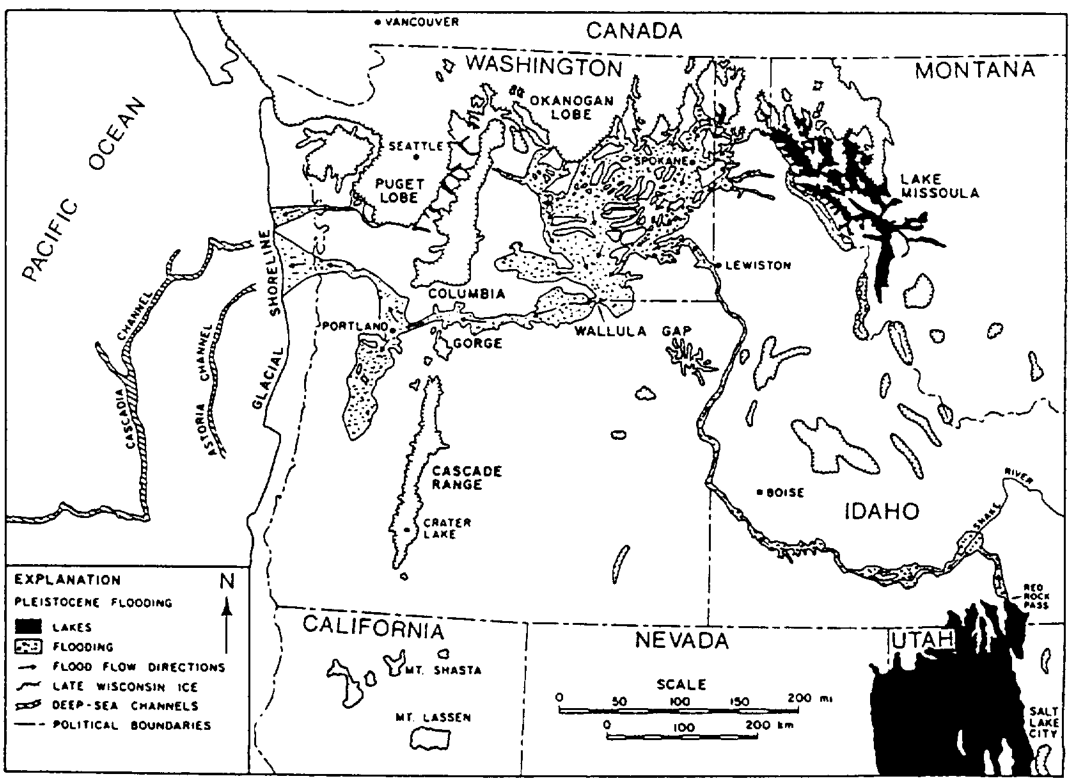

Fig. 1. Areas in the northwestern U.S. affected by catastrophic flooding during the last Ice Age. The Channeled Scabland covers much of central and eastern Washington, and resulted mainly from drainage of Lake Missoula. Figure source: Baker and Bunker (1985).

educational follow-up activities involving students, teachers, and parents in their home communities. (Part II of this Technical Report, to be printed in late 1995, will include additional information on how the educators were selected and the results of their education outreach efforts.) This meeting of K–12 educators and Mars Pathfinder scientists and engineers is intended to provide a forum for direct interaction between the two groups. Education outreach and enhancement is an important goal of the Mars Pathfinder project and of NASA in general (e.g., NASA, 1992; Edgett and Christensen, 1995; Edgett et al., 1995). We hope that the professional relationships fostered on this field trip will lead to additional interaction between educators, students, and communities, with NASA / Mars Pathfinder personnel (and other Mars scientists), throughout the course of the Mars Pathfinder mission.

Field Trip II— Lake Missoula Break-Out

Field Trip II examines catastrophic flood landforms associated with the break-out area where Lake Missoula was dammed by glacial ice. Like Field Trip I, this bus trip examines landforms that may be similar to features in Ares Vallis. The landforms include streamlined islands, giant current ripples, butte-and-basin scabland, and slackwater sediments from Lake Pend Oreille downstream through Rathdrum Prairie, Spokane Valley, and into the Cheney-Palouse scabland. The trip is designed to provide people who did not participate in Field Trip I with a sense of the immense flood landforms produced by catastrophic floods, while at the same time offering Field Trip I participants an opportunity to see the region through which much of the Lake Missoula flood water traveled before carving the rest of the Channeled Scabland. A highlight of the trip will be the examination of flood features near the southern end of Lake Pend Oreille, Idaho. O'Connor and Baker (1992) calculated that at peak discharge, at least 17 million m^3/s of Lake Missoula water poured through the Rathdrum valley from the break-out point near Lake Pend Oreille. The ice dam which contained Lake Missoula during the late Pleistocene was part of the Purcell Trench Lobe of the Cordilleran Ice Sheet. Present-day Lake Pend Oreille was once covered by the Purcell Trench Lobe, and much of Lake Missoula's flood waters emanated from this area.

More Information on Scabland and Mars Pathfinder

This field trip guide is deliberately geared toward interpretation of landforms that may be present at the Mars Pathfinder landing site in Ares Vallis. For more detailed information, readers should consult the references, particularly other field guides about the Channeled Scabland and Lake Missoula floods features: Baker and Nummedal (1978), Breckendridge (1989a), Othberg and Breckenridge (1992), Waitt et al. (1994), and O'Connor and Waitt (1995). A recent non-technical article about the Channeled Scabland was written by Parfit (1995). Non-technical books about the Channeled Scabland include those by Allen and Burns (1986) and Wies and Newman (1989). Reviews regarding martian outflow and other channels include: Baker (1982), Mars Channel Working Group (1983), and Baker et al. (1992). Mars Pathfinder and landing site selection was partly detailed in a technical report edited by Golombek (1994), and in the abstract by Golombek et al. (1995). Recent non-technical articles about Mars Pathfinder include those by Robertson (1994) and Bullock (1994).

Field Trip Road Logs

The road logs in this field guide were compiled in June 1995. References to artificial landmarks (road signs, status of road pavement, etc.) were accurate as of June 1995. Units of measure throughout are a mixture of English and metric units. English units are used to indicate miles that vehicles must travel and participants must hike. English units are used in the road log because odometers in U.S. vehicles measure distances in miles. Metric units are used when describing the dimensions of landforms or human-made structures. Some of the stop descriptions in the road logs are summaries of material in field guides by Nummedal (1978) and Waitt et al. (1994).

Field Trip Responsibility and Acknowledgments

Both field trips are convened by Kenneth S. Edgett and James W. Rice Jr. of Arizona State University, and led by Victor R. Baker of the University of Arizona. Educational activities associated with the field trips are coordinated through the Arizona Mars K–12 Education Program (Arizona State University / Mars Global Surveyor Thermal Emission Spectrometer Project) with assistance from Jo Dodds of O'Leary Junior High School, Twin Falls, Idaho. The road logs were compiled by K. Edgett and J. Rice with assistance and advice from V. Baker and Matthew P. Golombek. Photographs in this guide not credited to another source were taken by K. Edgett, June 7–15, 1995. The field trips are sponsored by (in alphabetical order) Arizona State University (Tempe, Arizona), the Jet Propulsion Laboratory (Pasadena, California), the Lunar and Planetary Institute (Houston, Texas), and NASA Headquarters (Washington, DC).

The editors are grateful to Maureen Harder for assistance with Field Trip I, Day 3 sites; Herman Harder for showing us the natural land bridge on his property in the Cheney-Palouse Scabland, and Virginia Harder for access to the loess island. We also thank Mikki Kisson of the Ice Age Floods Institute and Eugene P. Kiver and Dale F. Stradling of Eastern Washington University for suggestions and advice on sites to visit in the Channeled Scabland. We thank Jeff Akridge of Columbia Pacific Aviation for his role in setting up the overflights. Philip R. Christensen, Deb Wakefield, Brigitte Rigberg, Kelli Mellgren, Kathy Patoni, and Rebecca Rowell at Arizona State University are acknowledged for their assistance with the education program. Finally, we express many thanks to LeBecca Simmons of the Lunar and Planetary Institute for help in arranging the field trips.

THE SPOKANE FLOOD CONTROVERSY

Bretz's Outrageous Hypothesis

The Spokane Flood controversy is both a story of ironies and an illuminating display of the scientific method in action. In a series of papers published between 1923 and 1932, J Harlen Bretz stunned the geological community with his work on an enormous network of proglacial channels which were incised into the loess and basalt of the Columbia Plateau in eastern Washington. Bretz named this region the "Channeled Scabland." This area contained erosional and depositional features that were unique among fluvial phenomena (Bretz, 1923). It should be remembered that the field work done by Bretz was accomplished without the aid of aerial photographs and adequate topographic maps. He argued that the landforms present could only be explained as the product of an enormous but brief flood, which he named the "Spokane Flood." One look at a satellite image of the Channeled Scabland (Fig. 2) reveals the complex pattern of anastomosing channels, cataracts, and loess islands which typify the region.

Alternative Explanations for the Scabland Origin

Bretz met doubt all along the way with his theory about the Spokane Flood. In 1927, W. C. Alden warned of the difficulties with the flood theory even though he had no personal field experience in the region. Alden (1927) suggested that the rock basins might be collapsed lava caves. O. E. Meinzer (1927) claimed that the glacially swollen Columbia River could have cut the Dry Falls and deposited the huge gravel fan of the northern Quincy Basin. E. T. McKnight (1927) also subscribed to the glacially diverted Columbia River theory as the erosive agent responsible for the resultant landforms of the region. Yet another who was upset with Bretz's hypothesis was James Gilluly. Even though he had not been to the Scabland, Gilluly (1927) stated that the unusual landforms present in the region were created by long, continued erosion of present-sized streams. Gilluly would later change his mind when many years later he finally visited the Channeled Scabland. He was said to have commented, "How could anyone have been so wrong?"

J. T. Pardee found Bretz's flood hypothesis to be quite interesting. Pardee had been sent by Alden, who was the Chief of Pleistocene Geology for the U.S. Geological Survey at the time, to study the Scabland region. Communication between Bretz, Pardee, and Alden suggests that Pardee was considering the hypothesis that the sca-

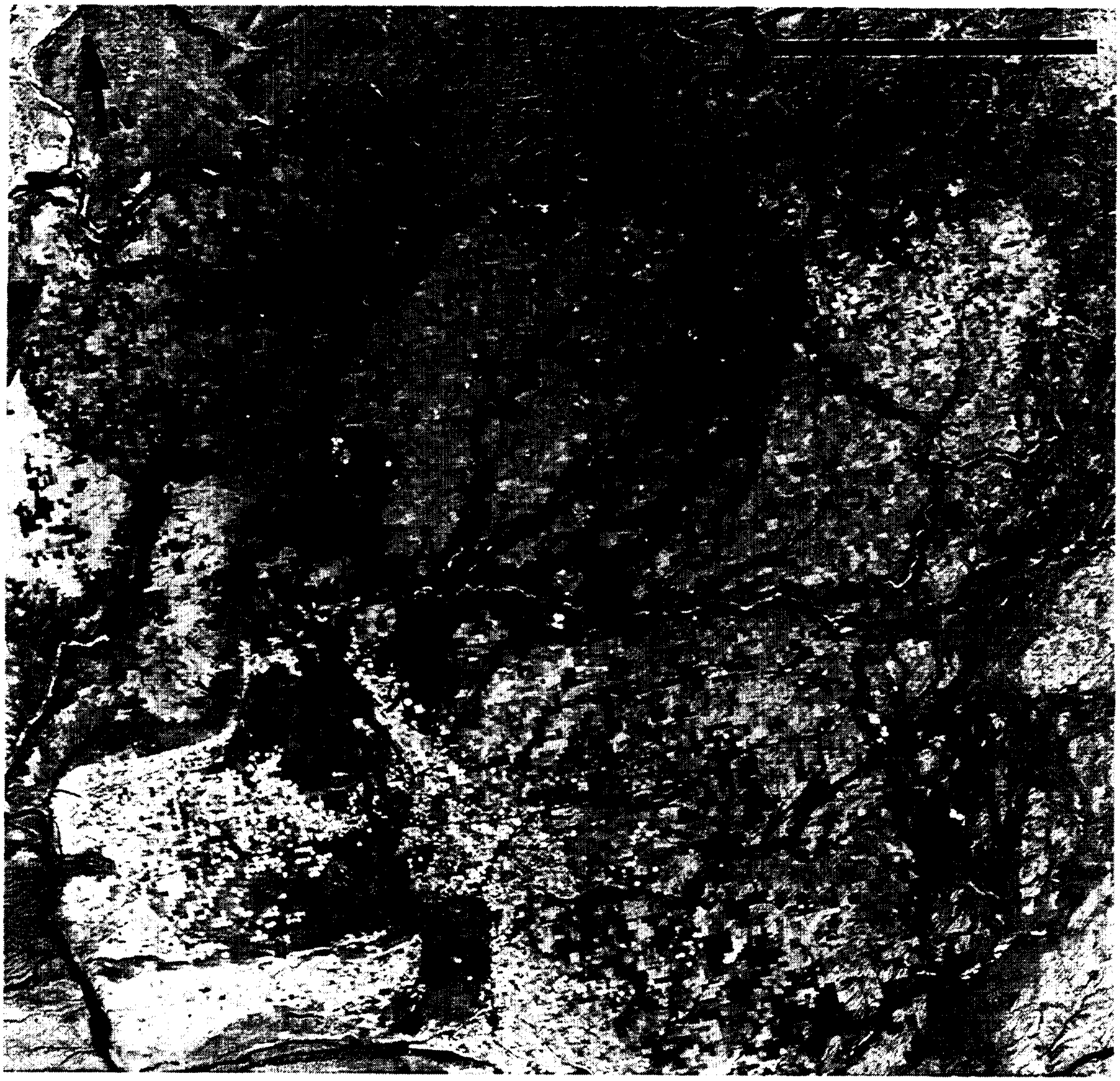

Fig. 2. Landsat image of the Channeled Scabland of Washington, obtained on September 29, 1992; exactly three years to the week before the field trips described in this guide. Image centered at 47° 27' N, 118° 49' W. From the U.S. Geological Survey EROS Data Center, Sioux Falls, South Dakota, Entity ID No. LM5044027009227390.

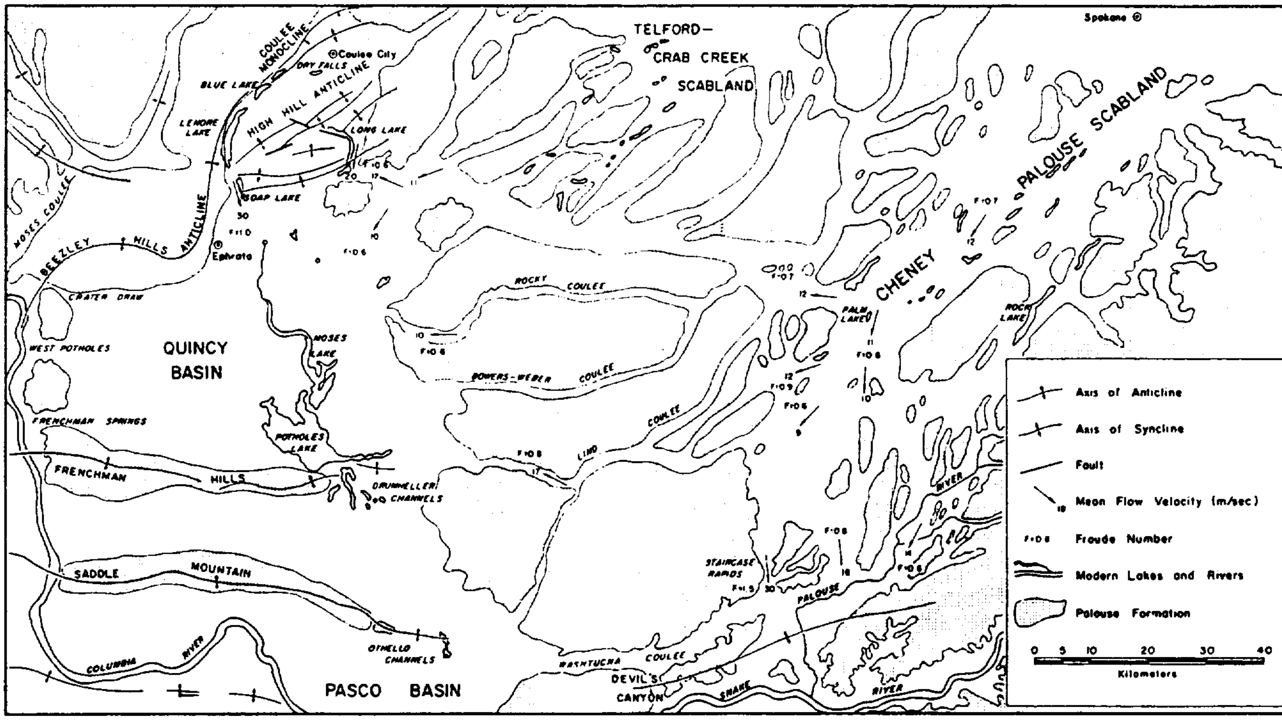

Fig. 3. Regional paleohydraulic features of the Channeled Scabland. Mean flow velocities were determined from high-water mark evidence and channel geometery by Baker (1973). Also shown is the regional structural pattern for the Columbia Plateau. Structure played an important role in determining where the channels flowed and whether there was deposition or erosion. This figure should be used as a reference to compare with Fig. 2. Figure from Baker (1978a).

bland might indeed be related to drainage of a large Pleistocene lake that he had studied in western Montana (Pardee, 1910). Pardee's observations would predate Bretz's work in the area by 13 years. However, Alden dissuaded Pardee from reporting on this hypothesis.

Eventual Acceptance of the Spokane Flood Theory

One of the major complaints with Bretz's Spokane Flood theory was the difficulty with identifying the source of this great flood. Bretz finally solved the source problem in 1928. Bretz (1930) later published the discovery that scabland flooding resulted from the rapid failure of an ice dam that formed glacial Lake Missoula.

Finally, Pardee (1942) shared his observations of glacial Lake Missoula, which firmly established the lake's role as the source of catastrophic floods that went through the scablands. Evidence for the ice dam failure includes several scoured constrictions in the Lake Missoula basin, enormous bars of current transported debris, and giant ripple marks with heigths of 15 m and spacings of 200 m. Thus, glacial Lake Missoula became the obvious source for the catastrophic floods required by Bretz's hypothetical origin of the Channeled Scabland. However, Pardee did not state the obvious connection, perhaps leaving that point generously to Bretz. In 1956 Bretz, H. T. U. Smith and George Neff answered with extensive detail all previous criticisms of the flood hypothesis. New topographic maps and excavations proved that the gravel hills called "bars" by Bretz were in fact subfluvial depositional bedforms. The most obvious confirmation of the flood hypothesis was the identification of giant current ripples on upper bar surfaces. These observations indicated that bars 30 m high were completely submerged by enormous floods.

PHYSIOGRAPHY OF THE SCABLAND REGION

The Channeled Scabland of eastern Washington is comprised of complex anastomosing channels, cataracts, loess islands, and immense gravel bars, all of which were created by catastrophic fluvial erosion of the loess and basalt surfaces of the Columbia Plateau. The erosion and deposition that produced the scabland topography resulted from the failure of the ice dam impounding glacial Lake Missoula. This lake discharged as much as 21.3 x 10^6 m^3/s into the vicinity of Spokane Valley (Baker, 1973).

Freeman et al. (1945) formalized the physiographic divisions of the regions covered in this report (Fig. 5). The entire field area lies in the Columbia Basin Subprovince of the Columbia Intermontane Physiographic Province. The Columbia Basin is a regional lowland surrounded by the Blue Mountains to the south, Cascade Mountains to the west, the Okanogan Highlands to the north, and the mountains of northern Idaho in the east.

The western part of the Columbia Basin, called the Yakima Folds, consists of a series of anticlinal ridges running eastward from the Cascade Mountains. Several of these ridges are transected by the Columbia River. From north to south, these ridges are: the Frenchman Hills, Saddle Mountains, and Horse Heaven Hills.

The far eastern portion of the Columbia Basin is characterized by relatively undeformed basalt overlain by as much as 75 m of Pleistocene loess. The loess has been dissected to form a rolling landscape termed the Palouse Hills. Elevation of the Palouse Hills declines from about 750 m on the northeastern margin to 100–120 m

Fig. 4. The outflow channels on Mars are much larger than the valleys of the Channeled Scabland of Washington. The small photograph in the lower left corner shows a Landsat image of the Channeled Scabland at the same scale as the Mars photomosaic. Note the size of the Mars Pathfinder landing ellipse (upper right) relative to the Channeled Scabland photograph. This figure is modified from NASA Photograph 84-H-430 (Meszaros, 1984), available from the National Space Science Data Center, Greenbelt, Maryland.

in the southwest. This gradient reflects the regional dip of the basalt toward the center of the Columbia Basin.

The Yakima Basalt comprises the bedrock in all but a few parts of the Channeled Scabland. This basalt unit is part of the extensive Neogene (23.7–1.6 m. y. a. (million years ago)) eruptions of plateau basalts that cover over 250,000 km^2 in parts of Washington, Oregon, and Idaho. Most of the lava was erupted in the Miocene Epoch (23.7–5.3 m. y. a.). The flows are thick, and several can be traced for over 150 km. Structural and lithologic variation can be found in the basalt sequence, including joint patterns, pillow-palagonite complexes, and sedimentary interbeds from Miocene lakes.

During the Pliocene (5.3–1.6 m. y. a.), extensive basalt deformation occurred. The entire Columbia Plateau was regionally tilted from an elevation of 760 m in the northeast to about 120 m in the southwest near Pasco, Washington. The east-west fold ridges (the Yakima Folds) are superimposed on this regional structure. The upraised northern rim of the plateau is significant for the flood history of the Channeled Scabland, because only a truly phenomenal amount of water could fill the great canyon of the Columbia River between Spokane and Coulee Dam. That filling would have had water spilling over the northern rim of the plateau and flowing south-westward, carving the huge scabland channels.

MULTIPLE SCABLAND FLOODS

Some flood events in the Scabland pre-date the most recent (Wisconsin— 75,000–10,000 years before present) ice age floods caused by Lake Missoula. The earliest episode of flooding in the Channeled Scabland occurred prior to the deposition of the extensive Palouse Formation (Baker, 1973). The earliest Missoula Flood deposits are overlain by younger pre-Palouse loess and petrocalcic soil. The early Quincy Basin flood deposits came from an unknown source to the west across the Babcock Ridge. These flood deposits are overlain by other flood deposits of Bull Lake age (Illinoian) which were also derived from a western source (Baker, 1973). Catastrophic

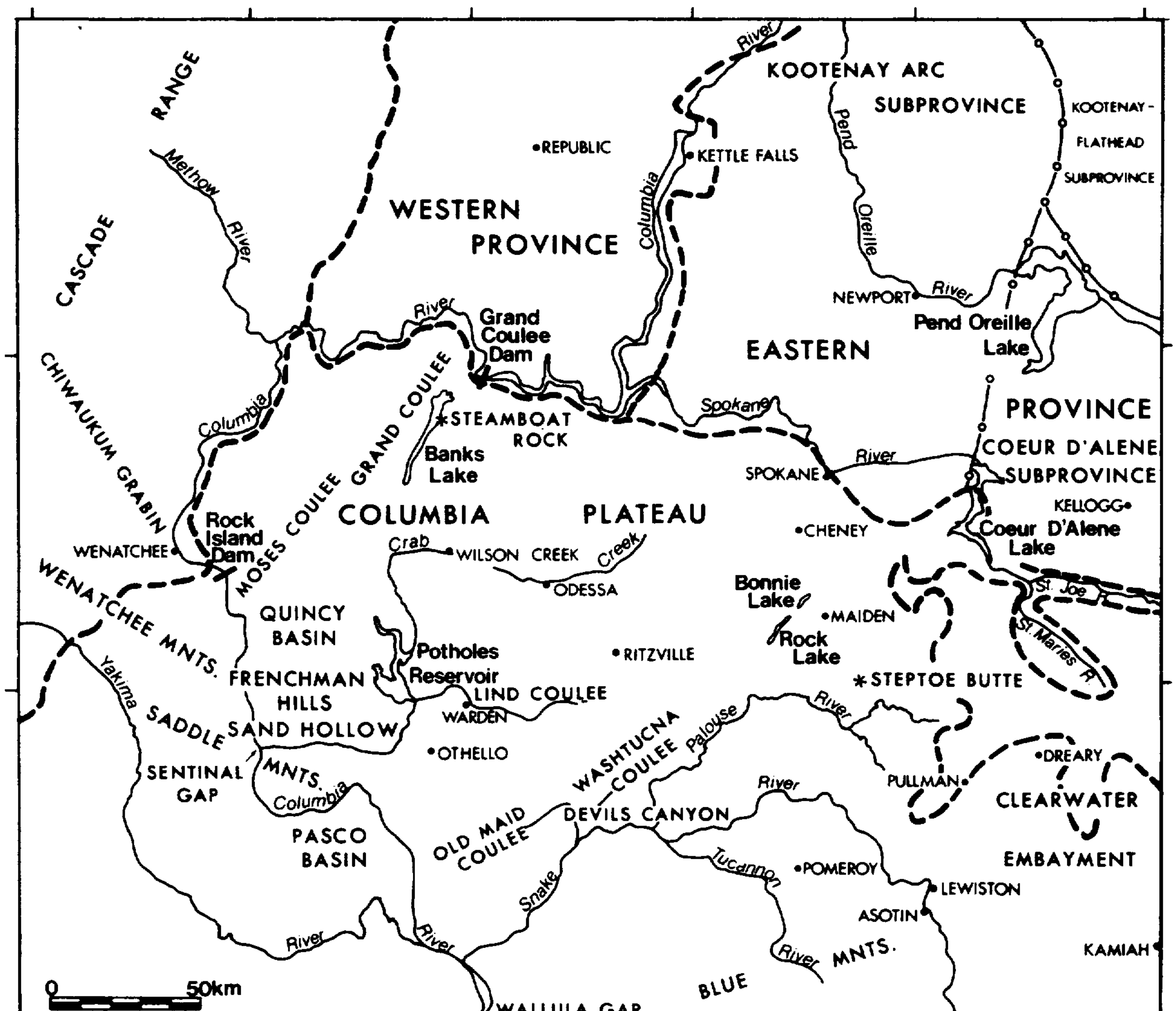

Fig. 5. Index map of localities in the Columbia Plateau region. Figure source: Baker and Nummedal (1978).

flooding from Lake Bonneville also affected the southern margins of the Channeled Scabland about 14,500 years ago (O'Connor, 1993).

The last major flood episode occurred between 17,000 and 12,000 years ago. It probably consisted of at least two major outbursts from Lake Missoula (Baker, 1973). The older flood affected Moses Coulee, the Grand Coulee, and the eastern Channeled Scabland. The second outburst involved less volume than the first and coincided with the retreat of the Okanogan ice lobe (Easterbrook, 1976). The very last phase of flooding also involved catastrophic flow down the Grand Coulee. Mount St. Helens Set S ash occurs as couplets and triplets in fine-grained clastic sediments called "slack-water" deposits. Mullineaux et al. (1978) have stated that tephra Set S dates the last major Scabland flood. They support the age estimate of 13,000 years for the flood with a radiocarbon date of 13,080 ± 350 on peat directly overlying the Portland delta, a Missoula Flood deposit located at Portland, Oregon. Waitt (1977) offers detailed evidence for late Pleistocene catastrophic flooding travelling down the Columbia River, through the area blocked by the Okanogan ice lobe until 13,500 years ago. Ice-rafted erratic boulders and dipping crossbeds in gravel indicate that this flood was up to 400 m deep.

Bretz (1969) proposed as many as eight seperate scabland floods; this was based on the physiographic evidence. However, Baker (1973) stated that some of the physiographic relationships which Bretz studied could be explained by a single flood. The number of late-Wisconsin age floods which poured through the region remains quite controversial today. Waitt (1980) found rhythmite beds (formed in slack-water deposits) around the Scabland which suggest that there was on the order of 40 late-Wisconsin floods. Atwater (1986) counted about 89 separate flood events, and Waitt et al. (1994) suggest that "a round number of 100 is currently the best estimate of the number of Missoula floods during the late Wisconsin glaciation."

Loess islands. The erosional loess remnants are the most obvious landforms of the Cheney-Palouse scabland tract. These streamlined hills have sharp upstream prows, steep faceted flanks, and long tapering tails (Baker and Nummedal, 1978). There are three different forms of streamlined islands: submerged, partially submerged, and unsubmerged (Fig. 7).

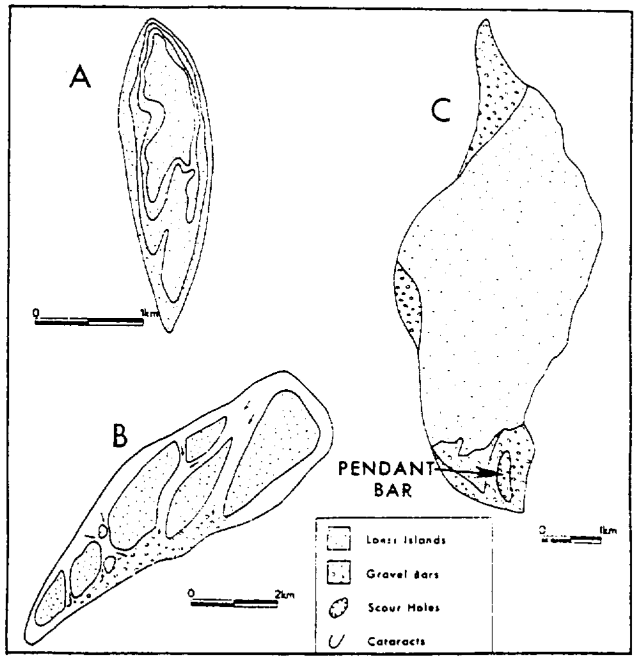

Fig. 7. Loess island forms in the Cheney-Palouse scabland, illustrating the three major morphologic types. (A) Subfluvially eroded loess island. (B) Partially submerged island, with arrows indicating subfluvial areas. (C) Unsubmerged loess island. The gravel pattern denotes depositional material. These maps are based on actual examples found in the Scabland. Source: Patton and Baker (1978).

LARGE EROSIONAL AND DEPOSITIONAL LANDFORMS OF THE CHANNELED SCABLAND

Erosional Landforms

Sequence of erosional landforms. The processes which formed the scablands are very similar to those in modern rivers, but they acted on an enormous scale (Baker, 1973). The progressive erosion of a typical scabland divide crossing is envisioned as follows (see Fig. 6, on next page): The initial flood water that overtops the crossing encounters soft Palouse loess (Phase I). The high velocity water easily erodes the loess and exposes the underlying basalt. This process leaves behind streamlined loess hills (Phase II). The now-exposed basalt entablature then yields to longitudinal groove development (Phase III). This process is associated with longitudinal roller vortices and vertical vortices (kolks) that pluck away at the basalt colonnades. The enlargement and coalescence of the resultant potholes surfaces then leads to the formation of the butte-and-basin topography that characterizes the Channeled Scabland (Phase IV). The final stage of this progression of landforms is the formation of a prominent inner channel (Phase V).

Butte-and-basin topography. This is the most common landscape in the scabland tract. The usual development is small channels and rock basins surrounding buttes and mesas. The total relief of this topography is on the order of 30–100 m (Baker and Nummedal, 1978).

Longitudinal grooves. When large expanses of basalt are eroded by catastrophic floods, a characteristic form appears in the form of a series of elongate grooves (Fig. 8). The grooves have their long axes parallel to the stream's flow. Their average depth is on the order of 5 m and width is 50 m (Baker, 1973).

Cataracts and inner channels. The cataracts and inner channels of the Scabland, particularly in the Dry Falls area, constitute some of the most spectacular landforms in the region. Dry Falls is the most impressive; it is 6 km wide and 120 m high. Bretz et al. (1956) observed that most cataracts form subfluvially (instead of plunge pool undercutting like at Niagara Falls in New York and Ontario). The headward retreat of cataracts creates the inner channels.

Depositional Landforms

Giant current ripples. These landforms create a pattern of parallel ridges and swales (Figs. 9–11), and were termed "giant current ripples" by Bretz et al. (1956). The giant current ripples are the most important bedforms used in paleohydraulic reconstruction

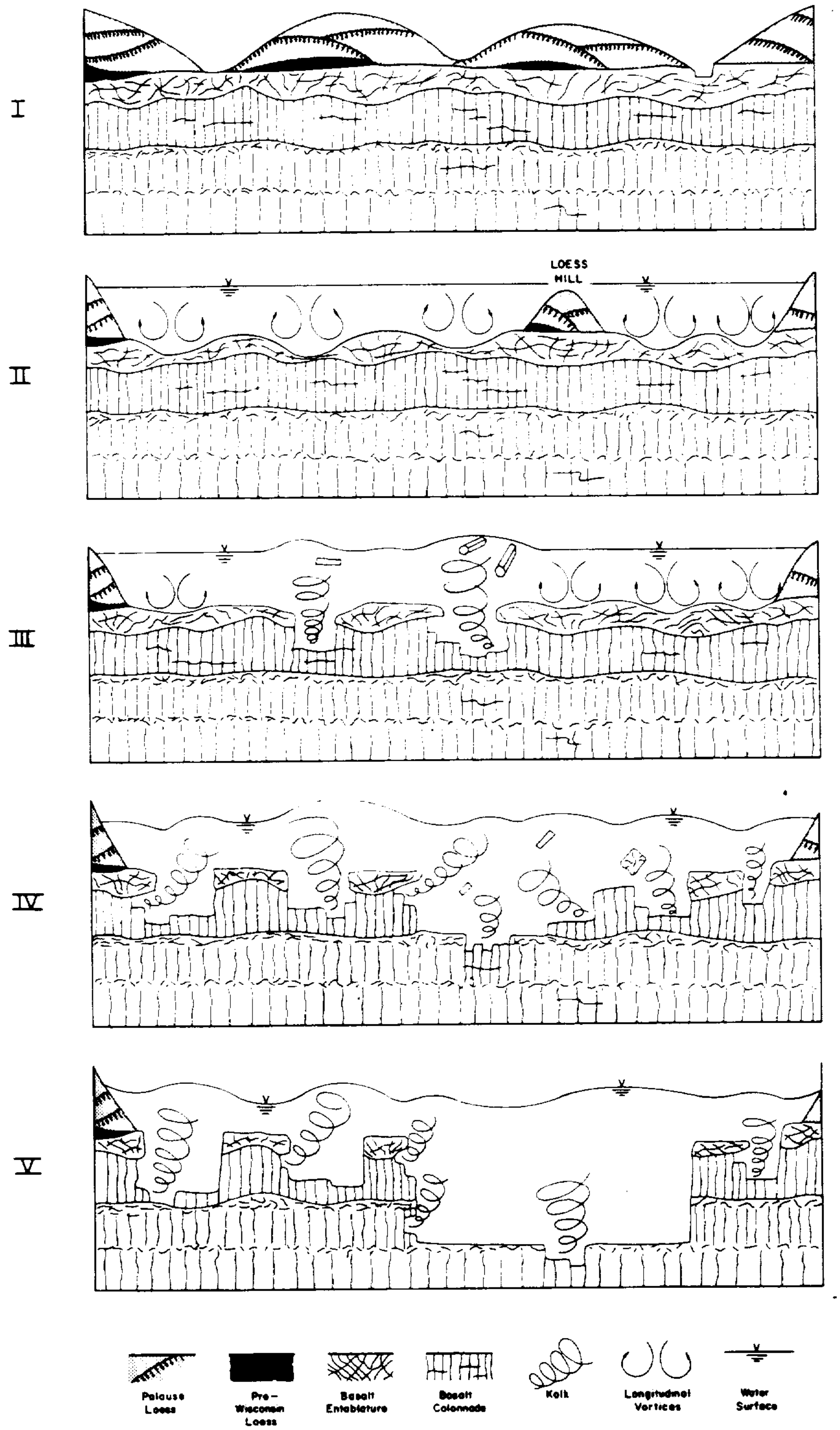

Fig. 6. Hypothetical sequence of flood erosion for a typical scabland divide crossing. This diagram should be helpful in understanding the processes which created landforms in the Grand Coulee and Cheney-Palouse Scabland, for example. Source: Baker and Nummedal (1978).

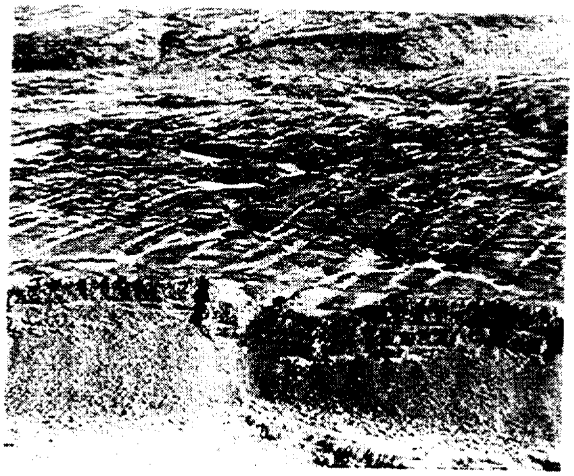

Fig. 8. Oblique aerial view of the longitudinal grooves eroded into basalt north of Dry Falls. The grooves are spaced about 50 m apart. Source: Nummedal (1978).

of the final major scabland flood (Baker, 1973). There are over 100 sets of these bedforms in Missoula flood channels. These ripples have chords ranging from 20–200 m and heights from 1–15 m (Baker and Nummedal, 1978). The ripples have asymmetric profiles, with the downstream facing slopes (lee sides) averaging 18–20 degrees; the upstream slopes (stoss sides) are 6–8 degrees. The giant current ripples are very difficult to recognize on the ground; they are best

Fig. 10. Oblique aerial view of Malaga, Washington, giant current ripples at low incident sun angle. Photo by David A. Rahm, from Baker and Nummedal (1978) with permission of V. R. Baker.

seen from the air. The sediment making up these ripples ranges from 1.5 m to granule-gravel size material. The median size particles fall into the pebble class (Fig. 12).

Pendant bars. Pendant bars (Fig. 7) are not confined to any certain geomorphic settings within the Cheney-Palouse scabland tract. These bars are found in all sizes of channels, but are rarely found in the deepest channels. Pendant bars are commonly found along the sides or margins of flow and where resistant basaltic knobs create flow obstructions from which the bars can accumulate (Baker

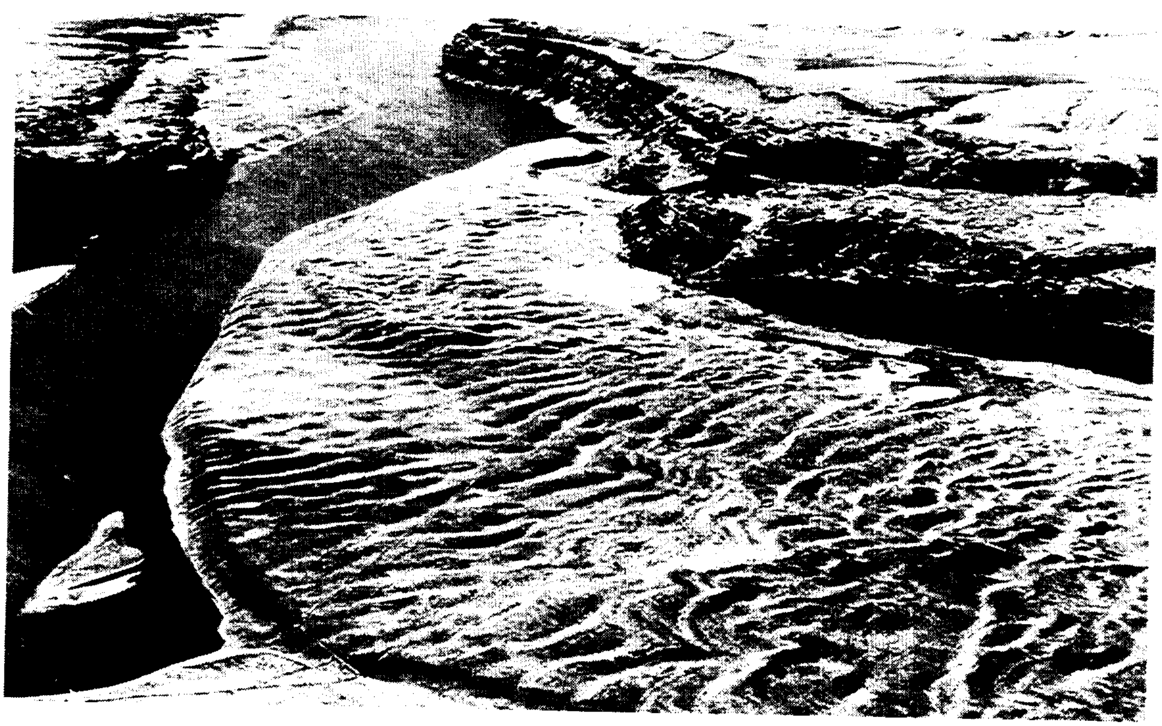

Fig. 9. Oblique aerial view of the West Bar giant current ripples, with the Columbia River to the left. Photograph 5595 by John S. Shelton, obtained from Baker and Nummedal (1978) with permission from V. R. Baker.

Fig. 11. Giant current ripples at Spirit Lake, Idaho. These ripples are overgrown with pine trees, which help to emphasize the location of ripple troughs in this oblique view. Source: Baker and Nummedal (1978).

and Nummedal, 1978). Pendant bars may extend downstream 1.5 km or more from their points of attachment, and have gravel accumulations from 10–30 m thick.

Expansion bars. Expansion bars are extensive gravel deposits immediately downstream from channel expansions. These bars are usually located where many small channels exit from an assemblage of loess islands. The flow expansion as well as shadowing effects of islands creat a low velocity zone in the flow; this results in the deposition of a bar (Baker, 1973). Other bars of this type form downstream of cataracts or where the channel is extremely wide. Both pendant and expansion bars commonly have giant current ripples superimposed on their surfaces. It should also be mentioned that the gravel bars located in the eastern sections of the Cheney-

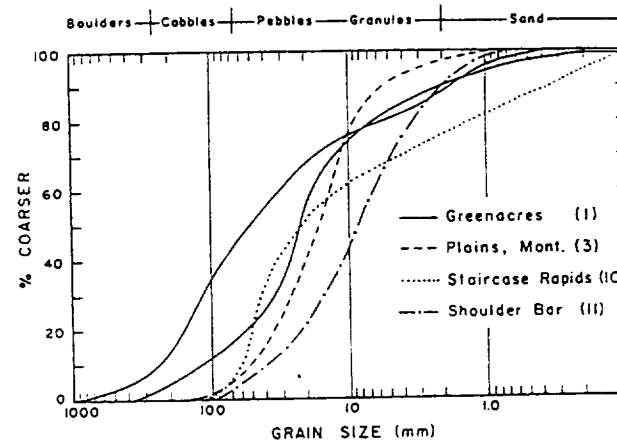

Fig. 12. Grain size distribution for sediment contained in giant current ripples in the Channeled Scabland. The numbers for ripple sets are keyed to locations described by Baker (1973). Note that the ripples are very coarse-grained.

Fig. 13. Flight path for September 25-26, 1995, overflights. Aircraft heads southeast from Grant County International Airport at 6:00 a.m., and returns once to the airport for a rest stop. The flight time is chosen to provide low-Sun angle views of Channeled Scabland landforms. Base map is a portion of the Landsat image shown previously in Fig. 2.

Palouse are smaller than those found in the west. The reason for this is the lateral spreading of the flood water, which resulted in lower flow depths than those of the great coulees of the western Columbia Plateau (Baker, 1973).

Ephrata Fan. The Ephrata Fan is an extensive, coarse gravel unit deposited subfluvially (under water). The fan was emerges into the Quincy Basin from the Soap Lake constriction at the mouth of Grand Coulee. The maximum known thickness of the deposit is about 40 m (Bretz et al., 1956). The surface of the fan displays a series of lobate depositional units, bounded on their downstream margins by slipfaces. The Ephrata Fan appears to have been built by bar-slipface migration (Nummedal, 1978). The sediments of the fan include a variety of lithologies brought from upstream locations to the Quincy Basin by the Missoula Floods (Gulick, 1990). Clast sizes range from house-sized boulders near the fish hatchery on Rocky Ford Creek to the sand of the Moses Lake dune field (see Field Trip I, Day 1, guide below).

FIELD TRIP I GUIDE TO OVERFLIGHT, SEPTEMBER 25 AND 26, 1995

To begin to understand the context and history of the Channeled Scabland, it is necessary to see the region from the air. People have lived in the Scabland region for more than 10,000 years, but it was not until aerial photographs of the region became available in the 1920's and 1930's that scientists began to realize that the terrain was carved by giant, catastrophic floods.

The overflights that accompany Field Trip I are critical to understanding the full context and history of the gigantic landforms produced by the Lake Missoula floods. The intuitive understanding that will be gained by experiencing the Scabland terrain from both the air and ground will be essential for interpreting the nature of the Mars Pathfinder landing site in Ares Vallis. The relevance to Ares Vallis is especially acute owing to the fact that Mars Pathfinder will not obtain descent images— the scientist and engineer alike will need to rely on the existing medium-resolution Viking images (~40 m/pixel; Golombek et al., 1995), coupled with images taken from the lander on the ground, to interpret the geological context of the landing site in July 1997.

There are two identical overflights of the Channeled Scabland, one on September 25, 1995, the other on September 26, 1995. Both depart from the Grant County Airport, Moses Lake, Washington, at 6:00 a.m. The flights each carry 18 participants and the field instructor, V. R. Baker. The flight path is indicated on the Landsat image shown in Fig. 13. The flights return twice to Grant County Airport, once for a rest stop, once for return at about 9:00 a.m. Total flight time is about 2 hrs. 20 mins.

Features seen on the flight include the following (in order of appearance): (1) Palouse Falls at Palouse and Snake River junction, (2) streamlined islands and giant current ripples in the Cheney-Palouse Scabland, (3) Sprague Lake, (4) Crab Creek channel, (5) Dry Falls, (6) longitudinal grooves above Dry Falls, (7) Lake Lenore / Lower Grand Coulee, (8) Soap Lake constriction point, (9) Ephrata Fan boulder deposits, (10) West Bar giant current ripples, (11) mouth of Moses Coulee, (12) Potholes Cataract, and (13) Moses Lake basaltic sand dune field. Many of these sites are also visited on the ground during Field Trip I.

FIELD TRIP I GUIDE: SEPTEMBER 24-27, 1995, CHANNELED SCABLAND OF WASHINGTON

Day 0— September 24, 1995
Moses Lake, Washington

- Orientation Session 6:00 p.m. to 9:00 p.m.

Day 1— September 25, 1995
Moses Lake, Washington Area

- Overflight Departs 5:30 a.m., Returns 9:30 a.m.
- Ground Trip Departs 10:00 a.m., Returns 6:00 p.m.
- Informal Discussion Session, 6:30 p.m. to 7:30 p.m.

Day 1 Ground Trip

Purpose. To follow along a major channel system (the Lower Grand Coulee) from erosional, through depositional, and then reworked deposits from Dry Falls, across the Ephrata fan, and into the dunes of the Quincy Basin. The Ephrata fan is a major depositional unit that includes sediments of a variety of clast sizes and compositions. Part of the Ephrata fan might be a miniature analog of the Ares Valles landing site.

Road Log and Stop Descriptions. On September 25, 1995, this field trip departs from the hotel being used by the participants. However, the road log begins and ends at the Interstate 90 on/off ramp, Exit 176.

Mileage

cum.	**inc.**	
0.0		Interstate 90 off-ramp at Exit 176, on west side of Moses Lake, Washington. Take W. Broadway Rd. toward downtown Moses Lake.
2.9	2.9	Left on Stratford Rd. (On some maps, it is J NE Rd.).
4.4	1.5	Note gravel pit to right. Vehicle is driving over a huge gravel deposit, the Ephrata Fan. Sediments were deposited by the catastrophic Missoula Floods. The Ephrata Fan emanates from the Grand Coulee. Much of today's field trip is focused on the Grand Coulee and Ephrata Fan; together these form a miniature analog to Ares Vallis and the Mars Pathfinder landing site region.
9.9	5.5	Note basalt columns in outcrop to right. Columns formed when the Columbia Plateau basalts cooled (Fig. 14). The Columbia River Basalt Group flood basalts were deposited over a period of time from about 17 million to 6 million years ago (e.g., Tolan et al., 1989). Similar flood basalts occur on the Moon and probably on Mars.
23.3	13.4	Corner of Stratford Rd. and 22.7 NE Rd. Stratford grain elevators should be to right. Turn left.

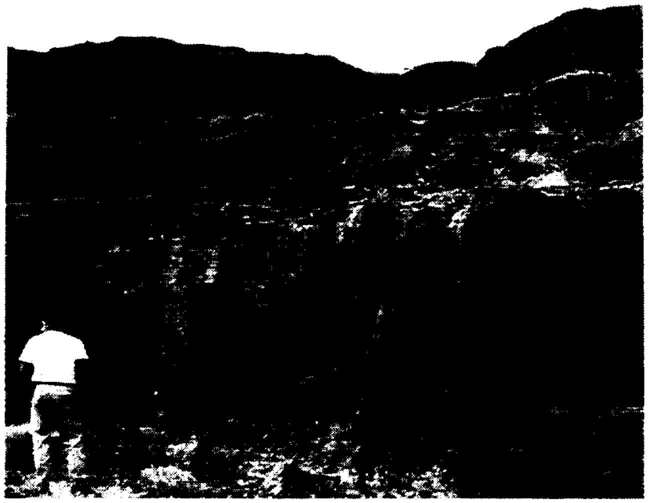

Fig. 14. Basalt columns in small mesa located near Deep Lake, Washington. Person for scale.

23.5	0.2	Turn left onto 23 NE Rd. Note vehicle is traveling in Crab Creek channel, a major conduit of Missoula Flood waters.
24.3	0.8	Intersection of 23 NE Rd. and S.R. 28. Go straight, across S.R. 28. Stay on 23 NE Rd.
25.2	0.9	Turn right onto Pinto Ridge Rd.
29.7	4.5	Overlook site. Slow vehicle and observe the view. To left in distance see west wall of Lower Grand Coulee. Straight ahead in distance is Banks Lake, formed by Dry Falls Dam. Dry Coulee is to immediate left.
33.7	4.0	Cross Main Canal of the Columbia Basin Project. This canal began delivering water from Banks Lake to farms in the Columbia Basin in 1951 (U.S. Bureau of Reclamation, 1978).
39.5	5.8	Turn left onto Main St. in Coulee City.
40.2	0.7	Turn right at 6 St., before grain elevators.
40.3	0.1	Turn left onto Walnut St., which curves to right and becomes I NE Rd.
40.8	0.5	Turn left onto U.S. 2. Drive across Dry Falls Dam. This earth-fill dam is 2,987 m long and 37.5 m high. The dam contains Banks Lake, the main reservoir for irrigation in the Columbia Basin (U.S. Bureau of Reclamation, 1978).
42.5	1.7	Turn left on S.R. 17.
44.5	2.0	Turn left, into parking lot. Park vehicle.

STOP 1— DRY FALLS INTERPRETIVE CENTER.

The Dry Falls is the main cataract which fed Missoula Flood waters from the Upper Grand Coulee to the Lower Grand Coulee system (Fig. 15). The Dry Falls are on the order of 6 km wide and 125 m high (twice as high and a third wider than Niagara Falls in New York and Ontario). The cataract developed as flood waters incised along the axis of the Coulee Monocline; the falls cut back into the rock from the Soap Lake area to the present location of the cliffs. The location and shape of the Lower Grand Coulee is largely controlled by the structure of the monocline. The weakened rocks on the steep (45°–60°) east-dipping slope of the monocline were more easily eroded by Missoula Flood waters than the more flat-lying basalt beds to the east. The lakes at the base of Dry Falls were plunge pools, and many large bouders are found immediately downstream of these pools. The Dry Falls Interpretive Center opened in 1994. *Estimated stay ≐ 1 hr.*

44.5		Depart Dry Falls Interpretive Center, turn left on S.R. 17 (heading south).
46.4	1.9	Turn left into Sun Lakes State Park. Now on Park Lake Rd.
47.7	1.3	Turn left on road to Deep Lake.
48.7	1.0	Keep to right, proceed onto road with white gate.
50.0	1.3	Note basalt columns to left and right (Fig. 14).
50.2	0.2	Pull into parking lot and stop vehicle.

STOP 2— DEEP LAKE.

This stop offers an opportunity to view the Lower Grand Coulee from the inside. Deep Lake (Fig. 15) was scoured by the Missoula Floods. Remnant buttes of basalt are seen in the vicinity. Longitudinal grooves occur on the surfaces upstream, above Deep Lake. The grooves cannot be seen from the lake, one must hike up the cliffs. Fig. 8 illustrates the longitudinal grooves in the vicinity. The spacing between longitudinal grooves range from 30 to 60 m, and they are up to 3 m deep (Baker, 1989). *Estimated stay = 45 mins., includes time for lunch.*

50.2		Depart Deep Lake site, return to Park Lake Rd.
52.8	2.6	Turn left onto Park Lake Rd.; follow around the east side of Park Lake (lake is to right).
53.2	0.4	On right, note hanging valleys on western canyon wall (Fig. 16). Hanging valleys are V-shaped and indicate earlier fluvial flow down the slope of the Coulee Monocline, which was later eroded out to become Lower Grand Coulee.

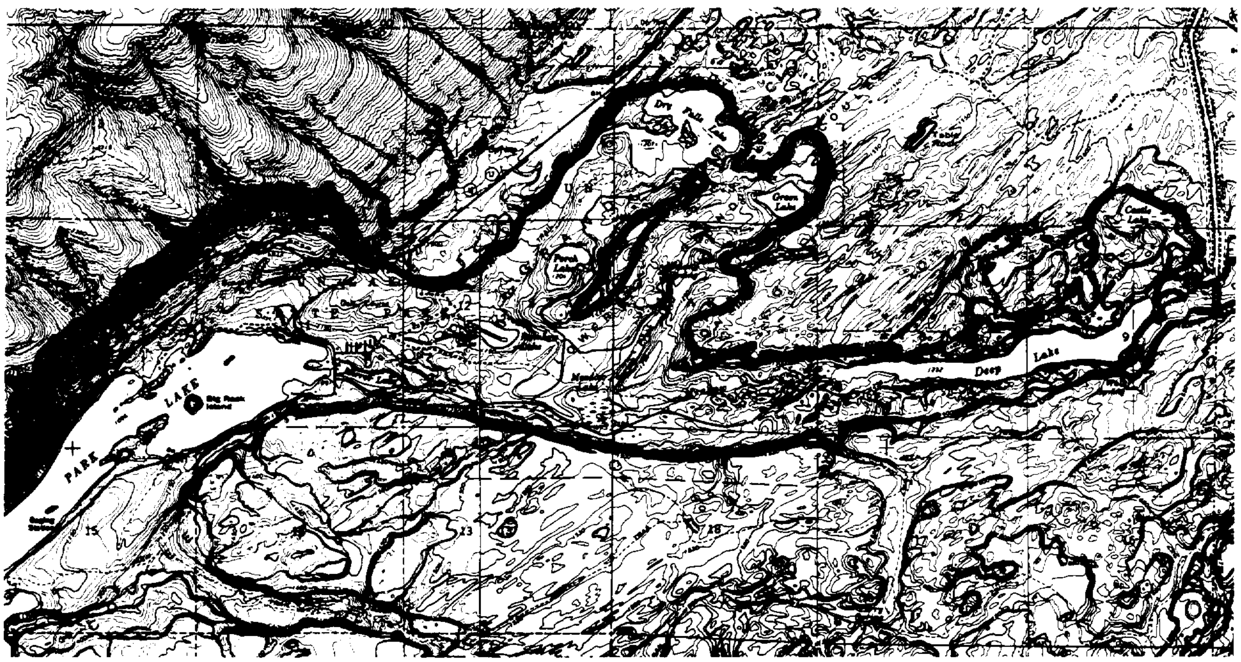

Fig. 15. Topographic map of Dry Falls cataract. Dry Falls Interpretive Center (Stop 1) is located near top center of figure, Deep Lake (Stop 2) is at the center right. Contour interval is 10 ft. Each box in the grid is a 1.6 km square. North is up. Source: U.S. Geological Survey and Nummedal (1978).

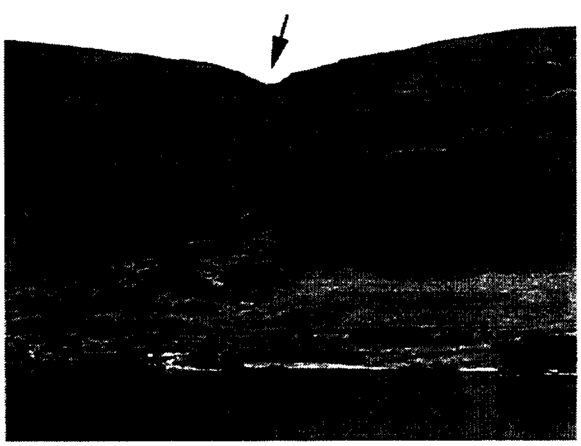

Fig. 16. Hanging valley (arrow) in western wall of Lower Grand Coulee above Park Lake (foreground). Valley indicates fluvial conditions prior to Missoula Floods.

54.9	1.7	On left, note gravel bar blocking the mouth of Jasper Canyon.
55.3	0.4	Turn left, back onto S.R. 17, heading south.
57.4	2.1	On left, note gravel bar blocking the mouth of Dry Coulee.
60.5	3.1	Lenore Lake. Slow vehicle, this is a good photography site. To left, Lake Lenore caves, inhabited by humans in past 10,000 years. To right, spectacular hanging valleys on canyon wall (Fig. 16).
67.0	6.5	Soap Lake. Soap lake occurs at a constriction point. Downstream from this location, Missoula Flood waters poured out onto the Ephrata Fan as if from a nozzled garden hose (Fig. 17). The flood-scoured bottom of Soap Lake is 62.5 m below the lake surface, although this surface is in turn overlain by 33.5 m of later flood gravels. Flood water emerged from the Soap Lake constriction to create the Ephrata Fan to the immediate south. The topography of the flood deposit slopes upward from Soap Lake to the bouldery portions of the Ephrata Fan in the south, attesting to the nozzle-like behavior of the flood that poured through the constriction point. Baker (1978a) speculated that a hydraulic jump occurred at this site. Soap Lake gets its name from its alkalinity; the primary salt in the lake is Na_2CO_3.
70.0	3.0	Intersection with S.R. 28. Proceed straight through; remain on S.R. 17.
70.1	0.1	Lake Bretz. Farming in the area immediately south of Soap Lake is made possible because of rich, fine soils deposited in post-Missoula Flood Lake Bretz. To the south, the surface is covered by boulders. In Lake Bretz, boulders were buried by finer sediments.
70.9	0.8	Turn left onto 19 NE Rd.

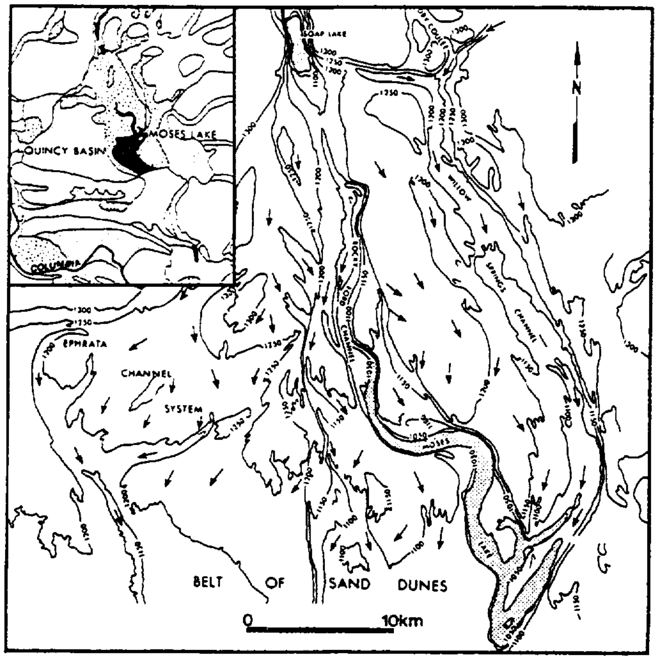

Fig. 17. Topographic map of Ephrata Fan complex in the upper Quincy Basin. Arrows indicate inferred surface flow directions. Contour interval is 50 ft. Note the change in topography from low to high going south from Soap Lake onto the fan. Also note that Moses Lake occupies part of the Rocky Ford Creek channel. Figure from Nummedal (1978).

72.8 1.9 19 NE Rd. curves sharply to right and becomes B.5 NE Rd. Proceed.

73.5 0.7 Along B.5 NE Rd., note boulders in the farm fields and those along the margins that were cleared from the fields. Boulders are some of the sediment deposited in Quincy Basin from the Grand Coulee. Vehicle is driving on the Ephrata Fan, which extends from Soap Lake southward past Moses Lake.

75.8 2.3 B.5 NE Rd. curves sharply to right. Proceed down into Rocky Ford Creek area. Note boulder field on plain to right.

76.0 0.2 Pull over as much as safely possible at the last outcrop on right.

STOP 3— EPHRATA FAN ROAD CUT.

This outcrop illustrates the bedding of the Ephrata Fan deposit, and also shows the range of grain sizes deposited within 10 km of the Soap Lake constriction point. Fig. 18 shows that the outcrop exposed at this site above the Rocky Ford Creek fish hatchery includes both forset beds and channel fill. The forsets are dipping south-southeast, whereas the channel fill material cuts through the forset bed units and is generally dipping toward the southwest. Clasts in this exposure range up to 0.5 m in diameter (Fig. 18).

The Ephrata Fan is thought to have developed largely underwater. The highest part of the fan stands 90 m higher than the scoured bottom of Soap Lake. The Fan consists of a series of lobate depositional bars which advanced along slip faces (resulting in the forset bedding observed).

Take a moment to look westward, out over the Ephrata Fan from this relatively high vantage point. Note that there are many large boulders on the fan to the west, and that the surface concentrations of boulders is variable. Compare this view with Viking lander images of the martian surface at Chryse Planitia and Utopia Planitia. *Estimated stay = 45 mins.*

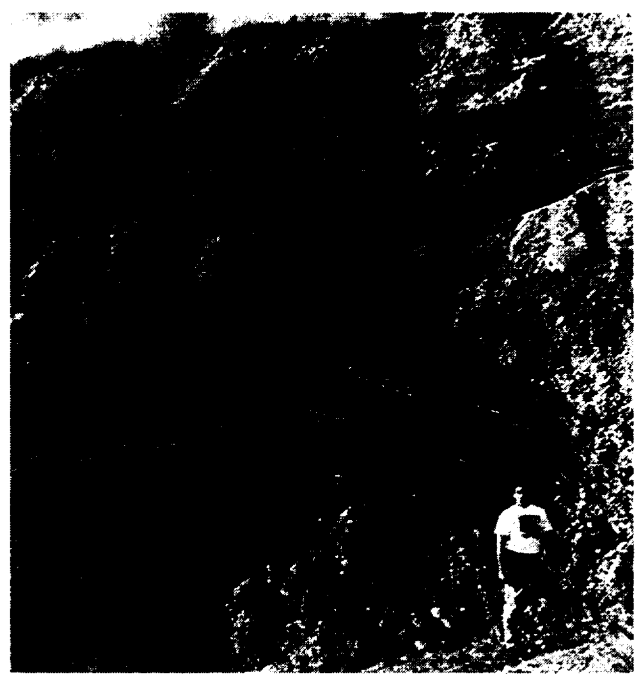

Fig. 18. Ephrata Fan road cut above the fish hatchery in Rocky Ford Creek. This location shows the nature of gravel beds in the fan. Note forset beds dipping to south (right), with unconformable channel cut on the left. Note that some of the clasts are as big as the person's head.

76.0 Depart Stop 3 and continue downhill past Rocky Ford Creek and fish hatchery.

76.4 0.4 Turn right onto Hatchery Rd. Proceed uphill. Note bouldery surface, reminiscent of the Viking lander images of Mars.

77.8 1.4 Pull over to right and park vehicle.

STOP 4— MONSTERS OF ROCK SITE.

Rocky Ford Creek, through which the vehicle has just passed, is thought by Baker (1973) to be the result of draining of the Quincy Basin. The drainage was in the form of high-velocity currents pouring southward, carving out Rocky Ford Creek, which includes

Fig. 19. Giant basalt boulder near Rocky Ford Creek is 18 m × 11 m × 8 m in size. This clast came from the Grand Coulee and was transported at least 8 km from the Soap Lake constriction point. Location is T21N, R27E, S17NE.

the Moses Lake bed. Waitt et al. (1994) and Bretz et al. (1956) prefer to interpret the Rocky Ford channel as the result of multiple, smaller Missoula Floods that poured over the Ephrata Fan later in its history. Regardless of origin, flow through this channel has concentrated large boulders at the surface in this location.

The largest boulder on the Ephrata Fan is shown in Fig. 19. It is 18 m × 11 m × 8 m is size, and has a prominent scour crescent in the sediment around it on the northwest (upstream) side of the boulder. The size of this boulder, and the fact that it is located at least 8 km from any potential source area, attests to the power of the Missoula Floods as they poured through the Soap Lake constriction point. Some of the boulders at this site were measured in 1995 (by M. Golombek, J. Rice, and K. Edgett) as part of a study of terrestrial analogs to martian landing sites and flood deposits (Golombek and Rapp, 1995). The surfaces represented here are more rocky than the Viking lander sites on Mars. *Estimated stay = 1 hr.*

77.8 Depart Stop 4, continue west on Hatchery Rd.

78.5 0.7 Turn left onto S.R. 17. Note changes in boulder populations as vehicle drives south along S.R. 17.

82.3 3.8 Turn right on S.R. 282, drive toward Ephrata, Washington. Again, observe boulder populations (or lack thereof).

85.0 2.7 Note silt mounds (Fig. 20) to left and right. The origin of such silt mounds has not been resolved, although they are found throughout the Channeled Scabland

Fig. 20. Silt mounds, also sometimes called "Mima mounds" (see text), are common throughout the Channeled Scabland. Their origin is uncertain, but vegetation trapping of windblown silt is a likely explanation. The mound shown here is located on private property at T19N, R38E, S23SE. Person is co-editor, J. W. Rice Jr.

region. (Their presence is noted several times in this road log.) The silt mounds are typically closely-spaced, several meters in diameter, and stand 1–2 m high. They contain mostly silt with some sand, and are commonly termed "Mima mounds," after similar-shaped features on the Mima Prairie south of Olympia, Washington. True Mima mounds appear to be periglacial features and they contain coarser materials (sand, pebbles) than the silt mounds in the Channeled Scabland. According to the summary by Waitt et al. (1994), some possible origins for the mounds include gopher colonies, run-off erosion of silty deposits, frost wedging or desication cracking, and vegetation anchoring. Washburn (1988) favored the combined effects of surface run-off and anchoring by vegetation as causes for the mounds. Olmstead (1963) suggested that the mounds result from aeolian accumulation of silt in depressions (because of higher moisture content), with subsequent vegetation growing on the silt deposits, anchoring additional windborne silt.

86.3 1.3 Commercial gravel pit to left was used as "Stop 7" on the 1978 NASA field trip to the Channeled Scabland (see Nummedal, 1978).

86.8 0.5 Turn left onto Dodson Rd. Turn is before the railroad underpass.

89.0 2.2 Proceed south along Dodson Rd. Areas farmed along this road denote the transition from rocky and coarse Ephrata Fan sediments to finer, more sandy sediment. Farms are typically located in areas where there are few boulders to clear from the fields.

100.7 11.7 Dodson Rd. overpasses Interstate 90. Continue south on Dodson Rd.

105.2 4.5 Note dark, somewhat vegetated sand dunes to left. Vehicle has entered western part of Moses Lake sand dune area. Dunes are reworked from sand-sized sediment deposited at distal end of Ephrata Fan.

106.5 1.3 Pull over to right and park vehicle.

STOP 5— BASALTIC AEOLIAN SAND DUNES.

These parabolic dunes by the side of Dodson Rd. represent a fraction of the larger Moses Lake dune field, which extends approximately 30 km from west to east. The dunes are unusual because they contain 60%–80% basalt lithic fragments; the remaining sand is mostly quartz (Petrone, 1970). The mafic composition contrasts with quartz dunes (of similar morphology and history) that are located 40 km south in the Pasco Basin on the U.S. Department of Energy Hanford Nuclear Site (Smith, 1992). The Moses Lake dunes formed by aeolian reworking of mostly basaltic sediments eroded from the Grand Coulee which settled in water ponded by the Quincy Basin during the Missoula Floods. The Moses Lake dunes represent the distal fine sediments of the Ephrata Fan (Nummedal, 1978).

The mafic dunes are a compositional analog to dunes and windblown sands on Mars (Edgett and Lancaster, 1993). Martian dunes are typically dark-hued, and appear to contain reduced iron and pyroxene minerals, indicating mafic compositions (e.g., Singer et al., 1979; Thomas, 1984; Mustard et al., 1993; Edgett and Christensen, 1994).

Windblown sand and dust were a common problem for homesteaders in the Moses Lake area during the first few decades of this century (Zickler and Ribail, 1983), but aeolian activity has been decreasing since the 1952 construction of the O'Sullivan Dam which contains the Potholes Reservoir (Petrone, 1970; Edgett, 1994). The Potholes Reservoir flooded a portion of the dune field. The region was also recently affected by volcanism; the 1980 eruptions of Mount St. Helens, located about 230 km to the southwest, blanketed the dune area with 2–4 cm of fine ash. The ash still covers inactive portions of the dune field. Active dunes contain a layer of ash at the location of their 1980 slip face (Edgett, 1994). The ash layer is exposed in some of the dunes at this stop along Dodson Rd. (Fig. 21). In recent years (1992–present), earth-moving equipment has been used to remove some of the sand from the dunes at this location. *Estimated stay = 30 mins.*

106.5 Depart, continue south on Dodson Rd.

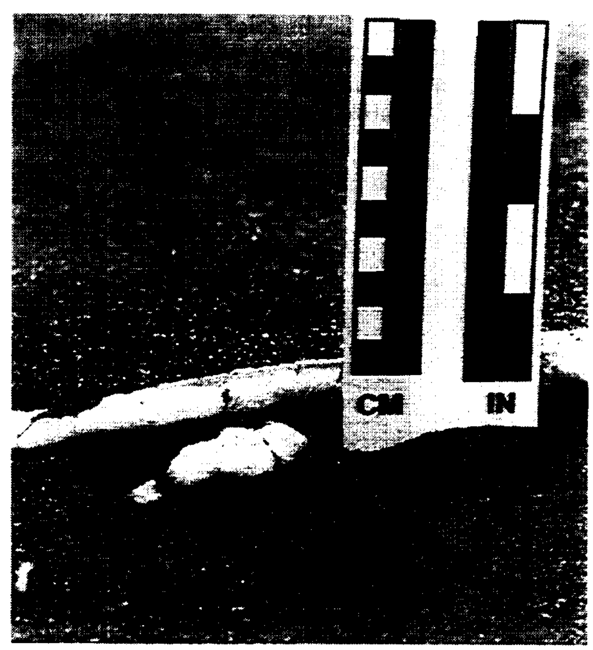

Fig. 21. Layer (white) of Mount St. Helens 1980 ash exposed in Moses Lake basaltic dune near Dodson Rd.

107.5 1.0 Note ridge straight ahead: the Frenchmen Hills. Ridge is formed by anticline fold in the Columbia basalts. This ridge is one of several in the region that have been considered as analogs to "wrinkle ridges" found on Mars and the Moon (e.g., Watters, 1988; Reidel et al., 1989). Such ridges are considered to form by compression (e.g., Plescia and Golombek, 1986).

110.4 2.9 Turn left onto Frenchmen Hill Rd.

115.0 4.6 Turn left on S.R. 262, also called O'Sullivan Dam Rd.

116.7 1.7
to
119.2 2.5 Slow vehicle, look left past farmed areas. Ridges and hills visible here are the sand dunes, similar to the dunes at Stop 5. Also can see Potholes Reservoir toward the front/left.

122.1 2.9 Entering O'Sullivan Dam. Potholes Reservoir is to left. Drumheller Channels to right. The O'Sullivan Dam, 5.6 km long and 61 m high, contains the Potholes Reservoir. Built in 1952, the dam and reservoir catch runoff from irrigated farmland, and allow the water to be recycled once more, for farms to the south, before rejoining the Columbia River system (U.S. Bureau of Reclamation, 1978). The Potholes Reservoir floods an area that used to have active sand dunes in the north, and the Drumheller ranch on Lower Crab Creek in the south (Drumheller, 1982). The channels to the right of the dam are named for the Drumheller family. The Drumheller Channels formed as a spillway as floodwaters poured out of the Quincy Basin over this low, eastern end of the Frenchmen Hills ridge.

122.4 0.3 Good view of Drumheller Channels to right. Note dipping of basalt layers, indicating the folded anticlinal nature of the Frenchmen Hills.

124.8 2.4 Another good view of Drumheller Channels to right.

127.0 2.2 To left, Lind Coulee enters Potholes Reservoir. Some of the water that once filled Quincy Basin during the Missoula Floods came through Lind Coulee (Fig. 3).

132.0 5.0 Turn left, onto S.R. 17.

133.9 1.9 Crossing Lind Coulee.

139.2 5.3 To left, past farmed areas, note dark dune ridges of the eastern end of the Moses Lake dune field.

141.9 2.7 Turn left, on-ramp for Interstate 90.

144.0 2.1 View of Moses Lake. The lake formed by damming of Rocky Ford and Crab Creeks by the eastward advance of the sand dunes, located to the south (Petrone, 1970). The channel filled by Moses Lake was carved into the Ephrata Fan during the waning stages of the catastrophic Ice Age floods.

145.0 1.0 Keep right, leave Interstate 90 at Exit 176. End of Day 1 Field Trip.

Day 2— September 26, 1995
Moses Lake, Washington Area

- Overflight Departs at 5:30 a.m., Returns 9:30 a.m.
- Ground Trip Departs 10:00 a.m., Returns 6:00 p.m.
- Mandatory Discussion Session, 6:30 p.m. to 7:30 p.m.

Day 2 Ground Trip

Purpose. To examine additional giant erosional and depositional landforms associated with the Missoula Floods in and near the Quincy Basin, particularly giant current ripples, slackwater sediments, scour and cataract features, and a giant landslide deposit. It is possible that some of these features, such as giant current ripples, might be present at or near the Ares Vallis landing site for Mars Pathfinder.

Road Log and Stop Descriptions. On September 26, 1995, this field trip departs from the hotel being used by the participants. However, the road log begins at the Interstate 90 on/off ramp, Exit 176. This trip involves much driving; thus it is essential for participants to stick to a tight schedule in order to see all of the geological features.

Milage
cum. inc.

0.0 Interstate 90 on-ramp at Exit 176, on west side of Moses Lake. Get on Interstate 90, heading west.

23.7 23.7 Get off Interstate 90 at Exit 151. Turn right, head toward S.R. 281 (north).

24.0 0.3 Go straight at stop sign.

25.6 1.6 Turn right, onto S.R. 281, heading toward Quincy.

33.3 7.7 In Quincy, turn left onto S.R. 28.

40.7 7.4 Turn left at Crescent Bar Rd. Follow signs for "Crescent Bar Recreation Area."

41.4 0.7 Vehicle parking and turn-around is on right.

STOP 1— WEST BAR GIANT CURRENT RIPPLES AND SLACK WATER DEPOSITS.

Overlook and slackwater outcrop are on left, about 0.1 mi. back up the road.

Giant current ripples are probably the most convincing feature that indicates the magnitude of the catastrophic Missoula Floods. This viewpoint above the Columbia River offers an opportunity to see one of the best-developed ripple bars in the region; the second stop on this trip (below) allows participants a chance to walk on similar ripples. West Bar is located on the western side of the Columbia River. It is best to visit the site early in the morning, to see the topographic relief at low sun-angle (Fig. 9).

The West Bar ripples are about 8 m high and spaced 110 m apart. The sediments in these ripples consist mainly of gravel and boulders up to 1.4 m in diameter (Baker, 1973). The maximum depth of the flood waters that poured through this region and over the ripple bed was about 200 m.

Crescent Bar, another coarse gravel deposit, is on the east side of the river, beneath this viewpoint. The gravels of Crescent Bar have an overlying set of rhythmite beds. The rhythmites are fine-grained (silt, sand) slack water deposits, representing a time of low-energy flow as might occur in an area where Missoula Flood waters were ponded. Such ponding occurred at this site. The slack water sediments indicate multiple periods of flooding in the region. There was more than on Missoula Flood. Indeed, Waitt (1980) showed evidence suggesting that there has been more than forty floods in the Channeled Scabland system. Fig. 22 shows a layer of volcanic ash exposed in the slack water deposits. This ash is part of the Mount St. Helens Set S ash, dated at about 13,000 years before present. See Baker (1989) for additional information about this site. *Estimated stay = 45 mins.*

41.4 Depart Stop 1, go back the reverse route, up Crescent Bar Rd. to S.R. 28.

42.2 0.8 Turn left at stop sign, onto S.R. 28.

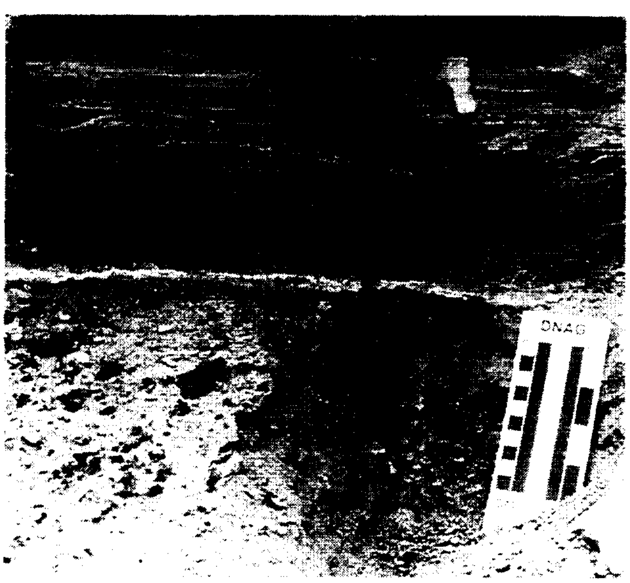

Fig. 22. Slackwater sediments on east side of Columbia River gorge near Crescent and West Bars. White layer in middle of photograph is one of the three Mount St. Helens Set "S" ash, dated at approximately 13,000 years ago. This date gives some constraint on the age of Missoula Flooding.

42.6 0.4 On left, view of West Bar giant current ripples.

42.9 0.3 Another view of West Bar to left. Also note that vehicle is driving down into the Columbia River gorge.

48.4 5.5 To right, vehicle is entering the mouth of Moses Coulee, a Missoula Flood channel that fed directly into the Columbia River system.

48.7 0.3 Note hanging valleys in Moses Coulee wall, to right. These V-shaped hanging valleys represent earlier channels that emptied into Moses Coulee, prior to massive floods.

49.6 0.9 Leaving Moses Coulee.

52.1 2.5 Rock Island Dam comes into view. Rock Island Dam was completed in 1933, and is located at the site of rapids which poured over pre-flood landslide deposits of giant basalt boulders that came from the west side of the Columbia River valley (Waitt and Atwater, 1989).

52.3 0.2 Note basalt columns to right.

60.7 8.4 To left, note outcrops on the other side of the Columbia River are no longer basalt, but other rock types. Vehicle has driven out of Columbia Basalt area.

63.9 3.2 Traffic light at Grant Rd. intersection. Continue straight on S.R. 28, get into left lane and follow signs toward Wenatchee.

64.0 0.1 Keep left, go across Stevens St. Bridge. Stay in left lane.

64.7 0.7 Turn left onto Mission St., following signs to Malaga.

64.8 0.1 Turn left onto Marr St. Sign on right says "Malaga-Alcoa."

65.0 0.2 At stop sign, turn right onto Wenatchee Ave. Vehicle is now headed southward on west side of Columbia River. Wenatchee Ave. becomes Malaga-Alcoa Hwy.

70.8 5.8 Turn right onto West Malaga Rd. Road curves sharply to right within 0.05 mi.

71.2 0.4 Turn right, park vehicle.

STOP 2— MALAGA GIANT CURRENT RIPPLES.

The Malaga ripples (Fig. 10) are mainly composed of pebbles. Waitt et al. (1994) noted that there are some gneiss and quartz diorite boulders in the deposit, as well. The mixture of lithologies reflects the composition of bedrock upstream, which in this area does not include much basalt. These ripples are thought to be young relative to other Scabland ripples;

they do not have an overlying Glacier Peak ash deposit that is dated at about 11,250 years before present (Waitt and Atwater, 1989).

This site was selected to offer participants an opportunity to walk on a set of giant current ripples. The perspective gained at this site could prove useful if Mars Pathfinder happens to land on a similar deposit. *Estimated stay = 45 mins.*

71.2		Depart Malaga ripple site. Turn left onto West Malaga Rd.
71.7	0.5	Turn left, back onto Malaga-Alcoa Hwy.
77.6	5.9	Turn left onto Marr St.
77.7	0.1	Turn right onto Mission St.
77.8	0.1	Turn right onto Stevens St., drive back across bridge over the Columbia River. Keep right, follow signs for S.R. 28.
83.0	5.2	To right, note Malaga giant current ripples can be seen in profile from across the river. The riverward side of the ripple field has been truncated by later fluvial action.
92.9	9.9	Moses Coulee visible to left. Continue following S.R. 28 up, out of Columbia River gorge.
103.7	10.8	Turn right on White Trial Rd. (also U NE Rd. on some maps).
108.3	4.6	Road curves sharply to left and becomes 5 NW Rd.
109.4	1.1	Turn right at sign for "Public Fishing, Public Hunting." Gravel road, curves to left almost immediately.
110.2	0.8	Keep left.
110.4	0.2	Keep right.
111.1	0.7	Keep right.
111.4	0.3	Turn right, park vehicle.

STOP 3— POTHOLES CATARACT.

Hike approximately 0.2–0.3 mi. to right (southwest). See Fig. 23 for map. Potholes Cataract is one of four main spillways by which flood waters ponded in Quincy Basin poured out of the temporary lake in which the Ephrata Fan was deposited. There are three cataract sites (Frenchmen Springs, Potholes, and Crater Coulee) plus the Drumheller Channels south of Potholes Reservoir.

Like Dry Falls, the Potholes Cataract might have been initiated under water. The distinct horseshoe shape is caused by headward erosion of the bedrock. The cataract was probably an efficient funnel during

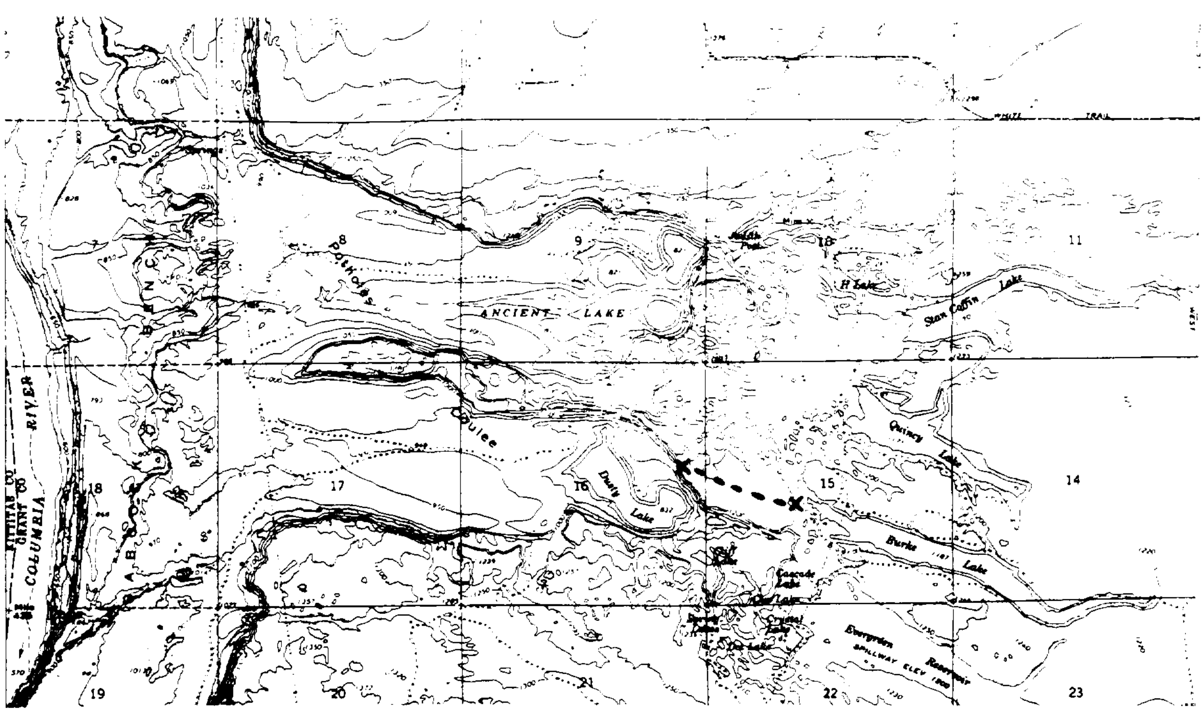

Fig. 23. Topographic map of the Potholes Cataract. Compare its shape with that of the Dry Falls in Fig. 15. Potholes Cataract formed by draining of Quincy Basin after it filled with Missoula flood water. Dashed line indicates hike for Stop 3. Contour interval is 10 ft., each box on the grid is about 1.6 km. North is up. Source: U.S. Geological Survey and Baker and Nummedal (1978).

Fig. 24. View to west-southwest of Dusty Lake from edge of southern Potholes Cataract.

maximum flood conditions, drawing the water surface sharply down over the cataract scarp and producing intensely scoured areas below (Baker, 1978b). This site is the southern of two Potholes Cataracts. The lakes in this area are formed in scoured zones. The lake down below the cliff at this site is Dusty Lake (Fig. 24). *Estimated stay = 1 hr., possible lunch stop.*

111.4 Depart Potholes Cataract site, turn right.

111.8 0.4 Keep right.

112.7 0.9 Keep right.

113.4 0.7 Keep left (road curves to left).

113.6 0.2 Turn right onto U NW Rd.

114.6 1.0 Turn left onto 1 NW Rd.

118.3 3.7 Turn left on Bev. Burke Rd. Follow signs to "I-90."

118.9 0.6 Turn right on S.R. 281. Follow signs to "I-90."

120.4 1.5 Turn right. On-ramp to Interstate 90, going west.

123.7 3.3 On left, note Frenchmen Hills, a "wrinkle ridge" analog, as discussed in Day 1 (mile 107.5) field notes.

126.3 2.6 On right, in distance, note piles of white material. These are outcrops of diatomaceous rock (diatomite) interbedded with Columbia Basalts. The diatomite indicates the presence of a lake in between episodes of basalt flooding during the Miocene. Stop 4 (below) will also relate to the existence of lakes and ponds between lava flow events.

128.3 2.0 Columbia River is in gorge to right.

131.6 3.3 Keep right.

131.9 0.3 Go right, leave Interstate 90 at Exit 137 to S.R. 26.

133.0 1.1 Keep left, stay on S.R. 26. Note quartz-rich climbing sand dunes to left. The modern Columbia River transports quartz sand from the north. This sand contrasts with the basaltic sands of the Moses Lake dune field.

133.6 0.6 Carefully pull over to right. Get out of vehicle, and very carefully cross the road to visit outcrop on left. Watch for high-speed traffic!

STOP 4— PILLOW LAVAS AND PALAGONITE.

The outcrop to the left contains excellent examples of basaltic pillow lava structures. Pillows form when basalt flows underwater. This outcrop is an indication of the presence of lakes on the Columbia Plateau at the time of basalt emplacement.

While this site is not directly related to the nature and history of the Missoula Floods, the outcrop of basalt and palagonite is directly relevant to Mars and the Mars Pathfinder mission. Palagonite is an amorphous (non-crystalline), iron oxide and silica gel that forms when basalt is erupted into a water-rich environment, or when basaltic ash is weathered. In this case, the basalt was erupted directly into water. Palagonite so far appears to be the best visible and near-infrared spectral analog to much of the surface material on Mars (see review by Soderblom, 1992; also see Roush and Bell, 1995). The Imager on Mars Pathfinder (IMP) should be able to distinguish palagonitic materials at the landing site, if present (Reid and Singer, 1995). *Estimated stay = 30 mins.*

133.6 Depart Stop 4, continue east on S.R. 26.

137.9 4.3 View of Saddle Mountains straight ahead, Frenchmen Hills to left. Both are anticlinal fold ridges cited as possible analogs to "wrinkle ridges" on other planets (e.g., Reidel et al., 1989). The Viking 1 lander landed on a wrinkle ridge in Chryse Planitia (Binder et al., 1977), and a wrinkle ridge occurs at the eastern end of Mars Pathfinder's landing ellipse in Ares Vallis.

157.9 20.0 To right, Corfu Landslide on the Saddle Mountains comes into view. Next stop will offer a chance to view the landslide area.

160.7 2.8 Turn left onto D SE Rd.

160.8 0.1 Pull over to right and park vehicle.

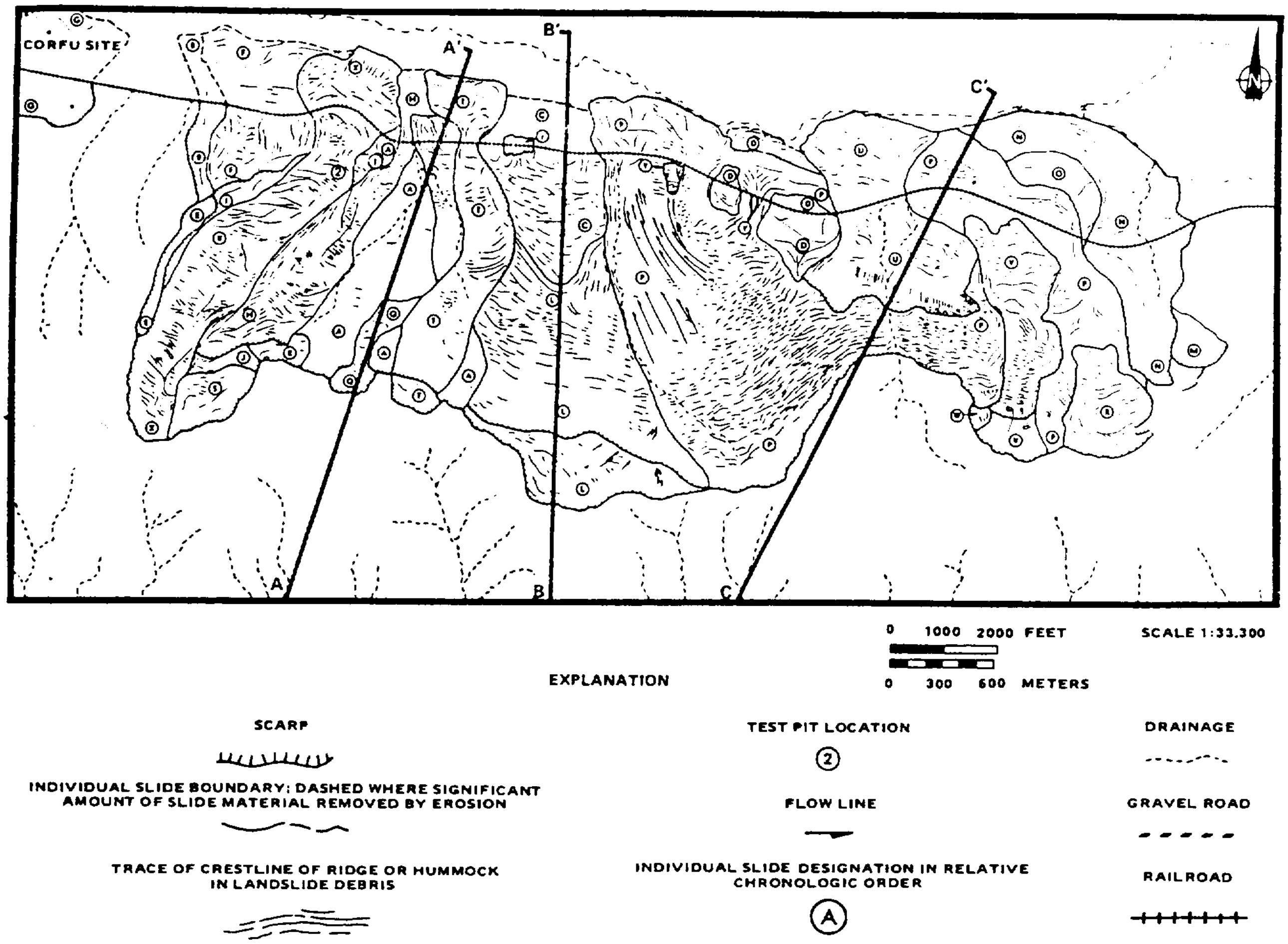

Fig. 25. Corfu landslide. At least 24 separate landslides occurred here following Missoula Floods. Mass movement was to the north (up). Sketch from Lewis (1985) with permission of thesis advisor, V. R. Baker. Lines marked A–A', B–B', and C–C' indicate cross sections, not shown.

STOP 5— VIEW OF CORFU LANDSLIDE.

The Corfu Landslide on the northern slope of the Saddle Mountains resulted from a combination of a relatively wet climate and repeated catastrophic flooding in the Channeled Scabland. Lewis (1985) estimated that nearly 1 km^3 of basalt and sedimentary rock slid off of the Saddle Mountains in a series of at least 24 separate events (Fig. 25). The giant flood events probably undercut the slope, allowing for slumping to occur. Smaller floods modified some of the landslide deposits. Some landslides were probably induced by seismic events. The earliest Corfu landslide deposit is about 13,000 years old, the most recent ones formed about 7,000 years ago (Lewis, 1985). *Estimated stay = 30 mins.*

160.8 Depart Corfu Landslide viewing site. Continue north on D SE Rd. Along the road during the drive uphill, some erratic boulders, rafted to the site by ice floes in the Missoula Flood waters, can be identified on the southern slopes of the Frenchmen Hills.

165.7 4.9 Turn right onto 12 SE Rd.

169.8 4.1 Turn left on H SE Rd.

172.3 2.5 Slow vehicle and look to right for overview of Drumheller Channels. Review Day 1 road log (mile 122.1 and 122.4) for more information.

172.8 0.5 Slow vehicle. View of Drumheller Channels to right, Potholes Reservoir straight ahead. Islands at the north end of the reservoir (in distance, ahead) were once active, basaltic sand dunes. The dunes were subsequently flooded and eroded nearly flat by the wind.

173.3 0.5 Proceed downhill, observing the landscape ahead and to the right.

174.4 1.1 Turn right onto O'Sullivan Dam Road (S.R. 262).

175.2 0.8 Entering O'Sullivan Dam. Review road log from Day 1. The purpose of coming this way again is to place the Day 2 stops back into context with the geological features seen on Day 1.

185.1 9.9 Turn left at stop sign, onto S.R. 17.

195.0 9.9 Turn left for on-ramp to Interstate 90.

198.1 3.1 Keep right, leave Interstate 90 at Exit 176. End of Day 2 Field Trip.

Day 3— September 27, 1995
Ritzville–Spokane, Washington Area

- Ground Trip Departs Moses Lake at 8:30 a.m.
- Arrive in Spokane, Washington, 3:00 p.m.
- Field Trip I ends in Spokane at 3:00 p.m.

Day 3 Ground Trip

Purpose. To investigate erosional and depositional landforms of the upper Cheney-Palouse Scabland tract. The landforms include scoured basalt flows and streamlined islands capped with loess. Participants will climb up onto a streamlined island to gain a perspective on the nature of these important landforms. Similar islands and scour features are apparent in Viking orbiter images of the Ares Vallis landing site area on Mars (Greeley et al., 1977; Golombek et al., 1995).

Road Log and Stop Descriptions. On September 27, 1995, this field trip departs from the hotel being used by the participants. However, the road log begins at the Interstate 90 on-ramp at Exit 176. The trip ends at the Division St. exit in Spokane, Interstate 90 Exit 281. Participants are delivered to hotel or airport after the trip.

Milage
cum. inc.

0.0 Interstate 90 on-ramp at west side of Moses Lake (Exit 176). Get on Interstate, heading east.

44.5 44.5 Keep right, leave Interstate 90 at Exit 221. Turn left on Washtucna Rd, which becomes Bauman Rd. ahead at the traffic light. Continue straight on Bauman Rd., through the 4-way stop.

45.4 0.9 Turn right at stop sign, onto Wellsandt Rd.

48.7 3.3 Beetle sculpture to right.

50.4 1.7 Turn right onto McCall Rd.

50.5 0.1 To left, in distance, note first view of butte-and-basin type scabland and streamlined loess islands.

51.6 1.1 Note silt mounds to left. Review Day 1, mile 85.0 notes for more information on silt mounds.

53.3 1.7 Entering butte-and-basin topography of the Cheney-Palouse Scabland tract. This area was scoured by the Missoula Floods, exposing and eroding the underlying Columbia basalts.

55.0 1.7 Note streamlined loess islands to left, right, and ahead. Streamlined islands occur in and near the Mars Pathfinder landing ellipse in Ares Vallis.

55.5 0.5 Turn right onto Marengo Rd., heading south. Vehicle will drive up and over a loess island.

56.6 1.1 Roadcut through loess deposit visible on right. Loess is the name given to windblown silt deposits consisting mainly of quartz, feldspar, mica, clay minerals, and carbonate grains (Pye, 1987). Loess is commonly made up of grains in the 20–40 μm range, and thick deposits usually form cohesive, vertical cliffs (Pye, 1987). The Palouse loess of eastern Washington, of which this island surface is composed, originated largely by glacial scour, probably followed by transport in glacial meltwater streams, followed by entrainment and deposition by wind. The loess deposits provide excellent, moisture-retaining soil for farming. Windblown dust deposits are common on Mars (Christensen, 1986), thus the properties of loess are relevant to the exploration of Mars (Francis, 1988).

57.8 1.2 Slow vehicle. Good view of loess islands to left.

59.3 1.5 Road goes from paved to gravel. Turn right, following signs toward "Harder's Hatchery."

59.4 0.1 Stop sign at railroad crossing.

59.5 0.1 Turn right, follow sign toward "Harder's Hatchery."

60.3 0.8 Railroad crossing.

60.4 0.1 Pull over to right.

STOP 1— MARENGO RAILROAD CUT.

The outcrop is on private property (not owned by the railroad). Obtain permission to visit the site. The railroad cut is located approximately 0.2 mi. to the right, up a dirt road overgrown by grasses. Hike up the road to the old railroad bed. Turn left at the railroad bed, outcrop is visible ahead.

This site provides excellent evidence that more than one flood passed through the Cheney-Palouse Scabland, and provides insight into the fact that some of these floods predate the Wisconsin glaciation associated with the most recent Missoula Floods (17,000–12,000 years ago). Loess deposits on top of ancient gravels in a variety of locations in the Cheney-Palouse scabland suggest at least six major episodes of pre-late Wisconsin floods (McDonald and Busacca, 1988). The earliest such episode is thought to have occurred more than 790,000 years ago, the most recent pre-late Wisconsin floods happened about 42,000 to 36,000 years ago (Busacca et al., 1989; McDonald and Busacca, 1988).

The railroad cut goes through a pendant bar at the south end of a large loess island about 1 km from Marengo, Washington. The outcrop contains two coarse flood gravel layers separated by three layers of loess and calcic (caliche) soil horizons (Fig. 26). The lower flood gravel represents pre-Wisconsin age floods. The upper gravel is from the most recent flooding, only about 13,000 years ago. Baker (1978c) discusses the Marengo outcrop in more detail.

With respect to Mars, this site is important because it serves as a reminder as to the nature of the deposits on the tail end of a streamlined island (Milton, 1973; Baker, 1978d). The streamlined islands on Mars likely contain gravel and boulders deposited by floods. *Estimated stay = 1 hr. 15 mins.*

60.4 Turn vehicle around, depart Stop 1 by going reverse route, back to McCall Rd.

65.1 4.7 Intersection of Marengo Rd. and McCall Rd. Note that McCall Rd. becomes Benge Rd. to right. Turn right.

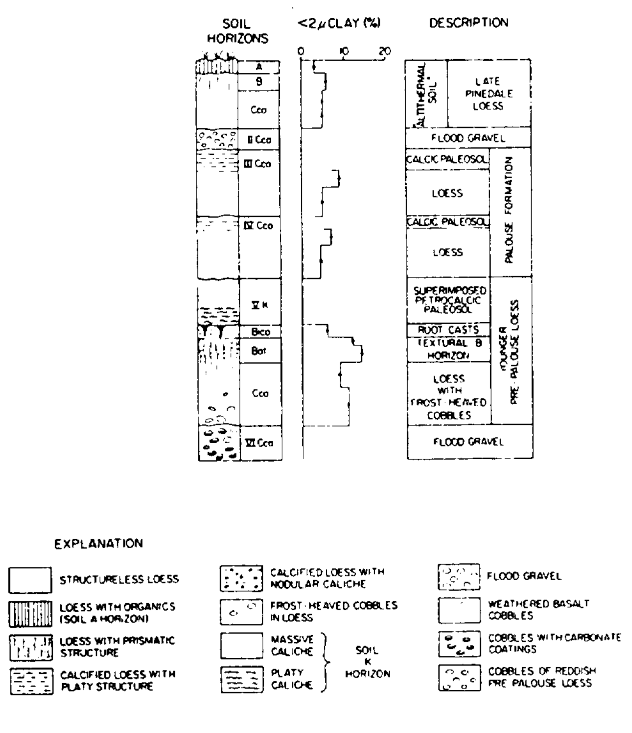

Fig. 26. Stratigraphic section at the Marengo railroad cut. The loess and lower gravel units represent flood, wind, and soil-forming episodes that predate the late-Wisconsin Missoula Floods. Source: Nummedal (1978).

67.0 1.9 Railroad crossing. Note loess island to right at approximately the 2:00 position. This island will be the site of Stop 2.

69.2 2.2 Turn right on Benge-Ritzville Rd. (Note that the road the vehicle was on is now called McCall Rd. again).

69.4 0.2 Turn right onto gravel road. (Benge-Ritzville Rd. curves sharply to left and is paved).

70.7 1.3 End of gravel road at gate. Turn vehicle around here (it might not be obvious, but busses have turned around here in the past).

STOP 2— STREAMLINED LOESS ISLAND.

This island occurs on private property (Fig. 27). Obtain permission to visit the site. With permission, pass through gated fence on left (east side of road) and walk up, onto the island along grass-covered dirt road.

A topographic map of this relatively small island is shown in Fig. 27. It rises 37 m above the surrounding scabland terrain. The island is covered with

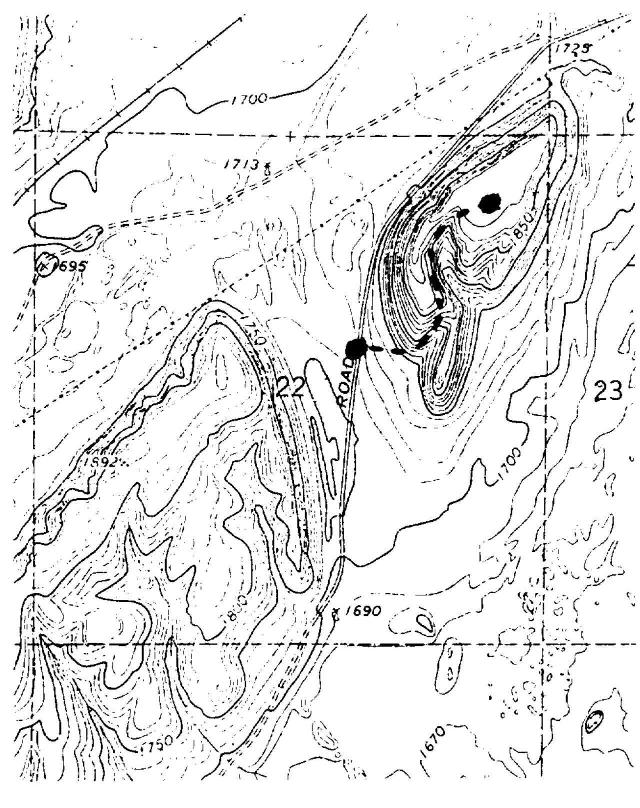

Fig. 27. Topographic map of the loess island visited in Stop 2. This island is located on private property. Dashed area marks approximate path to climb island. Contour interval is 10 ft., large box is 1.6 km. North is up. Source: U. S. Geological Survey 7.5 min. Marengo, Washington Quadrangle, 1964.

grasses, and is sometimes planted with crops. The island is one of many remnants of the Palouse loess in the Cheney-Palouse Scabland. Streamlined islands similar to this occur in the Ares Vallis Mars Pathfinder landing site region (Golombek et al., 1995; Komatsu et al., 1995). It is possible that the spacecraft will land near one of these islands. Notice that numerous other loess islands can be seen from the vantage point of the top of the island at Stop 2. Perhaps Mars Pathfinder will have a similar view after it lands.

The loess islands of the Cheney Palouse Scabland typically have sharp and steeply-sloped upstream ends, steep, faceted flanks, and long, tapering downstream tails (Patton and Baker, 1978). Some of these streamlined islands were once completely submerged, others were partly submerged or not submerged by the catastrophic floods (Patton and Baker, 1978). This particular island was probably not submerged. *Estimated stay = 2 hrs., includes time for lunch.*

70.7		Depart loess island site. Retrace route back to McCall Rd.
72.2	1.5	Turn right at intersection between McCall Rd. and Benge-Ritzville Rd.
74.9	2.7	On left, note road cut through gravel bar, with caliche layer at top of section. Sediments beneath caliche represent pre-Wisconsin aeolian and flood events. See Patton and Baker (1978) for more information about the outcrops along McCall Rd. in the Cheney-Palouse Scabland.
77.4	2.5	McCall Rd. becomes a gravel road.
79.4	2.0	Butte-and-basin inner channel of McElroy Creek. McCall Rd. becomes Lamont Rd., ahead.
87.9	8.5	Lamont Rd. and Revere Rd. intersection. Keep left (paved road). Drive through town of Lamont.
90.5	2.6	Turn left onto S.R. 23, head north toward Sprague.
98.5	8.0	Turn right to on-ramp for Interstate 90, north of Sprague. Head east toward Spokane.
105.0	6.5	Note streamlined islands to right and left.
122.0	17.0	Note streamlined islands and Granite Lake (followed by Willow Lake) to left. Lakes represent flood-scoured areas.
134.2	12.2	Keep right, leave Interstate 90 at Exit 281, the Division St. exit in Spokane. End of Day 3 Field Trip. **End of Field Trip I.**

FIELD TRIP II GUIDE: SEPTEMBER 30, 1995, LAKE MISSOULA BREAK-OUT, WASHINGTON AND IDAHO

Day 0— September 29, 1995
Spokane, Washington

- Orientation Session 4:30 p.m. to 5:30 p.m.

Day 1— September 30, 1995
Northeastern Washington, Northern Idaho

- Trip Departs Spokane at 8:00 a.m., Returns at 5:00 p.m.

Purpose. This trip investigates catastrophic flood features from the Lake Missoula break-out area at Lake Pend Oreille, Idaho, downstream through the Rathdrum Prairie, Spokane Valley, and into the Cheney-Palouse Scabland. Glacial Lake Missoula was ponded behind and broke through ice dams in the vicinity of southern Lake Pend Oreille, to carve the Channeled Scabland. Participants will examine landforms similar to those that might be found in the Mars Pathfinder landing site region in Ares Valles, such as giant current ripples and streamlined islands. Participants will also observe features created by the powerful scouring and erosion caused by the Missoula Floods. Multiple floods might have occurred in some of the martian outflow channels (e.g., Rice and DeHon, 1995; Moore et al., 1995), thus participants on this field trip will also have the opportunity to ponder evidence that multiple floods poured through the Spokane area.

Road Log and Stop Descriptions. On September 30, 1995, this field trip departs from the hotel being used by the participants. However, this road log begins and ends at the Interstate 90 on/off ramp at Division St. in Spokane, Exit 281.

Mileage		
cum.	**inc.**	
0.0		Get on Interstate 90 at Division St. on-ramp (Exit 281), heading east.
29.9	29.9	Leave Interstate 90 at Exit 12 in Coeur D'Alene, Idaho. Keep left, get on U.S. 95 heading north.
48.4	18.5	Turn right onto S.R. 54.
52.3	3.9	Traffic circle. Follow signs toward Farragut State Park.
52.7	0.4	Keep right, then left, to Farragut State Park Visitor Center, Idaho.
52.9	0.2	Parking lot at Visitor Center. Park vehicle, driver go inside, pay day-use fee, obtain park map. Field trip participants on September 30, 1995, do not have time to see the Visitor Center. It provides no information relevant to the Missoula Floods.
52.9		Depart Visitor Center parking lot. Farragut State Park opened as such in 1966. From 1942 to 1945, this

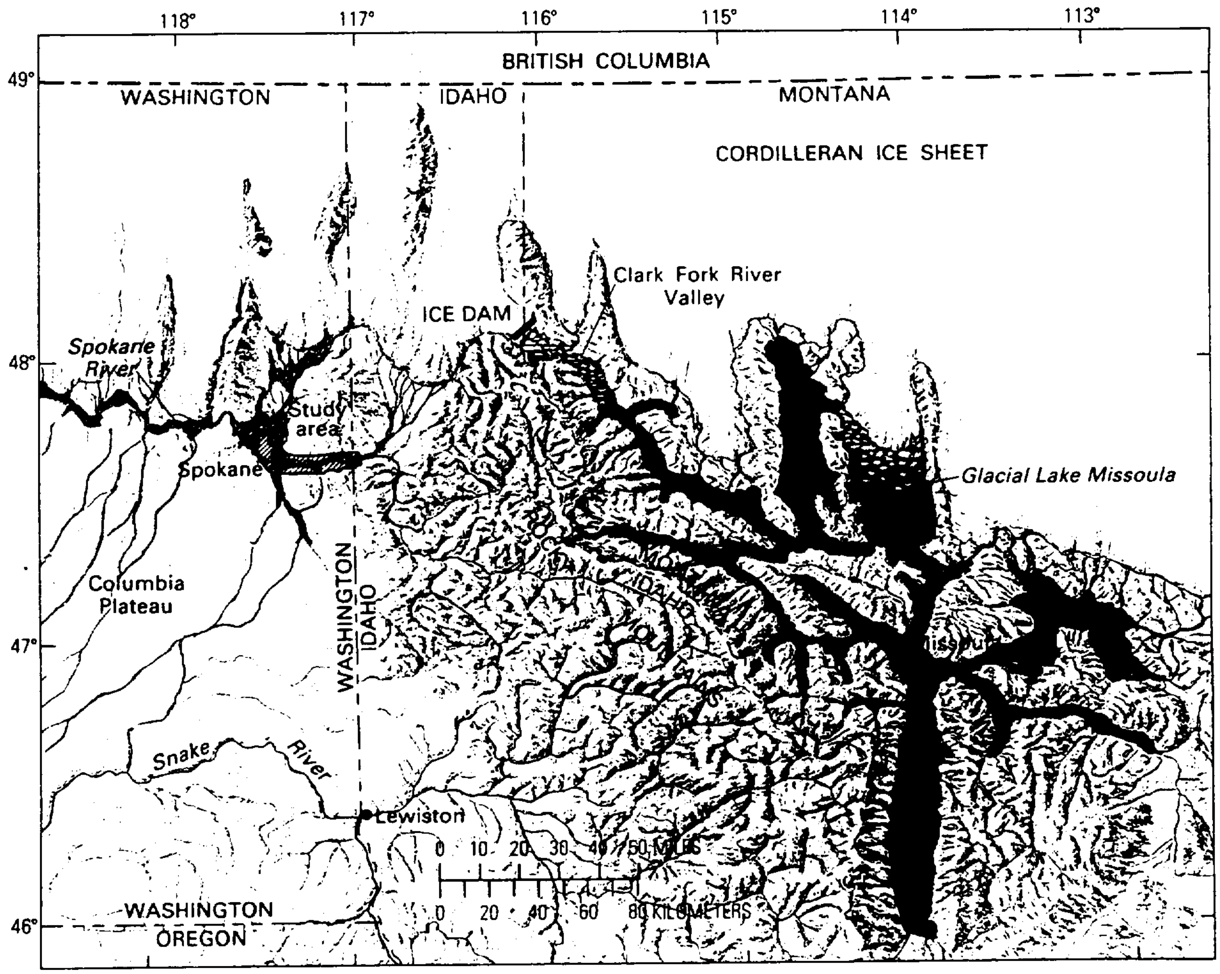

Fig. 28. Glacial Lake Missoula ponded behind an ice dam located at the west end of the Clark Fork River valley. Lake Pend Oreille is located beneath the ice lobe marked "ICE DAM." The region around Spokane, Washington, is labeled "Study area" because this figure comes from a U.S. Geological Survey report on the Spokane Aquifer by Molenaar (1988).

location was the site of the Farragut Naval Training Station. The Navy base was converted into a college that was used between 1946 and 1949, then the land was deeded to the state of Idaho as a nature preserve before becoming a state park (Merriam, 1975).

53.1 0.2 Turn right onto South Rd.

56.2 3.1 Turn right at "Sunrise Day Use Area" sign. Keep left, toward "Willow Day Use Area."

56.4 0.2 Park vehicle at Willow Day Use Area.

STOP 1— LAKE PEND OREILLE AND LAKE MISSOULA BREAK-OUT AREA.

The catastrophic floods which carved the Channeled Scabland of Washington began with the draining of Lake Missoula. The Purcell Trench Lobe of the Cordilleran Ice Sheet apparently advanced several times into the location of present-day Lake Pend Oreille, blocking off the Clark Fork River valley that enters Pend Oreille in the east (Fig. 28). The glacial lobe formed an ice dam. This dam broke and reformed several times (the exact number is still debated, see Waitt et al. (1994)) during the period about 12,000–17,000 years ago. Each time that the dam broke, Lake Missoula was drained. Much of the water poured right through the southwestern end of Lake Pend Oreille, where this field stop is located. It is useful here to examine a map such as shown in Figs. 1 and 28, to see the context of Lake Pend Oreille as the break-out site for the Missoula Floods.

Lake Pend Oreille is more than 350 meters deep, and is impounded by glacial moraines at this site. The lake has a U-shaped floor, thus it is likely that the Purcell Trench ice lobe was in part responsible for carving out this lake.

This material is summarized from Breckenridge

(1989b) and Othberg and Breckenridge (1992). *Estimated stay = 1 hr.*

56.4 Depart Willow Day Use Area.

56.6 0.2 Turn right onto South Rd.

56.8 0.2 Slow vehicle. Overlook at Lake Pend Oreille to right.

57.3 0.5 Slow vehicle. Overlook to right.

58.2 0.9 Turn left at stop sign in Bayview.

58.4 0.2 Slow vehicle. View of Lake Pend Oreille to left.

58.8 0.4 Road re-enters Farragut State Park.

59.0 0.2 Road curves to right, becomes Smylie Blvd. (also S.R. 54).

61.6 2.6 Follow traffic circle around toward left, toward town of Athol, Idaho (stay on S.R. 54).

65.6 4.0 Athol, Idaho. Intersection between S.R. 54 and U.S. 95. Go straight, stay on S.R. 54.

68.8 3.2 Entering Spirit Lake giant current ripple field. Watch for giant ripple forms out left and right windows. Giant current ripples are the most convincing features relating to the origin of the Channeled Scabland, because they contain clasts that range in sizes from pebbles to boulders that could only have been transported in catastrophic floods.

70.0 1.2 Signal to turn left. Parking will be on left. Do not turn vehicle around. Watch for traffic.

STOP 2— SPIRIT LAKE GIANT CURRENT RIPPLES.

Site is a road cut through a giant ripple crest. Examine the size of clasts included in this ripple (also see Figs. 29, 30). These ripples are on the order of 6–10 m high, and covered with a pine forest (Fig. 11).

The Spirit Lake ripples formed in a relatively "low energy" environment as Missoula Flood water diverged at this location around the mountainous area to the west which includes Rathdrum Mountain and Spokane Mountain. The southern channel is the Rathdrum Prairie. The road log next takes the participant south through this channel to an overlook site (Stop 3, below). *Estimated Stay = 30 mins.*

70.0 Depart Stop 2. Continue in original direction (west) on S.E. 54. Note depth of troughs between giant ripples.

73.4 3.4 Turn left on S.R. 41 at the stop sign. Leaving Spirit Lake ripple field. Note that the body of water known as Spirit Lake is located about 0.25 mi. to the right (west), but it cannot be seen through the trees.

Fig. 29. Road cut through crest of a giant current ripple at Spirit Lake, Idaho. Curve shows general shape of the ripple crest. Arrow indicates a person for scale.

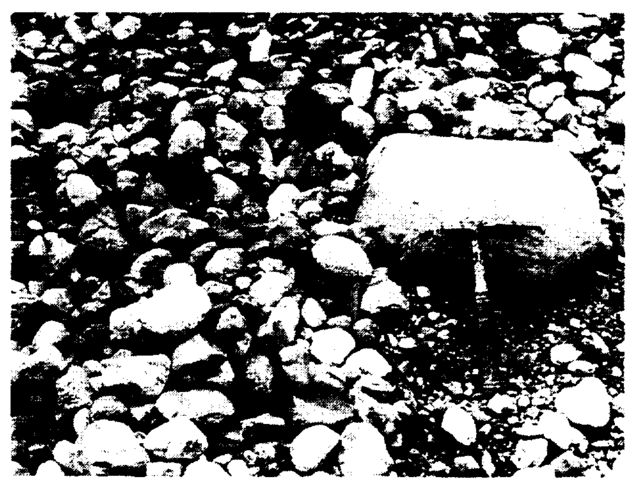

Fig. 30. Photograph of sediments exposed in the road cut through the crest of the giant current ripple shown in Fig. 29. Most of these pebbles and cobbles were previously rounded and stripped from glacial moraine deposits at the south end of Lake Pend Oreille and deposited here by the Missoula Floods.

83.5 10.1 Turn left just before the town of Rathdrum, Idaho. Follow signs for S.R. 41 south.

83.8 0.3 Turn right, continue following signs for S.R. 41. Drive south on S.R. 41 toward Post Falls, Idaho.

91.2 7.4 Keep right, get on Interstate 90 at on-ramp located about 2 mi. east of Post Falls, Idaho.

101.6 10.4 Leave Interstate 90 at Exit 296 off-ramp.

101.8 0.2 Turn left onto Liberty Lake Rd., Washington.

103.5 1.7 Liberty Lake Rd. and Liberty Rd. intersection. Keep right, stay on Liberty Lake Rd.

103.7 0.2 Liberty Lake Rd. becomes Garry Rd.

104.2 0.5 Garry Rd. becomes Molter Rd.

104.5 0.3 Pavement ends, gravel road begins.

105.2 0.7 Keep left, onto Quinimose Rd. (paved). Follow road as it winds up a hill.

106.1 0.9 Turn left onto Broken Lance Rd., entering Quinimose Estates housing development. Drive up hill.

106.6 0.5 Pull over to right. Hike to viewing area, at left. Vehicle may proceed up hill another 0.3 mi. to turn around at traffic circle, then return to this site on the left side of road.

STOP 3— RATHDRUM PRAIRIE / SPOKANE VALLEY OVERLOOK.

The Spokane Valley and Rathdrum Valley area is flanked to the north by the 1,792 m elevation Mt. Spokane and to the south by the 1,586 m Mica Peak mountains. These rocks are mainly Precambrian metamorphics with some younger (about 100 m. y.) intrusives. The valley below was flooded with Columbia basalts during the Miocene (5–24 m. y. a.), and later was a conduit for Ice Age streams and floods.

Missoula Flood waters rushed through this valley, carrying large volumes of rock debris and ice broken from the dam and adjacent glaciers. O'Connor and Baker (1992) calculated that at peak discharge, at least 17 million m^3/s of Lake Missoula water poured through the Rathdrum Valley area.

Downstream, additional ice dams sometimes caused ponding during flood events through the Spokane Valley, resulting in lake deposits in some areas around the city of Spokane. After the Missoula Floods, the Spokane River cut down through the flood sediments to form its present channel. The falls on the Spokane River might have been falls during an early Missoula Flood, and the river has now cut deep enough through flood sediments to re-locate the earlier falls or scabland terrain carved into basalt many thousands of years ago.

This material is a summary based on reviews by Molenaar (1988), Othberg and Breckenridge (1992), and Waitt et al. (1994). *Estimated stay = 1 hr. 10 mins., includes lunch time.*

106.6 Depart Stop 3. Drive back down Broken Lance Rd., turn right onto Quinimose Rd., follow back to Liberty Lake Rd.

109.7 3.1 Liberty Lake Rd. intersects with Liberty Rd. Turn left at stop sign.

111.4 1.7 Turn left to on-ramp for Interstate 90. Travel west on Interstate 90 toward Spokane.

137.9 26.5 On right, Willow Lake (first) and Granite Lake (second) are scoured areas caused by the Missoula Floods. Also note streamlined islands to right.

139.1 1.2 Silt mounds are visible to left and right. For more information, read discussion on silt mounds in text for Field Trip I, Day 1, mile marker 85.0.

154.9 15.8 Streamlined islands are visible to left and right. Similar islands occur in and around the Mars Pathfinder landing site in Ares Vallis.

160.5 5.6 Note scabland terrain visible to left. Vehicle will travel down into this terrain, known as the Cheney-Palouse Scabland tract.

161.4 0.9 Keep right, get off Interstate 90 at Exit 245 to Sprague. Go left at S.R. 23.

162.2 0.8 Turn left onto 4 St.

162.4 0.2 Turn left at stop sign.

162.5 0.1 Turn right at stop sign, onto "Old State Highway," which is not labeled.

164.8 2.3 Turn right onto Williams Lake Rd. Note vehicle is now heading into butte-and-basin scabland topography.

167.1 2.3 Railroad crossing. Note silt mounds in the vicinity.

168.7 1.6 Note streamlined islands to left, channel and butte-and-basin topography to right.

171.3 2.6 Williams Lake Rd. becomes Martin Rd.

175.3 4.0 Three-way intersection of Mullinix Rd., Mead Rd., and Martin Rd. Keep right, turning onto Mullinix Rd (gravel, not paved).

176.0 0.7 Note gravel bar road cut to left, formed of sediments deposited on the tail end of a streamlined island. The downstream end is commonly the site of deposition. In this case, the deposits are flood-borne gravels. Streamlined islands are common in and near the Mars Pathfinder landing site at Ares Vallis. Indeed, several downstream tails coming off of streamlined islands are present in the landing ellipse area.

176.3 0.3 Mullinix Rd. turns to right (south).

178.3 2.0 Keep left, onto Whitman Rd.

179.0 0.7 Intersection with Rock Lake Rd. Whitman Rd. becomes Miller Rd. on other side (east) of Rock Lake Rd. Proceed forward to Miller Rd.

180.1 1.1 Keep left, onto Belsby Rd.

181.5 1.4 Note that vehicle is driving up onto loess deposit.

183.1 1.6
to
183.4 0.3 Pull over to right, get out of vehicle, walk downhill about 0.3 mi., have vehicle meet passengers there.

STOP 4— ROCK COULEE NEAR HOLE-IN-THE-GROUND.

This canyon was carved by the catastrophic Missoula Floods. Waitt et al. (1994) describe it as a "three-tiered channel." There are three, perhaps four tiers or layers of Columbia Plateau basalt that have been cut by this channel. Immediately south of this site is Rock Lake, a deeply-scoured canyon with 244 m of relief to the bottom of the lake.

Hole-In-The-Ground is a 30 m-deep pit about 0.9 km long and 0.1 km wide located 60 m above the coulee floor on the opposide side of the canyon. Hole-In-The-Ground cannot be seen from this site, but is visible on topographic maps of the region. This pit was bored out by the Missoula Flood waters in a macroturbulent "subfluvial tornado," or "kolk" (Fig. 6; Waitt et al., 1994).

Rock Coulee is the most spectacular canyon erosion feature in the Cheney-Palouse scabland, and is all the more impressive because superficially it resembles some of the channels on Mars. Visitors might want to compare the multi-tiered Rock Coulee channel with some of the Viking images of straight, narrow channel systems on Mars, such as Ma'adim Vallis near Gusev Crater. *Estimated stay = 30 mins.*

183.4 Depart Stop 4, driving back up hill to intersection with Long Rd. (Note that large vehicles such as a bus should not attempt to go further down into Rock Coulee).

184.3 0.9 Turn right onto Long Rd.

191.6 7.3 Turn right onto Rock Lake Rd.

192.2 0.6 Rock Lake Rd. becomes Cheney Plaza Rd. Keep left.

202.0 9.8 Turn right on 1 St. in Cheney (located after two railroad crossings).

203.4 1.4 Turn right onto Cheney-Spokane Rd. at traffic light. Be careful not to miss this turn, the road is not clearly labeled.

214.7 11.3 Turn right at stop sign, onto U.S. 195 heading south.

216.2 1.5 Make U-turn to left at Meadowlane Rd. intersection (road to golf course). Travel north on U.S. 195.

216.8 0.6 Slow vehicle. Latah Creek outcrop is visible to right.

217.4 0.6 Turn-off for parking is to the right. This stop is optional, if time permits. Visitors must hike south along opposite side of streambed (assuming water is low) to visit the outcrop.

STOP 5— (OPTIONAL) LATAH CREEK SITE.

The site is actually located on the shores of Hangman Creek, but is known to geologists who have worked on this outcrop as the "Latah Creek" site (Fig. 31). The outcrops at this site contain slackwater sediments from the ponding of Missoula Flood waters (Kiver and Stradling, 1981). Rigby (1982) described a series of 15–20 rhythmites (individual units with a lower, gravelly portion and an upper portion of silt and clay). Within each rhythmite, Rigby (1982) found thin laminae interpreted as varves— the type of

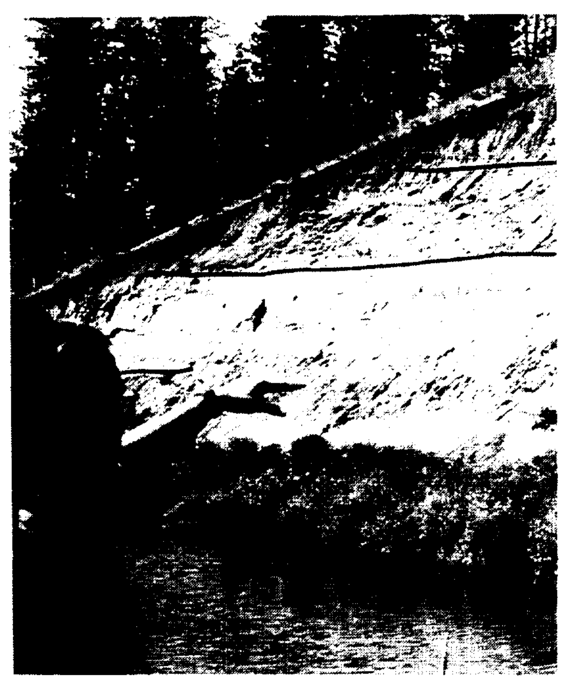

Fig. 31. Outcrop of rhythmite beds / slackwater deposits along shore of Hangman Creek, south of Spokane, Washington. Known as the Latah Creek site, this is a small outcrop just north of a public golf course. Lines drawn here indicate some of the rhythmite contacts. The deposits in this location are key evidence for multiple Lake Missoula floods.

annual layering found in lakes that occur in seasonally-variable climates. Rigby suggested that each of the rhythmites represents a major Missoula Flood. By counting varves, it is seen that these major floods were separated by periods of 10–60 years.

Kiver and Stradling (1989) consider this site to be among the most important in the Channeled Scabland, because it was the first site to provide "unequivocal evidence... that supports the hypothesis that numerous floods separated by decades of non-flood sedimentation occurred" in the region. *Suggested stay = 45 minutes.*

217.4 Depart Stop 5 site, continue north on U.S. 195.

219.7 2.3 Keep right, get onto Interstate 90, traveling east.

221.7 2.0 Leave Interstate 90 at Exit 281, the Division St. exit in Spokane. **End of Field Trip II.**

REFERENCES

Allen J. E. and Burns M. (1986) *Cataclysms on the Columbia.* Timber Press, Portland, Oregon, 213 pp.

Atwater B. F. (1986) Pleistocene glacial-lake deposits of the Sanpoil River valley, northeastern Washington. *U.S. Geological Survey Bulletin, 1661*, 39 pp.

Alden W. C. (1927) Discussion: Channeled Scabland and the Spokane Flood. *Washington Academy of Science Journal, 17*(8), 203.

Baker V. R. (1973) Paleohydrology and sedimentology of Lake Missoula flooding in eastern Washington. *Geological Society of America Special Paper, 144*, 79 pp.

Baker V. R. (1978a) Paleohydraulics and hydrodynamics of Scabland Floods. In *The Channeled Scabland*, edited by V. R. Baker and D. Nummedal, pp. 59–79, NASA, Washington, DC.

Baker V. R. (1978b) Large-scale erosional and depositional features of the Channeled Scabland. In *The Channeled Scabland*, edited by V. R. Baker and D. Nummedal, pp. 81–115, NASA, Washington, DC.

Baker V. R. (1978c) Quaternary geology of the Channeled Scabland and adjacent areas. In *The Channeled Scabland*, edited by V. R. Baker and D. Nummedal, pp. 17–35, NASA, Washington, DC.

Baker V. R. (1978d) The Spokane Flood controversy and the martian outflow channels. *Science, 202*, 1249–1256.

Baker V. R. (1982) *The Channels of Mars.* University of Texas Press, Austin, 198 pp.

Baker V. R. (1989) The Grand Coulee and Dry Falls. In *Glacial Lake Missoula and the Channeled Scabland, Field Trip Guidebook T310 for the 28th International Geological Congress*, edited by R. M. Breckenridge, pp. 51–55, American Geophysical Union, Washington, DC.

Baker V. R. and Bunker R. C. (1985) Cataclysmic Late Pleistocene flooding from glacial Lake Missoula: A review. *Quaternary Science Reviews, 4*, 1–41.

Baker V. R. and Milton D. J. (1974) Erosion by catastrophic floods on Mars and Earth. *Icarus, 23*, 27–41.

Baker V. R. and Nummedal D., editors (1978) *The Channeled Scabland.* A guide to the geomorphology of the Columbia Basin, Washington, prepared for the Comparative Planetary Geology Field Conference held in the Columbia Basin, June 5–8, 1978, NASA, Washington, DC., 186 pp.

Baker V. R., Carr M. H., Gulick V. C., Williams C. R., and Marley M. S. (1992) Channels and valley networks. In *Mars*, edited by H. H. Kieffer et al., pp. 493–522, University of Arizona Press, Tucson.

Binder A. B., Arvidson R. E., Guiness E. A., Jones K. L., Morris E. C., Mutch T. A., Pieri D. C., and Sagan C. (1977) The geology of the Viking Lander 1 site. *Journal of Geophysical Research, 82*, 4439–4451.

Breckenridge R. M., editor (1989a) *Glacial Lake Missoula and the Channeled Scabland, Field Trip Guidebook T310 for the 28th International Geological Congress.* American Geophysical Union, Washington, DC, 72 pp.

Breckenridge R. M. (1989b) Lower glacial Lakes Missoula and Clark Fork ice dams. In *Glacial Lake Missoula and the Channeled Scabland, Field Trip Guidebook T310 for the 28th International Geological Congress*, edited by R. M. Breckenridge, pp. 13–21, American Geophysical Union, Washington, DC.

Bretz J H. (1923) The Channeled Scabland of the Columbia Plateau. *Journal of Geology, 31*, 617–649.

Bretz J H. (1930) Lake Missoula and the Spokane Flood. *Geological Society of America Bulletin, 41*, 92–93.

Bretz J H. (1969) The Lake Missoula floods and the Channeled Scabland. *Journal of Geology, 77*, 505–543.

Bretz J H. (1978) Introduction. In *The Channeled Scabland*, edited by V. R. Baker and D. Nummedal, pp. 1–2, NASA, Washington, DC.

Bretz J H., Smith H. T. U., and Neff G. E. (1956) Channeled Scabland of Washington— New data and interpretations. *Geological Society of America Bulletin, 67*, 957–1049.

Bullock M. A. (1994) The soil of Mars. *Mercury, 23*(5), 10–16.

Busacca A. J., McDonald E. V., and Baker V. R. (1989) The record of pre-late Wisconsin floods and late Wisconsin flood features in the Cheney-Palouse Scabland. In *Glacial Lake Missoula and the Channeled Scabland, Field Trip Guidebook T310 for the 28th International Geological Congress*, edited by R. M. Breckenridge, pp. 57–62, American Geophysical Union, Washington, DC.

Christensen P. R. (1986) Regional dust deposits on Mars: Physical properties, age, and history. *Journal of Geophysical Research, 91*, 3533–3545.

Drumheller T. (1982) Ephrata, recorded September 9, 1975. *Memories of Grant County, 7*, 155–158.

Easterbrook D. J. (1976) Quaternary geology of the Pacific Northwest. In *Quaternary Stratigraphy of North America*, edited by W. C. Mahaney, pp. 441–462, Dowden, Hutchinson, and Ross, Stroudsbourg, Pennsylvania.

Edgett K. S. (1994) The basaltic aeolian dunes near Moses Lake, Washington, U.S.A.: Changes in Twentieth Century activity moderated by local human and volcanic influences (abstract). *Workshop on the Response of Eolian Processes to Global Change, Desert Research Institute Quaternary Sciences Center Occasional Paper, 2*, 33–35.

Edgett K. S. and Christensen P. R. (1994) Mars aeolian sand: Regional variations among dark-hued crater floor features. *Journal of Geophysical Research, 99*, 1997–2018.

Edgett K. S. and Christensen P. R. (1995) K-12 education outreach program initiated by a university research team for the Mars Global Surveyor thermal emission spectrometer project. Submitted to *Journal of Geological Education*.

Edgett K. S. and Lancaster N. (1993) Volcaniclastic aeolian dunes: Terrestrial examples and application to martian sands. *Journal of Arid Environments, 25*, 271–297.

Edgett K. S., Christensen P. R., Wakefield D. A., and Rigberg B. M. (1995) The Arizona Mars K-12 Education Program: Outreach for Mars Global Surveyor, Mars Pathfinder, and other missions (abstract). *Lunar and Planetary Science XXVI*, 359–360.

Francis P. W. (1988) Preparing for Mars: Loess, and why we should study it (abstract). *Lunar and Planetary Science XIX*, 346–347.

Freeman O. W., Forrester J. D., and Lupher R. L. (1945) Physiographic divisions of the Columbia Intermontane Province. *Annals of the Association of American Geographers, 35*, 53–75.

Gilluly J. (1927) Discussion: Channeled Scabland and the Spokane flood. *Washington Academy of Science Journal, 17*(8), 203–205.

Golombek M. P., editor (1994) *Mars Pathfinder Landing Site Workshop*. LPI Technical Report 94-04, Lunar and Planetary Institute, Houston, Texas, 49 pp.

Golombek M. P. and Rapp D. (1995) Size-frequency distributions of rocks on Mars (abstract). In this volume.

Golombek M. P., Parker T. J., and Moore H. J. (1995) Mars Pathfinder landing site characteristics (abstract). *Lunar and Planetary Science XXVI*, 481–482.

Greeley R., Theilig E., Guest J. E., Carr M. H., Masursky H., and Cutts J. A. (1977) Geology of Chryse Planitia. *Journal of Geophysical Research, 82*, 4093–4109.

Gulick C. W. (1990) Geologic map of the Moses Lake 1:100,000 Quadrangle, Washington. *Washington Division of Geology and Earth Resources Open File Report, 90-1*.

Kiver E. P. and Stradling D. F. (1981) Catastrophic flood deposits from Lake Missoula in the Spokane area (abstract). *Northwest Scientific Association 54th Annual Meeting, Oregon State University, Corvallis*, p. 46.

Kiver E. P. and Stradling D. F. (1989) The Spokane Valley and northern Columbia Plateau. In *Glacial Lake Missoula and the Channeled Scabland, Field Trip Guidebook T310 for the 28th International Geological Congress*, edited by R. M. Breckenridge, 23–35, American Geophysical Union, Washington, DC.

Komatsu G., Baker V. R., and Johnson J. R. (1995) Ares Vallis: Geomorphology of Mars Pathfinder landing site (abstract). *Lunar and Planetary Science XXVI*, 779–780.

Lewis S. W. (1985) The Corfu Landslide: A large-scale prehistoric compound-complex slide in south-central Washington. M.S. Thesis, University of Arizona, Tucson, Arizona, 48 pp.

Mars Channel Working Group (1983) Channels and valleys on Mars. *Geological Society of America Bulletin, 94*, 1035–1054.

McDonald E. V. and Busacca A. J. (1988) Record of pre-late Wisconsin giant floods in the Channeled Scabland interpreted from loess deposits. *Geology, 16*, 728–731.

McKnight E. T. (1927) The Spokane Flood: A discussion. *Journal of Geology, 35*, 453–460.

Meinzer O. E. (1927) Discussion: Channeled Scabland and the Spokane Flood. *Washington Academy of Science Journal, 17*(8), 207–208.

Meszaros S. P. (1984) Mars-Earth geographical comparisons: A pictorial view. *NASA Technical Memorandum, 86166*, Goddard Space Flight Center, Greenbelt, Maryland, 35 pp.

Merriam W. B. (1975) *Pend Oreille: The Story of an Inland Sea*. Washington State University, Pullman, Washington, 16 pp.

Milton D. J. (1973) Water and processes of degradation in the martian landscape. *Journal of Geophysical Research, 78*, 4037–4047.

Molenaar D. (1988) The Spokane Aquifer, Washington: Its geologic origin and water-bearing and water quality characteristics. *U.S. Geological Survey Water Supply Paper, 2265*, 74 pp.

Moore J. M., Clow G. D., Davis W. L., Gulick V. C., Janke D. R., McKay C. P., Stoker C. R., and Zent A. P. (1995) The circum-Chryse region as a possible example of a hydrologic cycle on Mars: Geologic observations and theoretical evaluation. *Journal of Geophysical Research, 100*, 5433–5447.

Mullineaux D. R., Wilcox R. E., Ebaugh W. F., Fryxell R., and Rubin M. (1978) Age of the last major scabland flood of the Columbia Plateau in eastern Washington. *Quaternary Research, 10*, 171–180.

Mustard J. F., Erard S., Bibring J.-P., Head J. W., Hurtrez S., Langevin Y., Pieters C. M., and Sotin C. J. (1993) The surface of Syrtis Major: Composition of the volcanic substrate and mixing with altered dust and soil. *Journal of Geophysical Research, 98*, 3387–3400.

National Aeronautics and Space Administration (1992) *NASA's Strategic Plan for Education: A Strategy for Change, 1993–1998*. NASA EP-289, Washington, DC, 65 pp.

Nummedal D. (1978) Field trip stop descriptions. In *The Channeled Scabland*, edited by V. R. Baker and D. Nummedal, pp. 131–168, NASA, Washington, DC.

O'Connor J. E. (1993) Hydrology, hydraulics and geomorphology of the Bonneville Flood. *Geological Society of America Special Paper, 274*, 82 pp.

O'Connor J. E. and Baker V. R. (1992) Magnitudes and implications of peak discharges from glacial Lake Missoula. *Geological Society of America Bulletin, 104*, 267–279.

O'Connor J. E. and Waitt R. B. (1995) Beyond the Channeled Scabland: A field trip to Missoula flood features in the Columbia, Yakima, and Walla Walla Valleys of Washington and Oregon— Part 1. *Oregon Geology, 57*, 51–60.

Olmstead R. K. (1963) Silt mounds on Missoula Flood surfaces. *Geological Society of America Bulletin, 74*, 47–54.

Othberg K. L. and Breckenridge R. M. (1992) Field trip to Missoula Flood features in the Rathdrum Prairie and vicinity, Idaho and Washington. Unpublished guide for the Idaho Science Teachers Association Fall Conference, October 1–3, 1992, 12 pp.

Pardee J. T. (1910) The glacial Lake Missoula, Montana. *Journal of Geology, 18*, 376–386.

Pardee J. T. (1942) Unusual current in glacial Lake Missoula, Montana. *Geological Society of America Bulletin, 53*, 1569–1600.

Parfit M. (1995) The floods that carved the west. *Smithsonian, 26*(1), 48–59.

Patton P. C. and Baker V. R. (1978) Origin of the Cheney-Palouse Scabland tract. In *The Channeled Scabland*, edited by V. R. Baker and D. Nummedal, pp. 117–130, NASA, Washington, DC.

Petrone A. (1970) The Moses Lake sand dunes. M.S. Thesis, Washington State University, Pullman, Washington, 89 pp.

Plescia J. B. and Golombek M. P. (1986) Origin of planetary wrinkle ridges based on the study of terrestrial analogs. *Geological Society of America Bulletin, 97*, 1289–1299.

Pye K. (1987) *Aeolian Dust and Dust Deposits*. Academic Press, New York, 334 pp.

Reid R. J. and Singer R. B. (1995) Mineral identification from well-calibrated multispectral imaging on the surface of Mars (abstract). *Lunar and Planetary Science XXVI*, 1155–1156.

Reidel S. P., Fecht K. R., and Tolan T. L. (1989) Field guide: Structural features of the Yakima Fold Belt, Columbia Plateau, Central Washington. In *MEVTV Workshop on Tectonic Features on Mars*, edited by T. R. Watters and M. P. Golombek, LPI Technical Report 89-06, pp. 77–123, Lunar and Planetary Institute, Houston, Texas.

Rice J. W. Jr. and DeHon R. A. (1995) Geologic map of the Darvel Quadrangle, Maja Valles region, Mars, 1:500,000 scale. *U. S. Geological Survey Miscellaneous Investigation Series Map I-2432*, in press.

Rigby J. G. (1982) The sedimentology, mineralogy, and depositional environment of a sequence of Quaternary catastrophic flood-derived lacustrine turbidites near Spokane, Washington. M.S. Thesis, University of Idaho, Moscow, Idaho, 132 pp.

Robertson D. F. (1994) To boldly go... *Astronomy, 22*(12), 34–41.

Roush T. L. and Bell J. F. III (1995) Thermal emission measurements 2000–400 cm^{-1} (5–25 μm) of Hawaiian palagonitic soils and their implications for Mars. *Journal of Geophysical Research, 100*, 5309–5317.

Singer R. B., McCord T. B., Clark R. N., Adams J. B., and Huguenin R. L. (1979) Mars surface composition from reflectance spectroscopy: A summary. *Journal of Geophysical Research, 84*, 8415–8426.

Smith G. D. (1992) Sedimentology, stratigraphy, and geoarcheology of the Tsulim Site, on the Hanford Site, Washington. M.S. Thesis, Washington State University, Pullman, Washington, 168 pp.

Soderblom L. A. (1992) The composition and mineralogy of the martian surface from spectroscopic observations: 0.3 μm to 50 μm. In *Mars*, edited by H. H. Kieffer et al., pp. 557–593, University of Arizona Press, Tucson.

Thomas P. (1984) Martian intracrater splotches: Occurrence, morphology, and colors. *Icarus, 57*, 205–227.

Tolan T. L., Reidel S. R., Beeson M. H., Anderson J. L., Fecht K. L., and Swanson D. A. (1989) Revisions to the estimates of the areal extent and volume of the Columbia River Basalt Group. *Geological Society of America Special Paper*, 238, 1–20.

U. S. Bureau of Reclamation (1978) *The Story of the Columbia Basin Project*. U. S. Government Printing Office, Washington, DC, 46 pp.

Waitt R. B. (1977) Missoula flood *sans* Okanogan lobe (abstract). *Geological Society of America Abstracts with Programs, 9*, 770.

Waitt R. B. (1980) About forty last-glacial Lake Missoula jökulhlaups through southern Washington. *Journal of Geology, 88*, 653–679.

Waitt R. B. and Atwater B. F. (1989) Stratigraphic and geomorphic evidence for dozens of last-glacial floods. In *Glacial Lake Missoula and the Channeled Scabland, Field Trip Guidebook T310 for the 28th International Geological Congress*, edited by R. M. Breckenridge, pp. 37–50, American Geophysical Union, Washington, DC.

Waitt R. B., O'Connor J. E., and Benito G. (1994) Scores of gigantic, successively smaller Lake Missoula floods through Channeled Scabland and Columbia Valley. In *Geologic Field Trips in the Pacific Northwest: 1994 Geological Society of America Annual Meeting*, edited by D. A. Swanson and R. A. Haugerud, pp. 1K-1–1K-88.

Washburn A. L. (1988) Mima mounds. *Washington Department of Natural Resources, Report of Investigations, 29*, 53 pp.

Watters T. R. (1988) Wrinkle ridge assemblages on the terrestrial planets. *Journal of Geophysical Research, 93*, 10236–10254.

Weis P. L. and Newman W. L. (1989) *The Channeled Scablands of Eastern Washington— The Geologic Story of the Spokane Flood*, second edition. Eastern Washington University Press, Cheney, Washington, 23 pp.

Zickler E. and Ribail M. (1983) Wilson Creek-Wheeler-Mitchell Coulee-Neppel, recorded May 11, 1982. *Memories of Grant County, 10*, 230–233.